www.sciencemag.org/cgi/content/full/science.1227670/DC1

Supplementary Materials for

Variable Clonal Repopulation Dynamics Influence Chemotherapy Response in Colorectal Cancer

Antonija Kreso, Catherine A. O'Brien, Peter van Galen, Olga Gan, Faiyaz Notta, Andrew M. K. Brown, Karen Ng, Jing Ma, Erno Wienholds, Cyrille Dunant, Aaron Pollett, Steven Gallinger, John McPherson, Charles G. Mullighan, Darryl Shibata, John E. Dick*

*To whom correspondence should be addressed. E-mail: jdick@uhnres.utoronto.ca

Published 13 December 2012 on *Science* Express
DOI: 10.1126/science.1227670

This PDF file includes:

Materials and Methods

Human colon cancer cell isolation, lentivirus production, and xenograft generation

Tumor cells were isolated from tissue obtained with patient consent, as approved by the Research Ethics Board at the University Health Network. A third-generation self-inactivating lentivirus vector with GFP expressed from the human phosphoglycerate kinase promoter was used (*31*). Tumor tissue was dissociated using collagenase A and red blood cells were lysed using ammonium chloride. Cells were analyzed using flow cytometry (with antibodies to EpCAM, CD31, CD45, and HLA) to determine the presence of human epithelial tumor cells, as well as contaminating non-epithelial cells. Isolated colon cancer cells were plated as described (*32*); viral particles were added at a multiplicity of infection of 1 to 10 for 16 to 40 hours. $5x10^4$ to $2x10^5$ cells were injected under the renal capsule of 8 to 10 week old non-obese diabetic/severe combined immune deficiency (NOD/SCID) and/or NOD/SCID/IL2R-gamma-null (NSG) mice. Animal experimentation followed protocols approved by the University Health Network Animal Care Committee. We assessed the presence of tumors by palpation. Starting 30 days following injection, we palpated mice every two weeks to monitor for tumor growth. When tumors were readily identified by palpation (generally, at this time they reached 5-10% of mouse body weight and parallel mice harbored tumors of approximately the same size) mice were sacrificed, tumors excised and weighed. Single cells were isolated from the tumor and $5x10^4$ to $2x10^5$ cells were re-injected to generate secondary tumors; this procedure was repeated for each transplant. Cells derived from xenografts were analyzed for the expression of EpCAM, HLA, and mouse H2Kd to ensure human cells were re-transplanted and to exclude contaminating mouse cells. Based on flow cytometric analysis, we estimate >80% of cells are tumor-derived.

Flow cytometry and fluorescence activated cell sorting

Cells were isolated from tumor tissue and passed through a 40-μm cell strainer to obtain single cells. Cells were stained with antibodies to human CD44 (Beckman Coulter) and CD133/1 (Miltenyi). EpCAM was used to mark epithelial cells; CD45, CD31, and mouse H2K (Beckman Coulter) were used to exclude hematopoietic, endothelial, and mouse contaminating cells, respectively. Flow cytometry analysis was performed on the BD™ LSR II or FACSCanto II (BD Biosciences). For limiting dilution analysis, GFP-expressing cells were sorted using FACSAria or MoFlo cell sorters. SYTOX Blue (Molecular Probes, 1 μM) or propidium iodide (Invitrogen, 1 μg/mL) was added to exclude dead cells.

Copy number alteration analysis

Genomic DNA from primary human tumor samples and xenografted tumor cells was isolated using the Qiagen Gentra Puregene Tissue kit. Tumor cells were profiled using flow cytometry to ensure absence of mouse contaminating cells and the presence of human epithelial tumor cells in the xenografted tumors. Based on flow cytometric analysis, we estimate >80% of cells are tumor-derived. DNA was subjected to copy number analysis using Affymetrix 6.0 SNP arrays. SNP array data was analyzed using a previously described workflow, including reference normalization (*33*), circular binary segmentation (*34*), and data were visualized in dChip (*35*). Samples lacking gross alterations were set as diploid reference samples in order to calculate copy number.

Targeted deep sequencing

Targeted deep sequencing, as previously described in (*36*), was used with the following modifications to the protocol: genomic DNA (500 ng) for each sample was sheared using the

Covaris S2 ultrasonicator (Covaris) to produce fragments of 3000 bp in length. Sheared products were purified using Zymo-5 columns (Zymo Research) and concentrated to a volume of 8-10 μL. Products were analyzed on a BioAnalyzer HS dsDNA chip (Agilent Technologies) to confirm proper shearing and quantified using Qubit® Fluorometer (Life Technologies). Up to 8 μL sheared DNA was mixed with 42 μL of Template Master Mix: 11.66 μL 10x High Fidelity Buffer (Invitrogen), 3.12 μL $MgSO_4$ (Invitrogen, 50 mM), 3.12 μL dNTP (NEB, 10 mM), 8.93 μL Betain (Sigma, 4 M), 4.46 μL RainDance Droplet Stabilizer (RainDance Technologies), 8.93 μL DMSO, and 1.79 μL Platinum High Fidelity Taq (Invitrogen, 5 U/μL). If necessary, nuclease free water was used to bring final volume to 50 μL. Microdroplet PCR (*37*) was used to amplify 71 kb of mutational hotspots in 42 cancer genes (*36*). Universal PCR was used to make sequencing libraries by incorporated the Ilumina adaptor sequences and a unique molecular barcodes onto the PCR products for each sample. Samples were quantified using the Qubit® Fluorometer and diluted to 10 ng/μL. Equal volumes of up to 12 samples were pooled together. qPCR was performed on the Eco Real-Time PCR System (Illumina) using the Kapa Illumina Library Quantification Kit (Kapa Biosystems).

Pooled libraries were sequenced on the Illumina MiSeq instrument (Illumina) using a 2X150 paired end protocol. Demultiplexed FASTQ files were generated from on instrument basecalls using Illumina's CASAVA software. The sequences were aligned to the human genome (hg19/GRCh37) using the Novoalign (Novocraft) short read aligner. Single nucleotide variants and short indels were identified using the Genome Analysis Toolkit (*38*) with standard filtering and annotated with ANNOVAR (*39*). Variants were removed for the following reasons: the variant fell outside the target region, there was not adequate coverage (100x) in the primary or reference sample, the variant in a xenograft samples arose due to differences between the mouse and human genomes.

Exome sequencing and variant calling

Genomic DNA was sonicated (Covaris) to generate fragments with size ranges of 300-500 bp. Fragmented DNA was then used as input for genomic library preparation using the NEBNext DNA Sample Preparation Kit (New England Biolabs); libraries were prepared manually. 500 ng of adapter-ligated DNA libraries were hybridized to the SureSelect Human All Exon 50Mb kit (Agilent) biotinylated RNA library baits for 72 hours. The enriched fragments were captured using streptavidin beads and then sequenced 2X101 bp Illumina HiSeq 2000 sequencing platforms. Intensities and basecalls were converted to FASTQ formatted reads using Illumina CASAVA which includes demultiplexing for barcoded samples. The FASTQ files were aligned to the UCSC hg19 human reference using Novoalign V2.07.14 and were further processed (i.e. BAM file conversion and sorting, duplicate read removal, read filtering) using Picard and SAMTools. Metrics and coverage data were generated using BEDTools. Variants were called using GATK v1.3.16, and samples were processed together though this pipeline as a set in accordance with recommended GATK best practices. The GATK workflow involved recalibration of base qualities and local realignment prior to SNPs and indels calling. Somatic candidates were initially identified as calls with a differing genotype between a reference (normal tissue) and tumor sample (always a pairwise comparison). Candidate somatic calls were then passed through in house scripts to filter based on depth of coverage, quality, frequency and for xenograft samples; likelihood to be due to differences in the human and mouse reference genome.

Passenger DNA methylation diversity analysis

Small (1-2 mm^2) tumor areas were microdissected from primary or xenograft microscope slides and 6 to 8 epialleles were sampled from each region by bisulfite sequencing of cloned PCR products (*40*). Diversity was measured as the number of unique 5' to 3' DNA methylation patterns

or as a pairwise distance between the epialleles within each small region, with more diverse populations having more unique epialleles or greater pairwise distances. Each tumor was represented by the average values for their microdissected regions (between 1 and 6 regions per tumor).

Passenger Epialleles

The sequences for the BRS and LOC epialles are provided in (*40*). Two new epialleles that show age related methylation in normal tissues, and are not in genes expressed in colon are illustrated below. These epialleles are autosomal (both on chromosome 19) and single nucleotide polymorphisms (in red) were used to distinguish between maternal and paternal alleles. Diversity (unique patterns or pairwise distances) was separately calculated for each allele and then averaged. CT54 was from a female patient, but its BRS locus (X-chromosome) had a polymorphism that distinguished maternal from paternal alleles. Bisulfite treated sequence with primer sites is underlined; converted "C" represented as "T", and CpG sites capitalized.

ABHD8: 9 CpGs

gggTttgaTTtTtaTaaaggtgtagTTatCGTtggaTtCGaCGTtTtTTagtggTTTTaCGgCGttgggggCGtgTTT
agTaggTaaTagaa(g/a)ataTCGtCGgtTaTTTCGgtTagTatggtgtgtTTtgtgagtg

ZNF471: 14 CpGs

gttTTtggggTTtgggagggaaaCGCGCGaCGgTtgagTTttCGgtgtgagtaCGCGtggggTtttgtgaCGTtgtTtgtg
TTtTtgtgatCGCGatgtTattCGgagCGCG(g/t)TTttTtgtgTTagtTCGtgggagtgtTattatTtttTtgtg

Southern blot analysis

Tumor genomic DNA was extracted and 5-35 μg was digested with BamHI. For several experiments, DNA was also digested with EcoRV to confirm the clonal pattern. After

electrophoresis and transfer to a positively charged nylon membrane, DNA was hybridized to a GFP probe. Samples were also digested with EcoRI, which cuts out the GFP, to confirm presence of the correct fragment. Three observers independently analyzed the presence of bands on Southern films and consensus was reached for insertion mapping.

Tracking single cells: methodology

To monitor the output of single CRC cells within the captured genetic clone over successive rounds of tumor formation, the progeny of single CRC cells was followed by carrying out clonal tracking experiments through the use of lentiviral integration site mapping by Southern blotting. A GFP sequence is integrated into the cellular genomes by the lentivirus, which allows it to be replicated alongside the host cells' genomes during cell division. Progeny descending from a labeled cell can be readily identified by the same viral insertion. The Southern technique conveniently requires the presence of at least $3x10^4$ cells for detection, ensuring that the detected band is derived from a cell with significant proliferative output, thus eliminating background noise associated with the output of cells that have limited proliferative potential. Generally, 10 to 30 μg of total tumor DNA was analyzed for Southern blot analysis. A typical mammalian cell has approximately 10 pg of DNA, therefore we estimate that $1x10^6$ to $3x10^6$ tumor cells were analyzed per lane in Southern blots. With the detection limit of $3x10^4$ cells, a clone would have to comprise about 1% to 3% of the analyzed tumor to be detected by Southern blot. Here, it is assumed that proliferation is correlated to the size of a marked clone, although other factors, including cell death, may play a role. Southern blotting is also quantitative, enabling the distinction between bands that are detected at low level versus those that are abundant. Serial transplantation combined with single-cell marking enabled us to track the longevity of the output of single CRC cells, including an assessment of their proliferative potential as measured by the size of their descendants, and tumor

re-generation potency as measured by serial transplantation. Since $5x10^4$ to $2x10^5$ primary tumor cells were injected at each serial transplant, representing at least 100-fold dilution of the isolated tumor cells, tracked tumor cells would be diluted out of existence if not for proliferation. Thus, by transplanting a limited number of CRC cells to challenge the system and by tracking their progeny using Southern blotting, we were able to measure the output of the most potent CRC cells. GFP-marked tumor cells were transplanted in two to six serial xenograft assays in NOD/SCID and NSG mice. Results from both strains of mice were similar and were pooled for analysis. Genomic DNA was isolated from the whole tumor at each transplant to assess the distribution of lentivirally tagged cells and two different restriction enzymes were used for Southern blotting to independently confirm the results. Lentiviral integrations were identified as distinct bands of unique size on a Southern blot. We assigned each band an identity number and recorded its presence in the tumor DNA of serial transplants. When a band was detected on the Southern blot at any of the exposure times, it was scored as positive and interpreted to represent outgrowth of a CRC cell (referred to as a 'LV clone' from now on). If bands of different sizes were consistently seen together but never separately across three or more recipients over more than one transplant, we assumed that they represented one clone with multiple lentiviral integration sites and scored the bands as one clone.

As a second method of detecting multiple inserts per cell, we carried out limiting dilution analyses, where GFP+ tumor cells were separated using FACS prior to injection at limiting doses into animals (data not shown). Using Poisson distribution statistics, cell doses at which at least 37% sites did not score positive for the presence of tumors were assumed to be generated by one cell. For all limiting dilution experiments, tumor DNA was isolated and analyzed by Southern blotting; we analyzed 335 tumors for sample CT38, 192 tumors for CT54, and 151 tumors for CT59. If bands of different sizes were consistently seen together but never separately in tumors that were generated using a limiting cell dose, these bands were scored as one LV clone with multiple insertions. Three

observers independently analyzed the presence of bands on Southern films and consensus was reached for insertion mapping.

Procedure for defining LV clone types

LV clone types were defined within the limits of each experiment. Type I, long-term persistent LV clones (purple arrowhead, Fig. 2A) were defined if the band was detected in every tumor that was re-transplanted further over an entire experiment; for example, (i) if the tumor was transplanted twice and the band is present in both transplants, it is classified as Type I, as well as (ii) if the tumor is transplanted six times and the bands are present in each transplant, including the tumor that was used for further transplantation, the band or clone was classified as Type I. Type II LV clones with limited or short-term tumor-initiating capacity (blue arrowhead, Fig. 2A) were defined by the presence of bands over multiple passages in mice, including detection in 1° and 2° recipients, but the characteristic absence in the last transplant. The number of transplants in which Type II clones were detected was unique to each experiment, but if the band was detected in at least two transplants and was not detected again, including the last transplant, it was characteristic of Type II behavior. Type III transient LV clones (green arrowhead, Fig. 2A) were defined by being detected in 1° recipients, but were not detected again over the entire experiment, irrespective of how many additional transplants were carried out. Type IV, quiescent or resting LV clones (red arrowhead, Fig. 2A) were defined by (i) not detected in 1° transplants and/or subsequent transplants, but then (ii) detected in one or more recipients in any succeeding transplant. The length of time Type IV then persisted was irrelevant to the definition of Type IV behavior, as long as the clone did not undergo a round of non-detection to surface again, which is defined as Type V or fluctuating clonal behavior (orange arrowhead, Fig. 2A). Type V behaviors were defined in experiments, which were transplanted enough times to observe the following clonal outcomes: (i)

detection in one transplant including the tumor of the recipient that was used for the subsequent round of injections, (ii) below the detection limit in the one or more of the following transplants, including recipients that were further transplanted, and (iii) detection in any successive transplant.

Insertion site determination

Lentiviral insertions were detected by splinkerette PCR as previously described (*41*).

Chemotherapy treatment

Transduced and xenografted colon tumor cells were re-injected into mice and when tumors were palpable, mice received intra-peritoneal injections of either vehicle (PBS) or oxaliplatin (Sigma, 5-15 mg/kg) twice a week for 2 to 4 weeks. Mice were sacrificed 2 to 5 days after the last treatment. To assess tumor re-initiation, control and oxaliplatin-treated cells were isolated and equal viable cell doses were re-injected into subsequent recipients, which did not receive any treatment. Viability was determined by Trypan Blue exclusion.

Quantitative analysis of Southern blot data

To quantify the blot data, a specific program was implemented in C++. This program simulates the peak shape, recovers and eliminates the background in columns, and fits peak parameters to the experimental data. Southern blots are digitized and columns are selected and reduced to a single vector of values by summation. Peak shape is simulated by assuming an isotropic linear diffusion process of the luminescent protein in the gel from its well. Further, as the images are obtained by manually putting a sensitive film on the gel, some motion blur is assumed. The background is obtained by sub-sampling the initial data and interpolating between sub-sampled points. Then the interpolated points are successively smoothed until the difference between two

adjacent points is no more than a set threshold. The peak parameters are the height and the position. They are fit by exhaustively checking all parameters around a manually input position. Finally, the area under the peak is assumed to be that of the idealized peak which was fit.

Measuring similarity between tumors

Transplanted tumors are compared to their primary tumor. As a significant fraction of the clones are not successfully transplanted, only those clones present in both the original and the transplanted tumor are considered. The similarity used is the angle between the vectors of the relative proportions of the clones considered in each tumor. The angle between the proportion vectors t_1 and t_2 is calculated as:

a = Acos((t_1 \cdot t_2)/(|t_1||t_2|))

This yields a result between 0 and pi/2 (as all values in the vectors are positive). The similarity s is then renormalized to lie between 0 and 1, where 0 represents orthogonal vectors and 1 parallel vectors.

s = 1-a/pi

For the purpose of this comparison, treated and untreated tumors were considered separately. The treated/transplanted comparison compares tumors, which were treated with their untreated transplant.

Mathematical fitting

The fraction of all clones recorded over each series of transplantation was recorded as a function of the number of transplantation. The median of each transplantation number group was fit with an exponential. This was done to verify the hypothesis that a constant fraction of the clones was lost during each round of transplantation. An excellent fit was obtained with an R^2 of 0.96.

The fit further indicated that only 70% of the total clones present were observed in each blot. This can be explained partly by: a threshold sensitivity effect of the film used to produce the blots: as the films were not pre-flashed, no faint bands below a certain threshold could be observed; and by clones that are below detection limits, but that become activated and expand to become detectable in subsequent xenograft recipients.

Monte-Carlo Simulation

The similarity study showed that clone multiplication kinetics were not significantly different. Furthermore, assuming exponential growth would have meant very finely tuned parameters to conserve tumor diversity, and thus would not have modeled the experiment robustly. However, significant dispersion was observed in the fraction of clones conserved in the transplanted tumor as a function of the number of observed clones in the tumor to be transplanted. A simple stochastic process was simulated to simulate this. Tumors with various number of clones were virtually transplanted until no clones were observed. The probability of any clone being transplanted was that observed in the mathematical fitting, with a dispersion of +- 50%. This reproduced the spread of experimental data, showing that no other stochastic process needed to be assumed to reproduce the experimental pattern.

Statistical analysis

All data was analyzed using GraphPad Prism version 5.0 for Mac OS X (San Diego California USA, www.graphpad.com). P-values were calculated using Student's two-tailed t-tests.

Supplementary Text

Marked CRC cells generate xenografts that maintain the characteristics of the patient tumor

We transduced cells from ten colorectal carcinomas obtained post-resection from a spectrum of primary (n=6) and metastatic (n=4) tumors, including microsatellite stable and unstable samples (Table S1). Following brief transduction using a GFP-expressing lentivirus, cells were injected into the renal capsule of immunocompromised mice. The transduced cells generated xenografts and maintained stable GFP expression over serial transplantation (Fig. S1, S2). The xenografts resembled the primary patient tumor morphologically (Fig. S3) and by expression of proliferation, cell death, and differentiation markers (Fig. S4). Xenografts did not reliably form when injecting CRC cells into orthotopic sites (Table S2). Genomic analysis of viral insertion sites from several experiments did not reveal a preference for integration near known oncogenes or tumor suppressor genes, suggesting that lentiviral insertion did not influence tumor growth (Table S3). These data indicate that brief exposure to lentivirus efficiently transduces and marks primary human CRC cells under conditions that permit their survival while maintaining their malignant properties.

Clonal outgrowth is maintained through serial rounds of tumor transplantation

To assess clonal dynamics in xenografts, we used high-resolution single nucleotide polymorphism (SNP) microarrays to compare genome-wide DNA copy number profiles of pre-transplant tumor cells and the corresponding xenografts for three biological samples. For each of these samples up to four serial transplants were undertaken, with two to four mice per transplant, encompassing 393 days (CT38), 341 days (CT54), and 261 days (CT59) of total tumor growth. The majority of CNAs detected in patient tumor samples prior to injection were recapitulated in all corresponding primary (1°) xenograft recipients (Figs. 1B, S6, S7). For diagnostic samples CT38

and CT59, an outgrowth of a minor genetic clone had occurred since several novel aberrations, which were below the detection threshold of the SNP arrays in the patient tumor, were detected in multiple corresponding 1° recipients (Table S4, Figs. S6, S7). We did not detect any CNAs in the third patient tumor sample (CT54) and no new CNAs were detected in the tumors of its corresponding 1° recipients (Fig. 1B). The CNA profile of all secondary (2°) xenografts closely matched the CNAs detected in 1° recipients (Fig. 1B). Moreover, the CNA profiles of quaternary (4°) and quinary (5°) xenografts, which have undergone several rounds of expansion, also recapitulated the aberrations detected in 1° and 2° xenografts (Fig. 1B). The presence of multiple xenograft recipients from the same patient sample with both identical and new CNAs strongly supports the existence of subclones that are present at low levels in the diagnostic sample. Thus, CRC clones were stably maintained over time in multiple recipients at multiple transplants as assessed by global DNA copy number analysis.

In addition to CNAs, somatic mutations are important drivers of cancer progression (*42*) and occur most frequently in restricted mutational hotspots of the genome. To gain insight into the prevalence of known driver mutations over time, the presence of single nucleotide variants (SNVs) in tumor DNA following rounds of xenografting was analyzed using targeted deep sequencing (*36*). Over 600 cancer hotspot mutations in 88 kb of sequence encompassing the mutational hotspot regions in 54 genes were sequenced to a median coverage depth of 1350X. Paired analysis of SNVs detected in patient tumors and matching normal intestinal mucosa illustrated variation in the total numbers of somatic SNVs between different patient tumor samples (CT38: 1 somatic SNV; CT54: 8 somatic SNVs; CT59: 11 somatic SNVs; Fig. 1C). For all three tumor samples, comparison of SNVs between the patient tumor sample and 1° recipients indicated that all somatic SNVs detected in the patient tumor were also present in 1° recipients (Fig. 1C, Tables S5-7). For CT59, the frequency of nine somatic SNVs was increased in 1° xenografts (SNV frequency ranges: patient

tumor, 9.3%-24.0%; 1° recipients, 33.4-63.1%; Fig. 1C), consistent with enrichment of a clone from the patient tumor sample. Of note, this analysis does not take into account copy number changes, loss of heterozygosity, or cellularity, although we estimate >80% of cells used for sequencing were tumor-derived. Next, the prevalence of somatic SNVs was examined over serial passage by tracking the frequency of each somatic SNV over consecutive transplants. For CT38, the somatically acquired SNV (in an intron of *RET*) was present at similar allele frequencies across patient and xenograft-derived tumors (patient tumor, 61.5%; 1° xenografts, 71.9±4.4%; 2° xenografts, 72.4±4.9%; 4° xenografts: 73.8±4.7%; Fig. 1C, Table S5). For CT54, the variant allele frequencies for four of the eight somatically acquired SNVs (TP53 N156H, CDH1, STK11, FGFR1) decreased from 1° to 2° transplantation, while one SNV (MSH K675X) was enriched in 2° recipients (Fig. 1C). The frequency of all eight somatic SNVs remained stable between the recipients of 2° and 5° transplants (Fig. 1C, Table S6), indicating that xenografting selects a genetic clone that remains stable over consecutive transplants. For CT59, the 11 somatically acquired SNVs (BRAF V600E, APC G487R, FBXW7 R104X, FBXW7 W408C, FLT3 C452X, HRAS A18V, KIT C902C, KRTAP19-6 G20G, PDGFRA P567L, TP53 R283H, and TP53 R196X) were present at comparable frequencies between the recipients of 1° and 2° transplants (Fig. 1C, Table S7), suggesting that xenografting maintains tumor cells that recapitulate a cell population present in the patient tumor sample. Importantly, no new somatic SNVs were detected in xenograft-derived tumors (Fig. 1C), indicating that out of the 660 mutational hotspots analyzed, no xenograft-specific somatic mutations were acquired. Consistent with the CNA data, targeted sequencing reveals that xenografting selects for clones that are stably propagated over multiple recipient mice and serial transplants.

To explore the degree of genetic variability after transplant into xenografts, we also used exome sequencing. The exome sequences of a MSS sample (CT38), its matching normal mucosa,

and two recipients from 1° transplants were analyzed. The average depth of coverage for the eight samples was 278X; 90% of the targeted exons were covered at least 28X (average 37X). A total of 316 somatic SNVs were detected in the diagnostic sample (26 synonymous, 6 stop-gain, and 61 non-synonymous, 223 located outside of exons). Paired analysis demonstrated very high retention of diagnostic SNVs in 1° xenografts with only 24 of the somatically-acquired SNVs enriched up to 4-fold and 12 SNVs decreased (more than 2-fold) or lost in 1° xenografts; congruent SNV profiles were seen when comparing the diagnostic sample to 2° or 4° recipients (Fig. S8A, Table S8). These data indicate that xenografting retains the major genomic aberrations of the diagnostic sample while selecting for a subset of CRC cells that are propagated as xenografts. To determine whether the clones selected in 1° xenografts remained stable over multiple transplants, we compared the somatically acquired SNVs from 1° recipients to 2° and 4° passaged recipients. A high level of genomic similarity was observed in serial xenografts irrespective of passage number (Pearson's r=0.944 and r=0.95, respectively, Fig. S8B), strongly supporting our prior genomic analyses.

We next sought to determine whether new SNVs could be detected in xenografts. If the same SNV appeared in each of two xenograft recipients, we reasoned that this is highly likely due to the emergence of a preexisting mutation present in the diagnostic sample, but that was below detection limits. Alternately, detection of a SNV in only a *single* recipient is more likely due to a bona fide *de novo* mutation arising through tumor propagation. We found no cases of non-synonymous SNVs that were detected in only one of the two 1° recipients (xenograft 'a' in Fig. S9A). We then looked for non-synonymous SNVs that were enriched (or detected ≥2%) in this recipient, but below the 2% cutoff in the parallel recipient and diagnostic sample. We found one non-synonymous mutation (APBA1 G178A) that was enriched in one of the two 1° xenografts (1° recipient 'a': 8.1% versus 1° recipient 'b': 1.7%, Table S9) and then detected in all subsequent 2° and 4° xenografts derived from this initial recipient. It is likely that the *APBA1* mutation was below

detection limit at diagnosis but was selected for in xenografts. Paired analysis of 2° xenografts with diagnostic tumors yielded similar results. In this case, 67 non-synonymous SNVs were *enriched* in only one of the two 2° xenografts (Fig. S9 and Table S10). These SNVs were present at low levels (less than 2%) in the diagnostic sample or 1° xenografts, indicating that they likely comprised minor cell fractions in the diagnostic sample. Of note, this analysis does not take into account tumor cellularity, although we estimate >80% of cells used for sequencing were tumor-derived. Collectively, the exome sequence of 1° and 2° recipients is consistent with selection of a pre-existing clone from the diagnostic tumor in the xenograft.

Finally, we examined how the exome of a late passaged xenograft compares to its diagnostic sample and earlier xenografts. Analysis of two recipients from 4° passage revealed enrichment of 235 non-synonymous SNVs in one of the two 4° xenografts, which were either not detected or detected at low levels (less than 2%) in prior xenografts and the diagnostic tumor sample (Fig. S9 and Table S11). Of these, 15 non-synonymous SNVs were only detected in one of the two 4° recipients, suggesting that they are newly acquired SNVs. These newly detected SNVs were present at a frequency of <15% in any recipient and never presented as the predominant tumor clone. In summary, these data are consistent with selection of a CRC clone from the diagnostic tumor sample that survives and contributes to tumor growth over consecutive transplants and, while some new mutations are gained over the course of several transplantations, it largely recapitulates the exome of the diagnostic sample.

As a fourth independent assessment of the stability of xenograft tumor propagation and the relationship between xenograft and primary tumor, we carried out passenger methylation pattern analysis that serves as an epigenetic molecular clock to assess divisional history (*40*). This approach was applied to determine whether serial xenografting perturbs tumor cell population diversity. Passenger DNA methylation patterns were analyzed at several CpG rich regions (*40*). For the two

analyzed samples (CT38 and CT54), high levels of methylation pattern diversity were found in the patient tumors that were largely maintained across all passages in their xenografts (Fig. S10), indicating that population diversity was maintained with xenograft age. Together with the findings that tumor phenotype and growth are maintained with each transplant, these genomic data provide strong evidence that the xenograft model allows for sequential propagation of CRC cell clones that are representative of the tumor cell population within primary human CRC tissue.

Detailed copy number alteration analysis of CRC tumors through serial xenotransplantation

To determine whether repeated rounds of *in vivo* tumor expansion in xenograft assays select for particular genetic CRC clones, we performed high-resolution genome wide DNA copy number profiling of tumor cells prior to transplant and the corresponding xenografts using single nucleotide polymorphism (SNP) arrays. We analyzed three biological samples and for each we profiled two to four recipients at several *in vivo* passages, encompassing up to 400 days of tumor growth and 24 tumor recipients in total (Fig. 1B). The major genetic copy number aberrations (CNAs) displayed in patient samples prior to injection were recapitulated in the corresponding 1° recipients (Fig. 1B). In sample CT38, loss of a 63-Mb region on chromosome 5 (5p15.2 – 5q13.3) and gain of chromosome 20 were seen both in the patient tumor sample and all three 1° recipients (Fig. S6A,B). Likewise, in sample CT59, both the patient sample and all four 1° recipients harbored losses of a 2-Mb and 4-Mb region on chromosome 1 (1p13.2 – 1p13.1 and 1p13.1 – 1p12), as well as a gain of a 39-Mb region on chromosome 1 (1q32.2 – 1q44) (Fig. S7). We did not detect any CNAs in the third patient sample (CT54) and no new genetic aberrations were detected in the tumors of its corresponding 1° recipients (Fig. 1B). Overall, major CNAs that were detected in the patient samples were recapitulated across all 1° recipients.

Paired CNA analysis revealed several novel aberrations amongst recipients after transplant. For sample CT38, we detected two CNAs, a 31-kb deletion on chromosome 12 (12p13.1) and a 42-Mb deletion spanning chromosome 18 (18q22.3 – 18q12.1), which were detected in all 1° recipients, but were below the detection limit in the patient sample (Fig. S6C,D, Table S4). For sample CT59, we detected eleven CNAs in the 1° xenografts using paired copy number analysis, including 225-kb and 303-kb deletions on chromosome 1 (1p35.1 and 1q31.1, respectively) and a 50-Mb deletion on chromosome 2 (2p25.3 – 2p16.3), which were below the detection limit in the patient sample, but were observed in all four 1° recipients (Fig. S7). 7-Mb, 124-kb, and 568-kb deletions on chromosome 6 (6p25.3, 6p22.3, and 6q24.3, respectively) were detected at low levels in the patient, but further loss was evident across all 1° recipients. In addition, a 1-Mb loss on chromosome 16 (16q22.1) and a 2-Mb loss on chromosome 18 (18q21.31 – 18q21.32) were below the detection limit in the patient sample, but were observed in all four 1° recipients (Fig. S7). Likewise, all 1° xenografts generated by CT59 primary tumor cells contained a 561-kb gain on chromosome 2 (2q33.1), a 70-Mb gain on chromosome 7 (7q21.13 – 7q36.3) and a 5-Mb gain on chromosome 17 (17p13.3), which were below the detection limit in the patient sample (Fig. S7). In the third sample (CT54), we detected no CNAs that were specific to the xenograft. The detection of identical CNAs in multiple xenograft recipient mice indicates outgrowth of a clone from the primary patient sample, rather than *de novo* generation of variants due to xenotransplantation, which would be a random process where each mouse would be different.

Next, we sought to determine whether the clonal outgrowth we detected in 1° xenografts would be propagated upon several rounds of transplantation. In the three samples we tested, the CNA profile of 2° xenografts closely matched the CNAs detected in 1° recipients (Fig. 1B). In sample CT59, a 296-kb gain on chromosome 2 (2p16.3) was dominant in both 2° recipients, but was below the detection limit in the patient sample and 1° recipients (Fig. S7). Comparing the

CNAs of 4° recipients from CT38, which have undergone several rounds of expansion, demonstrated a complete recapitulation of all aberrations detected in 1° and 2° xenografts (Fig. 1B, Fig. S6). Thus, we observed maintenance of genetic clones in our serial xenografts over time. Our data indicate that xenografting CRC specimens allows for expansion of a genetic clone present in the patient tumor.

CRC tumor population heterogeneity through serial xenotransplantation

The SNP CNA and LV studies illustrate tumor propagation heterogeneity between individual cells with similar genetic background. However, this propagation heterogeneity may not reflect the tumor cell dynamics in a primary tumor if xenotransplantation selects for subpopulations of tumor cells more adapted to the mouse microenvironment. We used passenger methylation patterns at "epigenetic molecular clocks" (*43*) to detect potential population bottlenecks caused by xenotransplantation. Previous studies demonstrated that passenger methylation patterns become homogeneous after single cell cloning and xenotransplantation (*40*), indicating the ability to detect severe population bottlenecks. Passenger methylation patterns were analyzed at multiple loci (8 to 14 CpG sites per locus). Polymorphic SNPs were used to distinguish between maternal and paternal patterns for the autosomal loci ABHD8 and ZNF471, and the X-chromosome BRS locus in the female patient with CT54.

To allow comparisons between the primary tumor and its xenografts, multiple small 1-2 mm^2 tumor regions were microdissected from stained microscopic sections (1 to 6 regions per tumor) using laser capture microscopy. Methylation patterns were read with bisulfite sequencing of clone PCR products. Heterogeneity within these small tumor areas is measured by sampling between 6 to 8 epialleles per microdissected region and then counting the numbers of unique

patterns or tags and calculating the pairwise distance (PWD) between the tags. Greater heterogeneity is indicated by more unique tags and greater PWDs.

Tumor heterogeneity appeared to be maintained after xenotransplantation because methylation pattern diversity was not consistently different between the primary cancers (CT38 and CT54) and their xenografts (Fig. S10). There was a trend for increased diversity in the xenografts compared to their primary tumors, with significantly higher xenograft PWDs and unique tags for the BRS locus for CT54, and significantly higher xenograft PWDs for the LOC locus for CT38 (two-tail t-test, $p < 0.05$). Diversity in the first xenografts after transplantation was not significantly different from their primary tumors except at one locus (ABH for CT38). Overall the passenger methylation pattern analysis provides evidence that the population diversity in the primary tumors is maintained or increases after xenotransplantation.

Passenger methylation pattern diversity can also measure potential reductions in tumor cell population diversity caused by chemotherapy. The CT38 oxaliplatin treated xenografts had lower PWDs (0.97 versus 1.25) and significantly lower unique tags (2.4 versus 3.1) compared to their same aged untreated xenografts. No differences in diversity were observed for untreated and oxaliplatin treated CT54 xenografts (Fig. S10). These findings are consistent with little or minor reductions in tumor cell diversity and the lack of a severe population bottleneck induced by oxaliplatin treatment, consistent with the no apparent change in the absolute number of LV marked clones in the oxaliplatin treated xenografts.

Reproducible patterns of CRC cell outcomes

To obtain a measure of the clonal distribution over time, the proportion of each LV clone type was determined for every xenograft by normalizing for differential inter-sample marking efficiency and averaging between all recipients at a given passage (Fig. 2D). Type I, Type II, and

Type III behaviors were seen in 7, 8, and 9 of 10 samples, respectively; 4 of 10 samples had all three types. Type IV and Type V clones with variable proliferative activity appeared in early as well as late passages and were detected in 8 and 4 samples, respectively. Importantly, all samples contained functionally distinct cells. In some cases, our classification is limited by experimental design (Fig. 2C). For example, sample CT19 was transplanted only twice due to long latency (546 days, Fig. 1A) precluding the ability to define Type II and Type V behavior, which requires a minimum of three passages. Likewise, the long-term Type I behaviors classified in 2° xenografts for sample CT19 may not persist through as many transplants as Type I clones in CT54, which were evident in six consecutive transplants. Despite the reduced number of overall passages for some samples, the total time of lineage tracking was invariably more than 250 days. Of note, transplanting LV clones, which were previously minor, into multiple parallel recipients and finding them to dominate across all mice (Fig. S11), supports the notion that this behavior is stable and not random. Collectively, each LV clone type was identified in four or more patient samples, establishing that the varied clonal behaviors are reproducibly found in primary CRC.

We determined the cumulative numbers of each LV clonal behavior across all experiments. Type I, II, III, and IV clones each accounted for ~22% of marked clones, while Type V intermittently proliferating clones were the least frequently observed (12%) (Fig. 2B). These findings indicate that colorectal tumors contain a heterogeneous pool of functionally distinct CRC cells that vary in their longetivity and proliferative kinetics despite sharing similar genomic profiles.

Patterns of clonal growth

Variation in clonal behaviors could be stochastic or they could reflect specific classes of CRC cells that function in a predictable deterministic fashion. If the process is stochastic then the probability of any LV clone contributing at any transplant will be reflected in its relative

distribution in the previous donor tumor; abundant LV clones have a higher probability of persisting than less abundant clones. By contrast, the emergence of dominant LV clones from minor or undetected LV clones would be a low probability event, especially simultaneously within multiple recipients at a given transplant. Examination of clonal output as measured in parallel recipients at each passage did not support the stochastic model. For example, a Type I clone that dominated tumor growth in later transplants of sample CT54 (upper arrowhead, Fig. S11A) was not abundant in each of the 1°, 2° or 3° recipients that were selected for further transplantation (upper arrowheads, Fig. S11A). Indeed, the 3° xenograft is dominated by a different clone (lower arrowhead, Fig. S11A). However, upon further passage, the dominant 3° clone is strikingly surpassed by the apparently activated Type I clone (upper arrowhead) in all four 4° recipients, which then continues to dominate tumor growth in all 5° and 6° recipients. Whereas random growth dynamics would predict clonal dilution of minor marked clones over multiple transplants, the observed clone is in relatively low abundance over 3 rounds of transplantation and then, despite being a minority of injected cells, dominates all four 4° and subsequent recipients. Sample CT51 also showed unexpected distribution of LV clones upon transplantation. The 1° transplant contains several dominant LV clones (depicted by the upper arrowhead, Fig. S11B) and a minor LV clone (lower arrowhead, Fig. S11B). Upon re-transplantation into three 2° recipients only the previously minor marked clone dominated, rather than the clones that were dominant in 1° transplant (lower arrowhead, Fig. S11B). Taken together, this data is consistent with the notion that LV clones can behave in a predictable fashion.

Mathematical modeling of the clonal patterns

All the Southern blots were digitized and the relative size of the clonal populations that had been previously identified was quantified using image analysis. These relative sizes were tracked

through serial xenografts. Relative clonal population size represents a surrogate measure for clonal proliferation. Because only a fraction of the tumor is injected at every transplant, some LV clones may be lost due to dilution. To investigate this possibility we determined the fraction of observed LV clones in every consecutive transplant over the total number of marked LV clones in the experiment. The median was used as the estimator of the main parameter of the distribution. An excellent fit (R^2=0.96) was obtained when fitting the median at each transplant to an exponential curve (Fig. S12A). The exponential decline in the number of LV clones indicates that transplantation is a dominant factor in the disappearance of LV clones. Moreover, this analysis also indicated that the sensitivity of the Southern to detect clones was approximately 70% (that is, undetectable clones that appeared in subsequent xenografts). There is significant spread of data around the medians in Fig. S12A. We implemented a Monte-Carlo model to determine whether any other factors influencing clonal loss are contributing to this dispersion and to resolve whether the exponential decline can be predicted solely on the basis of two stochastic effects: (i) the loss of LV clones due to the transplantation process and (ii) the sensitivity of detection of a Southern blot. The simulation shows that as the initial number of observed LV clones goes up, a smaller dispersion is seen (Fig. S12B). The symmetry of the dispersion as well as the good reproduction of the experimental spread by the model indicates that the two stochastic processes in the model suffice to explain the observations and do not require any further assumptions to be imposed on clonal function itself. Since the Monte-Carlo model simulates the contribution of the two stochastic processes and reproduces the observations of clonal loss, any further significant stochastic influences on the clonal size/proliferation is not justified to reproduce observed data. As this is the simplest model that reproduces the data, it is also the most likely to be true. Thus, clonal loss is not due to the imposition of stochastic processes on clonal function/proliferation, which remains stable, but rather on randomness due to the transplantation process. With the knowledge that

transplantation contributes to clonal loss, to examine clonal dynamics (constant or newly emerging) and variation in clonal population size, we performed comparisons on matching sets of clones that were present in any two sequential tumor samples (e.g. 1° to 2°; 2° to 3°; 3° to 4°; etc). In tumors where no emergent LV clones (Type IV or V) are observed, the relative clonal population size of LV clones, which have been successfully transplanted, is very similar in paired samples (Fig. S12C "No Emergent"). On the contrary, we found that the presence of emergent LV clones correlates to significant variation in the LV clone proportions (Fig. S12C "Emergent"). Thus, activation of previously dormant LV clones corresponds to tumor-wide changes. Oxaliplatin treatment of the tumor also leads to large changes in LV clone proportions. Quantitative analysis of re-transplanted cells showed preservation of the tumor structure after oxaliplatin treatment (Fig. S12C "Untreated", "Treated" and "Treat/Trans"). The tumors derived from treated samples where emergent Type IV clones are selected show even higher levels of similarity. Indeed, these post-oxaliplatin treatment tumors are generally smaller (Fig. 3A) than controls supporting the notion that Type IV derived tumors may be distinct.

Collectively, this modeling and data quantification predicts that at least some of the clonal loss that distinguishes between Types I, II, and III clones may be due to stochastic processes involving the transplantation process and the sensitivity of detection. Clonal proliferation seems to be relatively constant and not influenced by stochastic processes. Nevertheless, the data suggests that active clones are distinct from the dormant LV clones (Type IV or V). Thus, the interpretation that the five experimental categories that depict our results actually represent five distinct classes remains uncertain. However, the data and the modeling clearly support the conclusion that there are at least two functionally distinct classes (constant and dormant/emergent). Moreover, oxaliplatin treatment differentially affects LV clones and thereby alters the tumor structure. We would like to raise a few final thoughts on interpreting the modeling of clonal behavior. When the first lineage

tracing studies were performed on murine repopulating hematopoietic stem cells by us and other groups in 1985, very similar data was obtained showing long-term and short-term repopulating cells (*44-46*). If the same modeling had been applied, it would have predicted that the repopulating pool was relatively uniform and the differences in short-term and long-term may be due to stochastic processes. However, in the last 5 to 8 years a series of new cell surface markers were developed that enabled prospective isolation of each class thereby proving the existence of distinct classes of long-term and short-term hematopoietic stem cells. Stochastic models of stem cell function cannot be proven, but only disproven (*47, 48*). Thus, we are cautious about extrapolating too much functional meaning to the modeling at this stage, especially as very limited cell surface markers are available to purify initiating cells from colon or any other solid tumor.

Absence of major genetic changes between untreated and oxaliplatin treated tumors

To determine whether the altered clonal patterns after oxaliplatin treatment were due to major changes in genetic subclones, DNA of xenografts from control and oxaliplatin treated groups was profiled by genome-wide CNA analysis. New DNA copy number changes were not detected in the oxaliplatin-treated tumors as compared to control tumors and the CNAs between the two groups were congruent (Fig. 3F, Fig. S6). In addition, SNVs was analyzed following oxaliplatin treatment through targeted deep sequencing. For CT38, the frequency of the somatically acquired SNV in *RET* remained stable following oxaliplatin treatment (Ctrl: 73.8±4.7%; OX: 75.1±2.4; Fig. 3G, Table S5). Likewise, for CT54, the eight somatically acquired SNVs were present at similar allele frequencies across control and oxaliplatin-derived tumors (Fig. 3G, Table S6), indicating that oxaliplatin treatment did not select for a distinct genetic subclone. Importantly, out of the 660 analyzed SNVs, no new SNVs were acquired in the oxaliplatin-treated tumors. In keeping with this similar genetic profile, passenger DNA methylation pattern analysis indicated that tumor cell

population diversity was maintained between untreated and oxaliplatin treated tumors (Fig. S10). The absence of a detectable bottleneck or selection for novel genetic clones after chemotherapy treatment provides strong support for the existence of intrinsic mechanisms, within a genetic lineage, that link variable clonal growth kinetics and tumor propagation behavior with therapeutic tolerance.

Caveats associated with the xenograft tumor environment

Xenografting human cells in immunodeficient mice can introduce selection pressures due to the lack of features of the human tumor microenvironment. In some cases, aspects of the microenvironment are provided by implantation into an orthotopic site, while in other tumor models features of the microenvironment are provided by using non-dissociated tumor fragments. The published literature for CRC mainly cites orthotopic models that are either developed using (i) whole pieces of CRC tissue, which are not dissociated into single cell suspensions, but are sutured to the cecal wall, or (ii) injection of cell suspensions from commercially available CRC cell lines but not primary CRC into the cecal wall or other sites including subcutaneous. However, to our knowledge, reports where orthotopic engraftment with single dissociated primary CRC cells is reliably achieved are rare. In our total experience, we have transplanted 143 primary and metastatic tumors that represent the entire spectrum of CRC subtypes under the renal capsule; 130 of these samples yielded tumors. Thus, our overall success rate is 91% for the renal capsule method. In our early development of this model we attempted to transplant liver metastases into the liver of immune deficient mice and primary CRC into the cecum (Table S2). Although sporadic cases would initiate tumors from orthotopic sites, none of these orthotopic sites yielded the highly robust success rate of the renal capsule. Thus, the renal capsule is the only single cell derived model that permits the experimental design our study requires. While no xenograft method is perfect, the renal

capsule xenograft model is arguably the most accurate reflection of human CRC that can be achieved to date in an experimental setting.

The design of our study resulted in a degree of selection. For example, the whole tumor that is resected from a patient is not taken entirely for xenografting, but rather a small piece is used for xenografting. Likewise, some cells are lost during dissociation and transduction and the xenograft environment will also exert pressures on the cells. Our CNA analysis revealed small changes between the primary sample and the first set of xenografts in some samples. However each of the subsequent rounds of xenografts are each highly similar to the primary xenograft. The key message of our manuscript is that there is significant variation in the tumor repopulation function of individual CRC cells within a single sample as detected across multiple xenografts. This large-scale functional variation is not due to large-scale changes in CNAs and mutational hotspots as assessed by targeted sequencing. The passenger methylation analysis further supports this finding. Thus, the potential presence of selective forces that permit the outgrowth of only some of the genetically diverse subclones that must be present in the donor sample (because multiple primary xenografts all have the same clone) does not alter the main conclusion of our work that comes from comparing the xenografts to each other, where the genomic data indicates strong concordance.

Selection pressures during xenograft formation

There is a widely accepted dogma in cancer research that clonal dynamics, and ultimately tumor evolution and response to therapy, are driven by the acquisition of new mutations. Our work points to an additional layer of complexity that needs to be considered. We find that within a population of CRC cells, the individual tumor cells exhibit highly variable functional repopulation properties. There are two interpretations of this result: each of the different LV clonal behaviors is due to the outgrowth of specific and unique genetic subclones; or these highly variable functional

properties that are observed across serial xenografts occur without major changes in the genetic identity. Three independent methods applied to the serial xenografts came to the same conclusion that genetic clones remained stable over serial transplantation. Our interpretation of this result is that the functional differences are not linked to known subclonal genetic properties. This conclusion is not dependent on whether the first set of xenografts is genomically identical to the donor sample or whether there are differences reflective of the outgrowth of subclones. The outgrowth of only a subset of the clones that are present in the donor sample could be due to sampling bottlenecks: only a small portion of the tumor is given to us following surgical resection from the patient, tumor cell dissociation and lentivector transduction might lead to some cell loss, and the xenografting process may exert selective forces. We know the outgrowth in the first xenograft must represent an outgrowth of a genetic subclone present in the donor sample rather than a stochastic tumor progression event because multiple recipients all contain the same subclone. Thus, our main conclusion of non-genetically driven functional variation is valid for those genetically diverse subclones that are present in the donor sample. We are careful in universalizing our conclusions as we cannot conclude it will be true for every subclone present nor for those subclones that were not or could not be xenografted.

In addition, our data is strongly indicative of the existence of genetically diverse subclones in human CRC. CNA analysis of diagnostic samples compared to 1° xenografts showed that the majority of CNAs detected in the diagnostic sample prior to injection were recapitulated in all corresponding 1° recipients. For CT38 and CT59 an outgrowth of a minor genetic clone had occurred since several novel aberrations, which were below the detection threshold of the SNP arrays in the patient tumor, were detected in multiple corresponding 1° recipients. It is generally accepted that tumors comprise multiple genetic clones and we selected one genetic lineage in the xenograft that was faithfully recapitulated across all subsequent passages. This result is confirmed

in the genomic analysis of single cell derived populations shown in Fig. S14. This was an important finding as it strengthened our conclusion that the functionally distinct LV clones were all part of one genetic lineage once the xenograft was established.

An alternative explanation for the presence of CNAs in 1° xenografts, which were not detected in the matching diagnostic sample, is that they were below the detection limit in the diagnostic sample because of contaminating non-tumor cells. A piece of flash-frozen tissue from the diagnostic tumor was used to extract DNA for CNA analysis, which could have included a mixture of stromal cells, normal epithelial cells, and/or blood cells. However, only tumor cells generate xenografts and this may have been captured by the CNA analysis, where a higher percentage of tumor cells in the xenograft would have enabled detection of CNAs that were previously masked in the diagnostic sample. We find this across several CNAs where the CNA $\log_2$ ratio segment intensity increases across 1° xenografts as compared to the diagnostic sample. This can serve as an alternate explanation for the detection of several CNAs in 1° recipients that were not detected in the diagnostic sample.

Even though tumor sampling or the xenografting process can exert selective pressures during initial xenograft growth leading to the outgrowth of subclones, we believe that the xenografted tumor is still relevant and important. Several reports support the relevance of clones growing out in xenografts, supporting the validity of using xenografts to study human cancer and supporting the interpretations of our results, namely that for some patient samples clones from the primary tumor, which was below the detection limit of CNA analysis, were captured in the xenografts. Thus, we conclude that the genetic clone that grows out in the 1° xenografts is a subclone from the patient tumor at the time of resection and, importantly, the clone is stable upon further passages. This enabled us to identify functional heterogeneity within genetically similar lineages.

The limited sampling of the primary tumor and subsequent xenografting discussed above will generate a population bottleneck. Such restriction will result in more limited diversity of the subsequent rounds of population expansion as occurs during serial xenografting. This principle fits well with our experimental results showing overall stability of the genetic clones within serial xenografts. Moreover, the diversity as measured by divisional history through passenger DNA methylation patterns at several CpG rich regions within the processed and transduced donor sample (a limited sampling of the entire tumor) was largely retained between xenografts. While this method may not be sensitive enough to detect all selective pressures that the xenograft environment exerts, it certainly has the capacity to detect severe bottlenecks due to clonal dominance by single cells. It has been reported that xenografts initiated by a single cell have significantly less methylation pattern diversity than xenografts initiated by many cells from the same cell line (*40, 43*). In our system, we do not find evidence for such a severe bottleneck during initial xenografting or subsequent transplantation, supporting the stability of the xenograft model. This is an important consideration because during clonal evolution, it is expected that a single cell that has gained a selective advantage would outgrow other cells and dominate the tumor and we should be able to detect such a clonal evolution event with the methylation pattern analysis. We do not find changes in methylation pattern diversity during xenograft initiation and over serial xenografts. Thus, the marked functional variation in repopulation was not linked to a severe population bottleneck during xenografting which might have occurred if, for instance, one genetic driver mutation is responsible for a long term Type I clone but not for any other LV clonal behavior.

Stability of the xenografts

Individual CRC cells from MSI-H tumors are genetically unstable and likely continue to accumulate mutations during xenografting. However, novel mutations in one cell within a tumor

cannot be easily detected unless the cell clonally expands to produce many progeny that carry the new mutation. The lack of detectable genomic changes we observe over time does not necessarily imply that instability does not exist. Rather, the three methods we used including population analysis using passenger DNA methylation analysis imply that no new genomic changes are detected because there is no strong selection for cells with mutations that drive clonal dominance. It is intriguing that we see functional variability in LV clones, but do not see associated changes in known driver gene mutations, indicating that cells exhibit functional diversity that is not necessarily driven by genetic diversity.

The most difficult issue in the study of MSI-H tumors is whether the mutations are neutral or background mutations, which do not influence the function of LV clones that we measured over serial transplants or whether they are significantly influencing growth of LV clones. Because MSI-H tumors have a high basal level of mutation rates, there is increased probability that with every cell division the newly acquired mutation will result in a new cell that has changed growth dynamics. However, until the genome of each new cell is sequenced it is difficult to draw conclusions about whether the mutations that MSI-H tumors have accumulated are affecting cellular behavior, including growth of LV marked clones. Even if the entire genome were sequenced, it would be difficult to have confidence in separating passenger versus driver mutations. Other parameters need to be assessed, such as histology and growth rates. We found that MSI-H tumors recapitulate the histological appearance of the parent tumor over several serial transplantations and do not exhibit increased aggressiveness in terms of time to tumor formation, or show any other alterations in growth that we could detect. We chose to sequence validated mutations, which have been previously implicated to influence tumor progression across a spectrum of human cancers, through targeted deep sequencing (~1300x) in order to directly gain insight into mutations that have known associations with affecting cell growth. This method allowed us to

examine the relevance of a mutation that occurred in a tumor and enabled us to pick up low-level mutations in many known oncogenes and tumor suppressor genes. However, out of 600 analyzed mutational hotspots (in 71 kb, containing 5,271 known single nucleotide variants (*36*)), we see little evidence that MSI-H tumors have accumulated mutations in driver genes over serial xenografting. In addition, sequencing driver mutations in tumors derived by two different single-cell derived LV clones from a MSI-H tumor (Fig. S14) supports the conclusion that the functional differences in LV clonal behaviors are not driven by these specific underlying driver mutations. Although we have sequenced the exomes of CT38 and its corresponding xenografts, our analysis does not include whole genome sequencing, leaving open the possibility that an unknown DNA mutation could explain the diverse clonal behavior. However, our population studies do not support the existence of such a bottleneck. Thus, while MSI-H tumors are genetically unstable, this instability does not necessarily translate to changes in important driver genes, which we have confirmed through targeted deep sequencing, showing that a large collection of frequently mutated genes were not changed.

Cancer-initiating cells in CRC

CRC harbors cancer stem cells, which are detected using xenotransplantation assays and are operationally termed cancer-initiating cells (C-ICs) to denote their functional definition. To date eight independent scientific groups have prospectively purified C-ICs in over 90 different CRC specimens (*49-55*). Although no universal cell markers have been identified to enrich for C-ICs across all samples, combinations of markers applied to individual samples demonstrate that most colorectal tumors are organized hierarchically, with C-ICs driving tumor growth. C-ICs are characterized by their unique ability to self-renew as measured by serial tumor initiation assays. Thus, sequential rounds of xenotransplantation effectively record the output of C-ICs when

performed clonally using limiting dilution assays, even when tumor cells are injected without prior phenotypic fractionation of C-ICs. This *in vivo* experimental model then serves as a tool to measure the defining qualities of C-ICs. Since we used serial xenograft transplantation in our assays to follow the output of single marked CRC cells, we essentially assayed the key properties attributed to C-ICs. Therefore, our experimental data reveals that C-ICs in primary human CRC are not functionally homogeneous. However, we remain cautious in extrapolating our claims to the existence of discrete functional C-IC classes within a C-IC compartment, since CSC cell surface marker expression is variable amongst individual samples (*56*), and no methods are known that would prospectively purify such putative C-IC classes at this time. Future studies need to focus on markers and mechanisms to determine the basis of CRC cell heterogeneity.

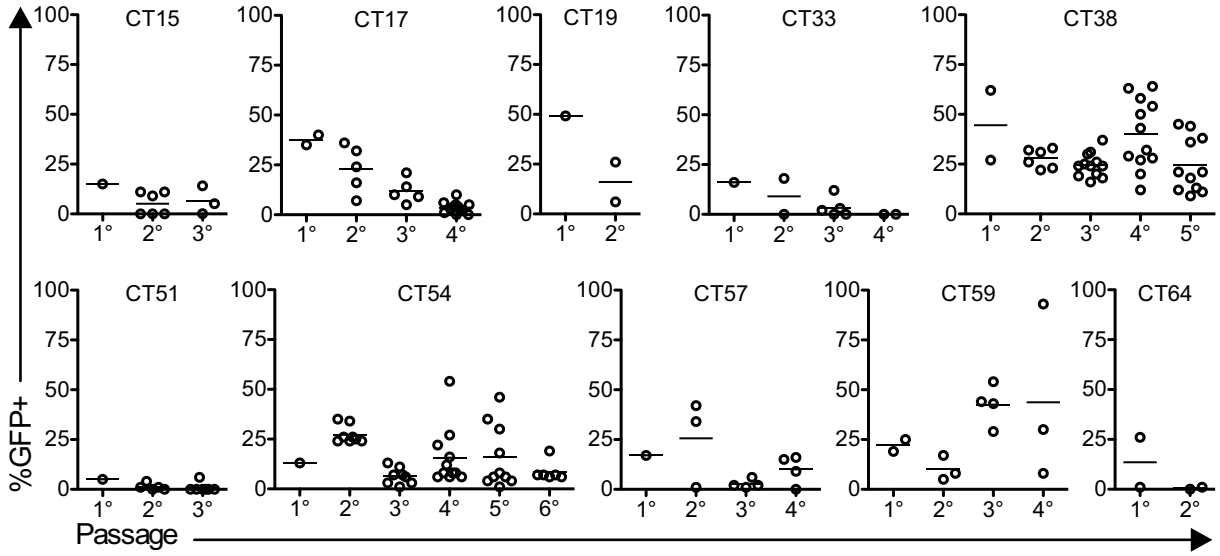

Fig. S1. Transduced CRC cells generate xenografts that maintain GFP expression.

Diagnostic tumor samples were transduced with a lentiviral vector encoding GFP and $5x10^4$ to $2x10^5$ viable cells were transplanted into immunodeficient mice. Once tumors formed (1°), an equal number of cells were transplanted into the next passage. Marked cells were assessed by flow cytometry for GFP expression. Each circle represents the percentage of GFP-expressing tumor cells from one recipient and horizontal lines indicate median GFP expression.

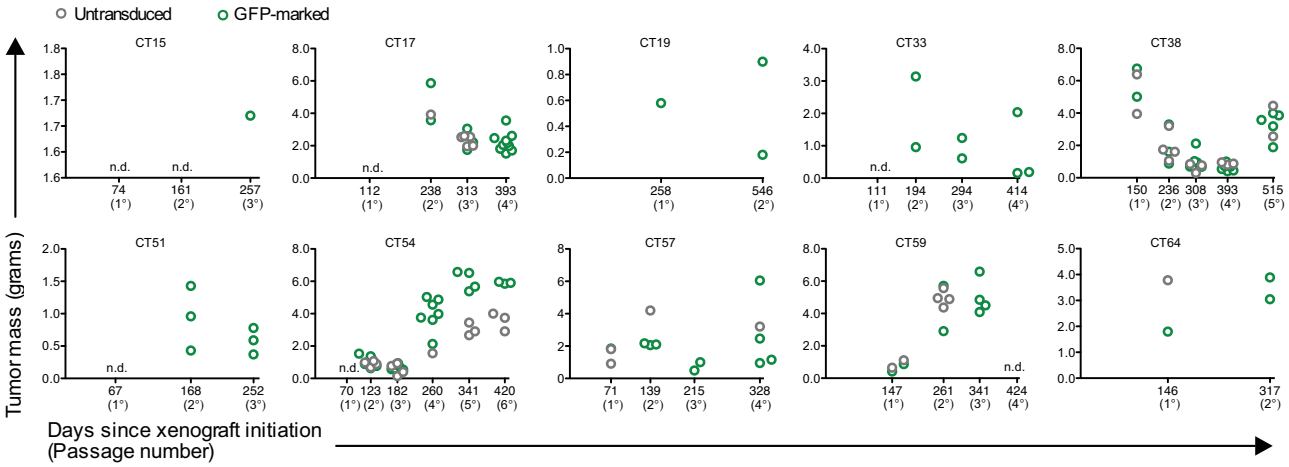

Fig. S2. Comparison of tumor weights generated by transduced and untransduced CRC cells. Following primary tumor tissue dissociation and single cell suspension generation, cells were either (i) directly injected into immunodeficient mice without exposure to lentivirus (grey circles) or (ii) marked with a lentivirus and then injected to generate tumors (green circles). When animals reached endpoint, or a tumor mass was readily palpable in the renal capsule, mice were sacrificed, the tumor removed and weighed to generate the tumor mass measurements on the y-axis. Transduced and untransduced tumors were serially transplanted in parallel as indicated on the x-axis.

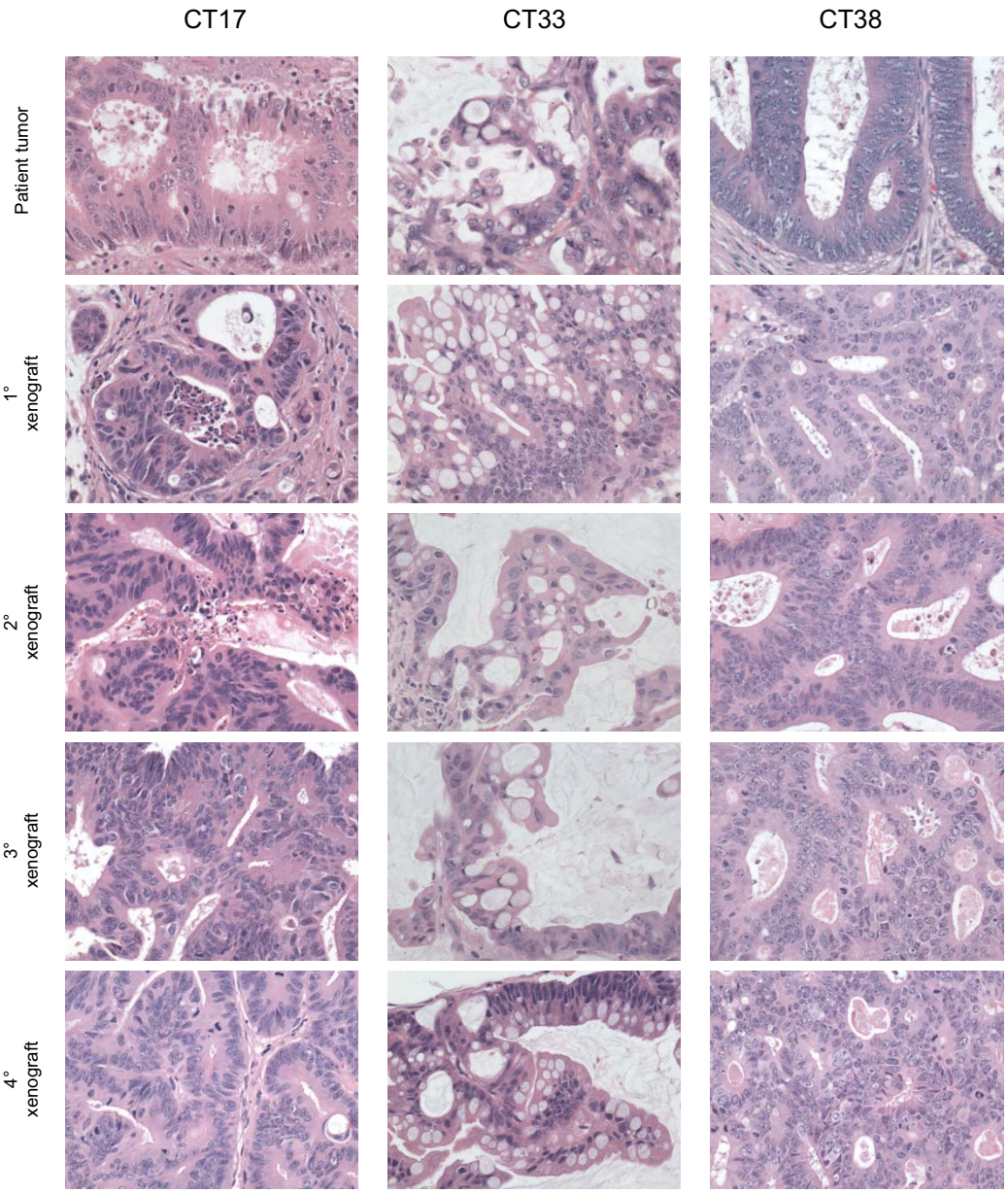

Fig. S3. Morphology of xenografted tumors and corresponding patient tumor samples.

Representative haematoxylin and eosin images of samples CT17, CT33, and CT38. For each image, at least 3 slides were analyzed for each tumor and generally 2-4 tumors were stained for the H&E analysis.

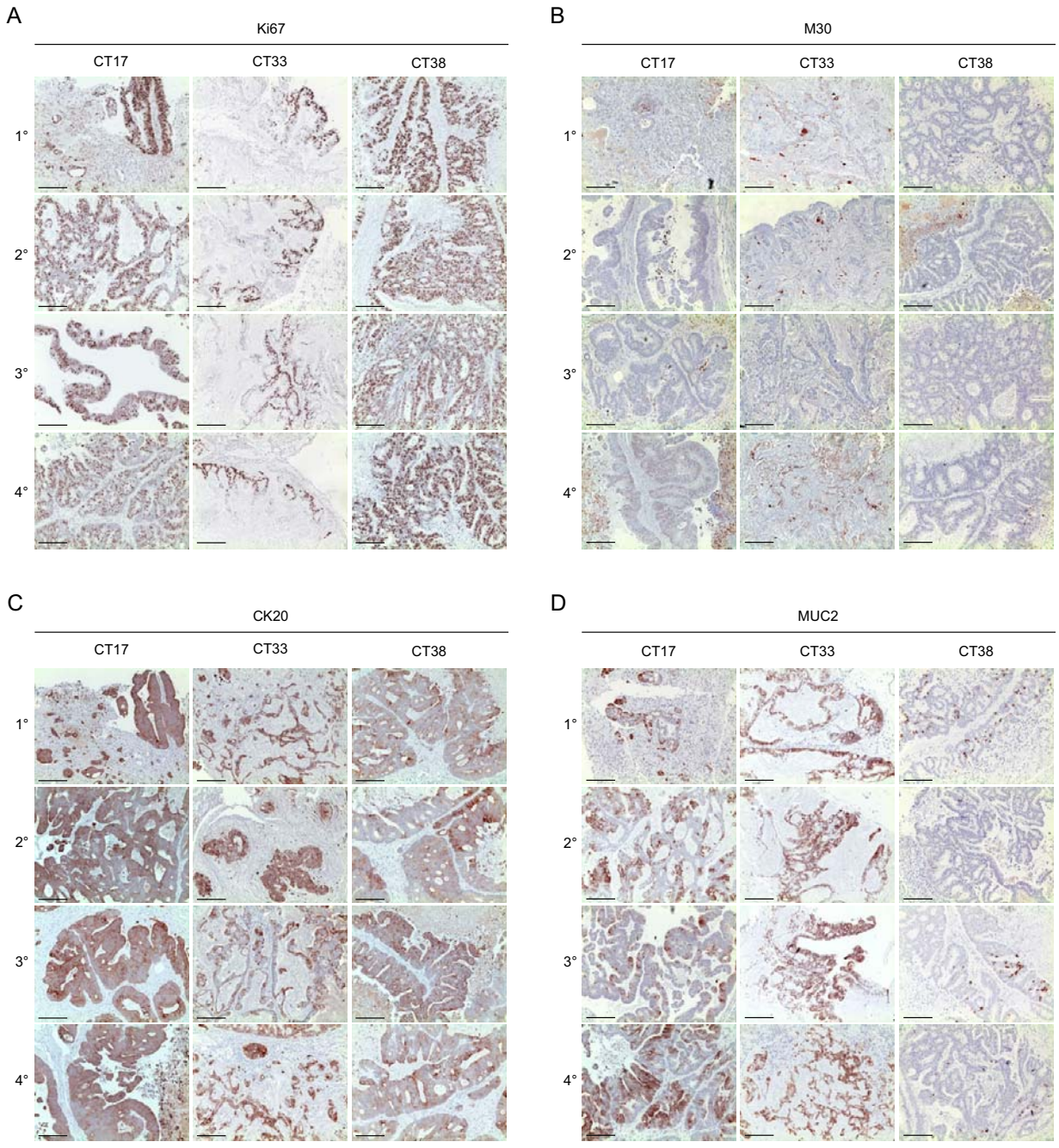

Fig. S4. Marker expression of xenografted tumors.

Representative images show expression of proliferation marker Ki67 (**A**), epithelial-specific cell death marker M30 (**B**), and differentiation markers CK20 (**C**) and MUC2 (**D**). Scale bar indicates 200 μm. For each image, at least 3 slides were analyzed for each tumor and generally 2-4 tumors were stained for each analysis.

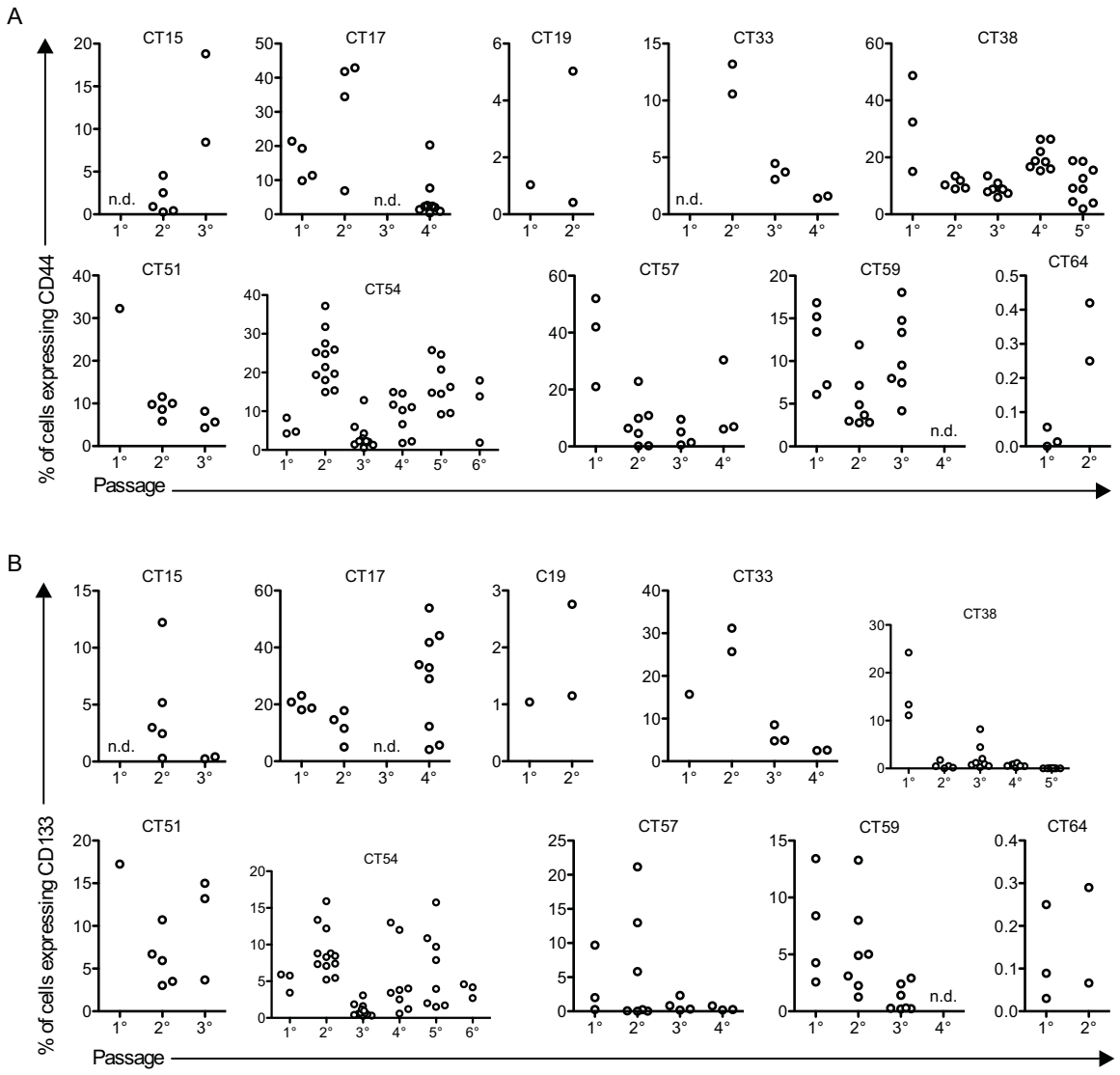

Fig. S5. CD44 and CD133 expression in xenografted tumors.

Following single cell suspension generation, cells were stained with antibodies to CD44 and CD133 and marker expression was analyzed using flow cytometry. Each circle represents data of one tumor that was generated by injecting CRC cells into parallel recipients.

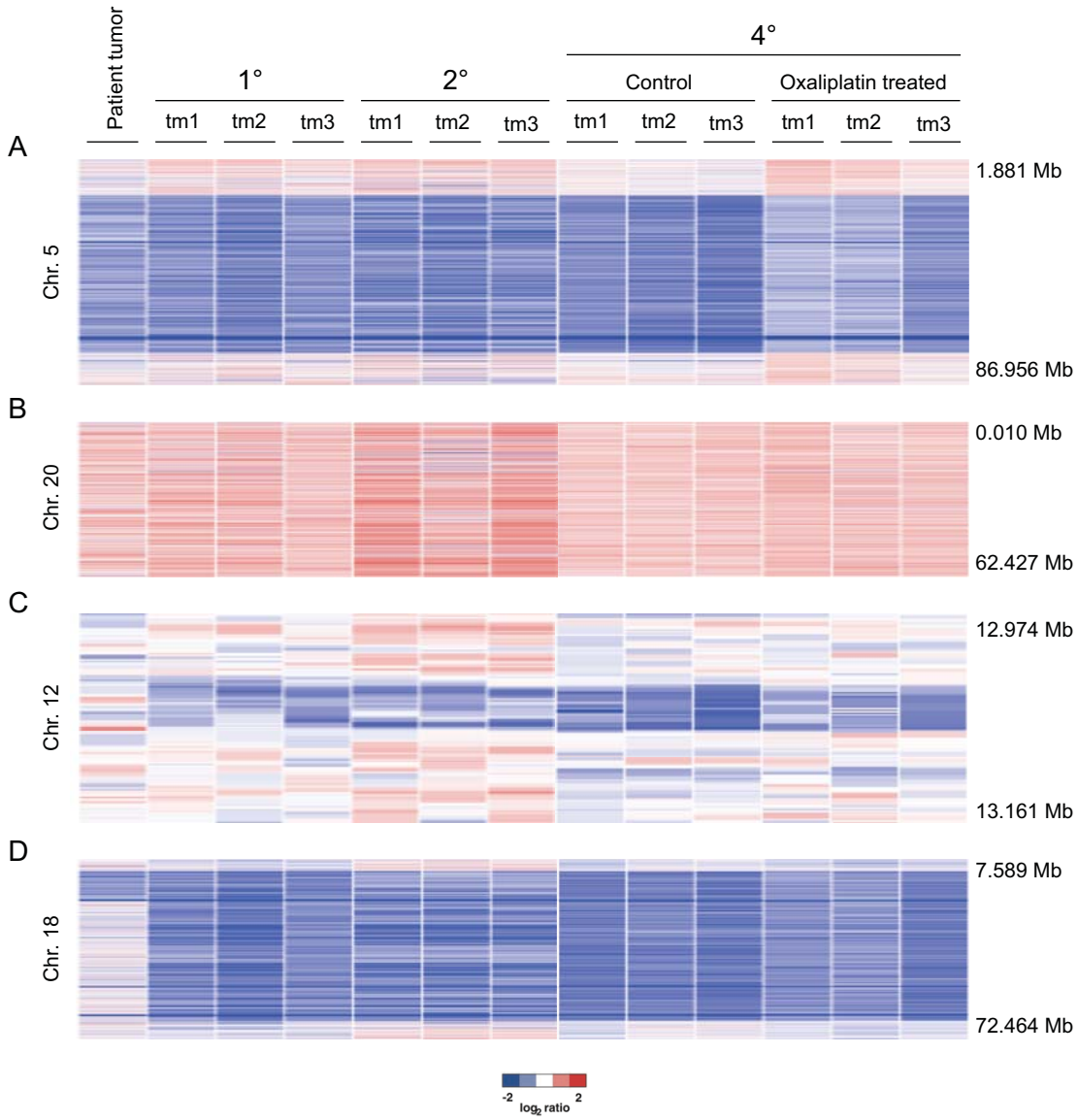

Fig. S6. Paired copy number alteration analysis in colon cancer sample CT38 and the matching xenografts.

Copy number heat maps showing gains and losses in the patient sample and the corresponding 1°, 2°, and 4° (both control and previously oxaliplatin treated) xenografts. Log_2 ratio copy number data is shown (median smoothing format; blue, deletion; white, normal; red, gain). Each lane contains the data for one tumor. Data is not normalized for copy number changes and tumor cellularity, although generally >80% of cells are estimated to be tumor cells.

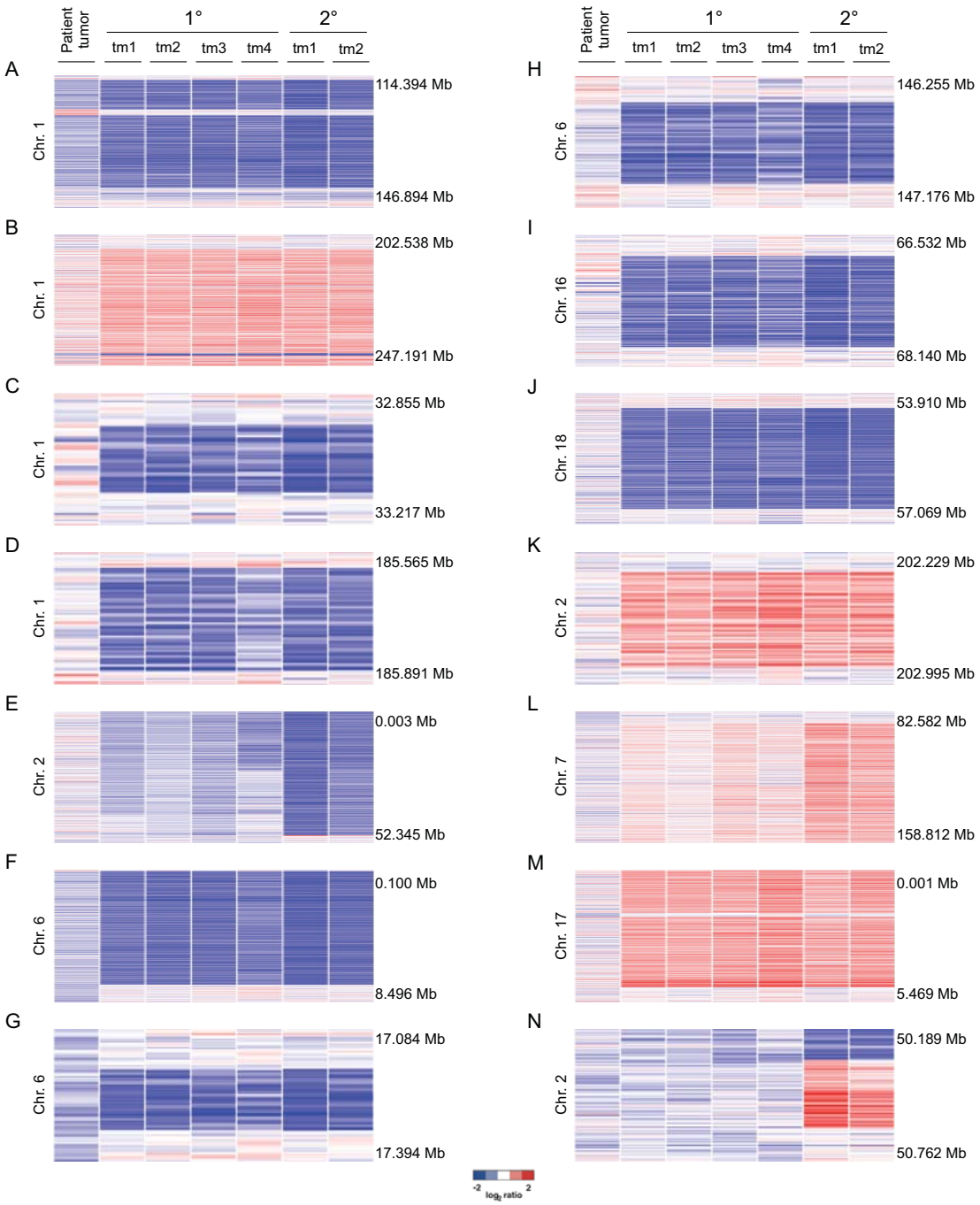

Fig. S7. Paired CNA analysis in colon cancer sample CT59 and the matching xenografts.

Copy number heat maps showing gains and losses in the patient sample and the corresponding 1° and 2° xenografts. Log_2 ratio copy number data is shown (median smoothing format; blue, deletion; white, normal; red, gain). Each lane contains the data for one tumor. Data is not normalized for copy number changes and tumor cellularity, although generally >80% of cells are estimated to be tumor cells.

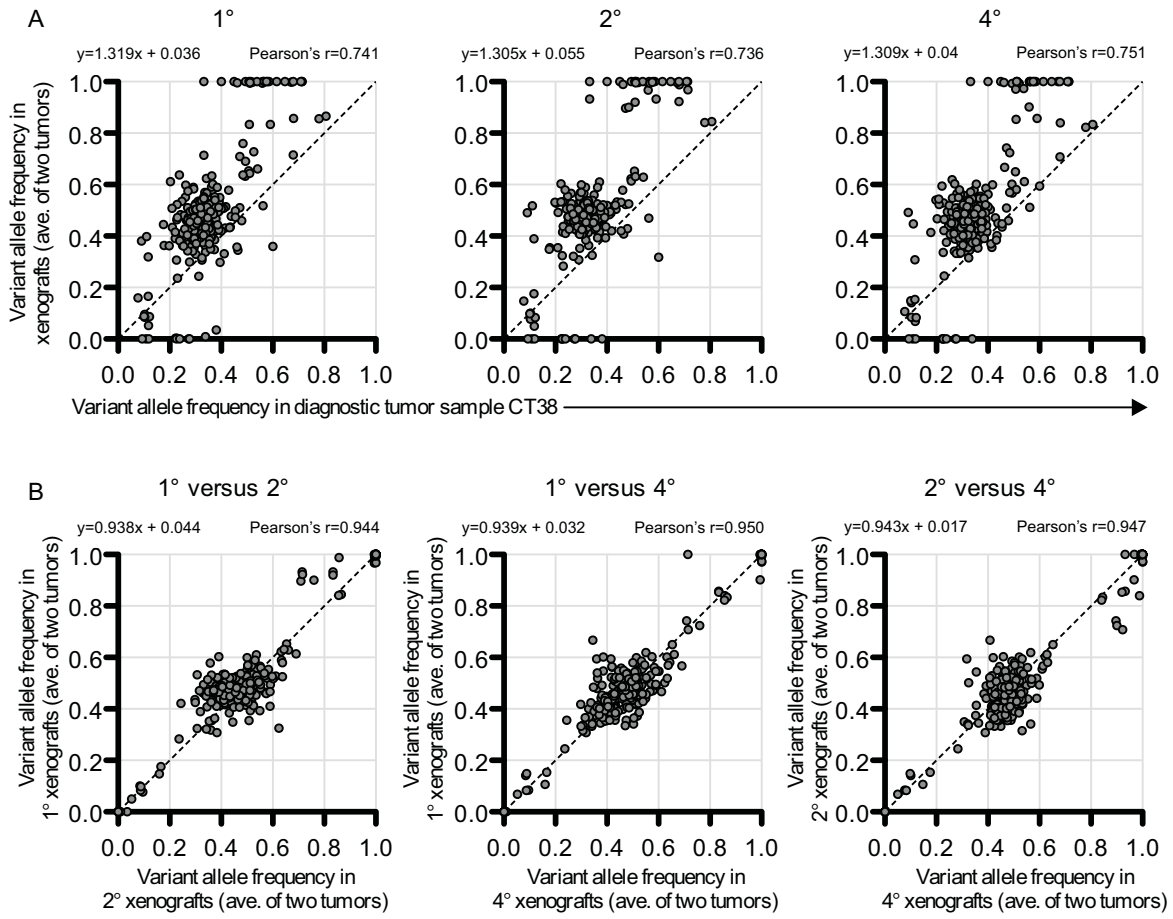

Fig. S8. Exome sequencing of CT38 diagnostic sample and matching xenografts.

Tumor cells from diagnostic sample CT38 were transplanted into two 1° recipient mice. A tumor from one of these recipient mice was used for further transplantation into two 2° recipients. This process was repeated up to 4° transplantation. DNA from diagnostic tumor sample, its matching mucosa, and two xenografts from 1°, 2°, and 4° passages was profiled using exome sequencing to an average depth of 278X. (A) Somatic SNV frequencies are shown for the diagnostic sample (x-axis) and xenografts (y-axis). The SNV frequency for each passage is the average SNV frequency between the two sequenced tumors of a particular transplant. (B) Somatic SNV frequencies as determined by comparing the average SNV frequency of 1° to 2° xenografts, 1 to 4° xenografts, and 2° to 4° xenografts. The SNV frequency for each transplant was generated by averaging the frequency of two recipients for each particular transplant.

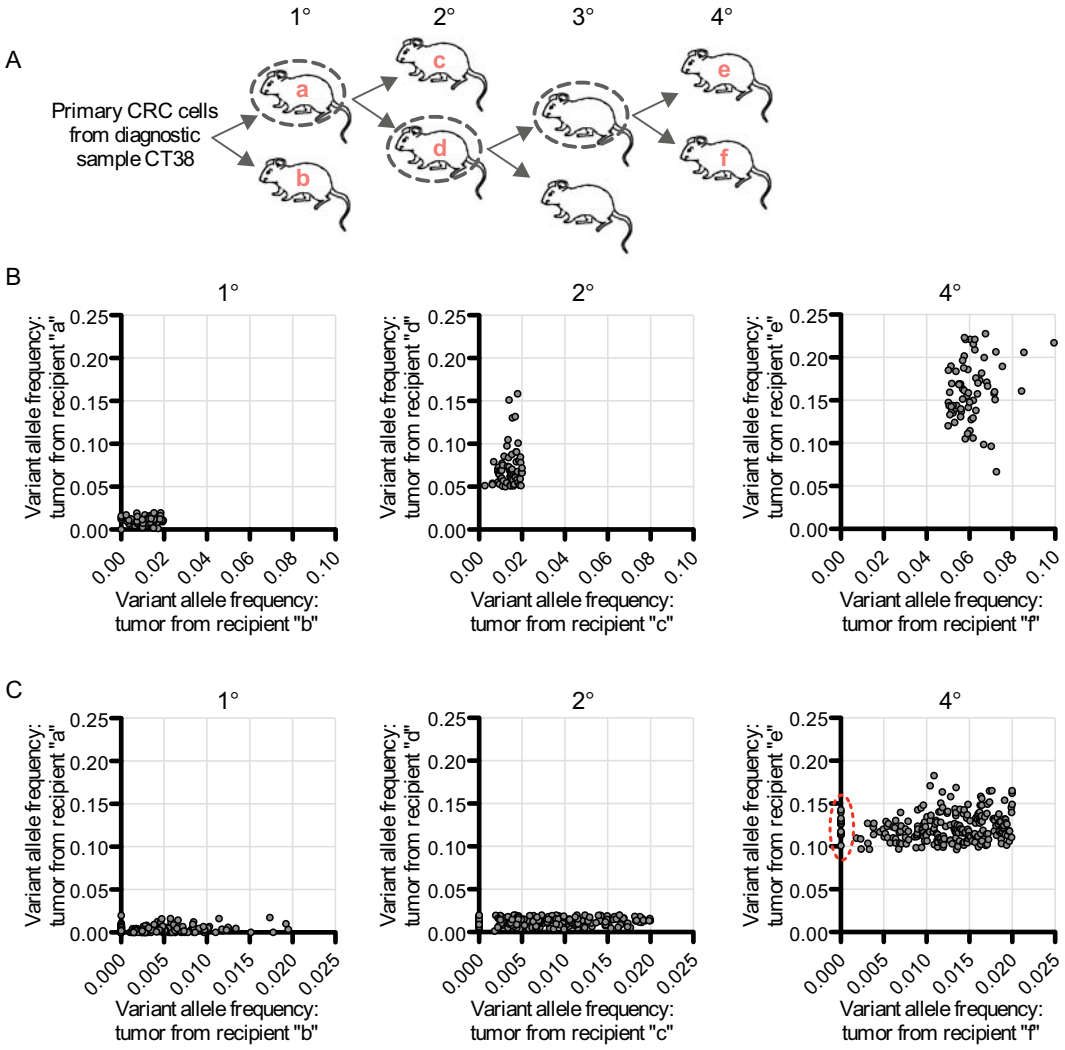

Fig. S9. Non-synonymous SNVs that are enriched in 2° and 4° recipients.

(**A**) Tumor cells from diagnostic sample CT38 were transplanted into two 1° recipients (recipient 'a' and 'b'). Once tumors formed, cells from one of the tumors were re-transplanted into two 2° recipients (recipient 'a' was re-injected into recipients 'c' and 'd'). This process was repeated for each subsequent transplant. The recipient whose tumor was used for transplantation is circled. For each transplant, tumor DNA from both recipients was analyzed by exome sequencing. To discover xenograft-specific non-synonymous SNVs, non-synonymous SNVs that were enriched or detected in only one of the two tumors from parallel recipients were considered. These SNVs were detected above 2% in the tumor that was used for further transplantation and were detected in subsequent

recipients, but were detected at a frequency of less than 2% in the other tumor that was not injected further at the same passage. The frequency of these 'enriched' SNVs was then noted across all transplants. (**B**) Non-synonymous SNVs that were enriched in recipient 'd' of 2° transplant as compared to recipient 'c' of the same passage (shown in middle graph, titled '2°'). The frequency of these SNVs was then tracked in 1° and 4° passages. (**C**) Non-synonymous SNVs that were enriched in recipient 'e' of 4° transplant as compared to recipient 'f' of the same passage (shown in graph on the right, titled '4°'). The frequency of these SNVs was then tracked in 1° and 4° passages. Red dotted circle on graph titled '4°' encircles those SNVs that are only detected in one recipient but not the other recipient of this passage.

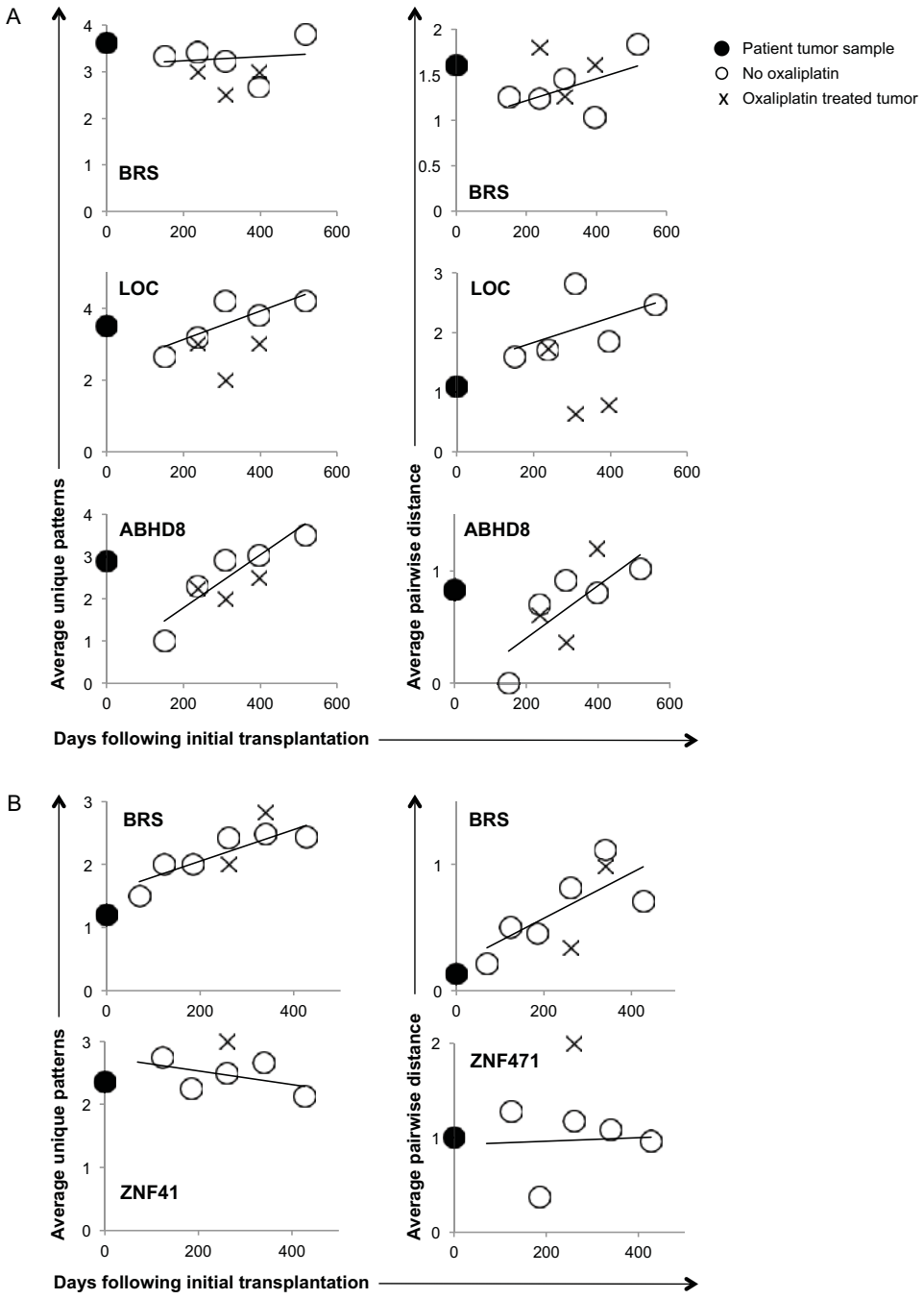

Fig. S10. Diversity in CRC samples and corresponding xenografts.

Sample passenger DNA methylation patterns from different regions of the primary cancers CT38 **(A)** and CT54 **(B)**, and their xenografts. Two measures of tumor population diversity were computed. Left column, average unique patterns: average number of unique patterns observed when

6 to 8 epialleles were sampled from a small patient tumor or xenograft region. Right column, average pairwise distance: average number of differences between the 6 to 8 epialleles sampled from a small patient tumor or xenograft region. Multiple loci were tested (BRS, LOC, ABH, ZNP). Each circle represents data of one tumor. In general there appears to be no evidence for a severe bottleneck with xenotransplantation, and population diversity is maintained with xenograft age. Oxaliplatin does not have any consistent effect on population diversity.

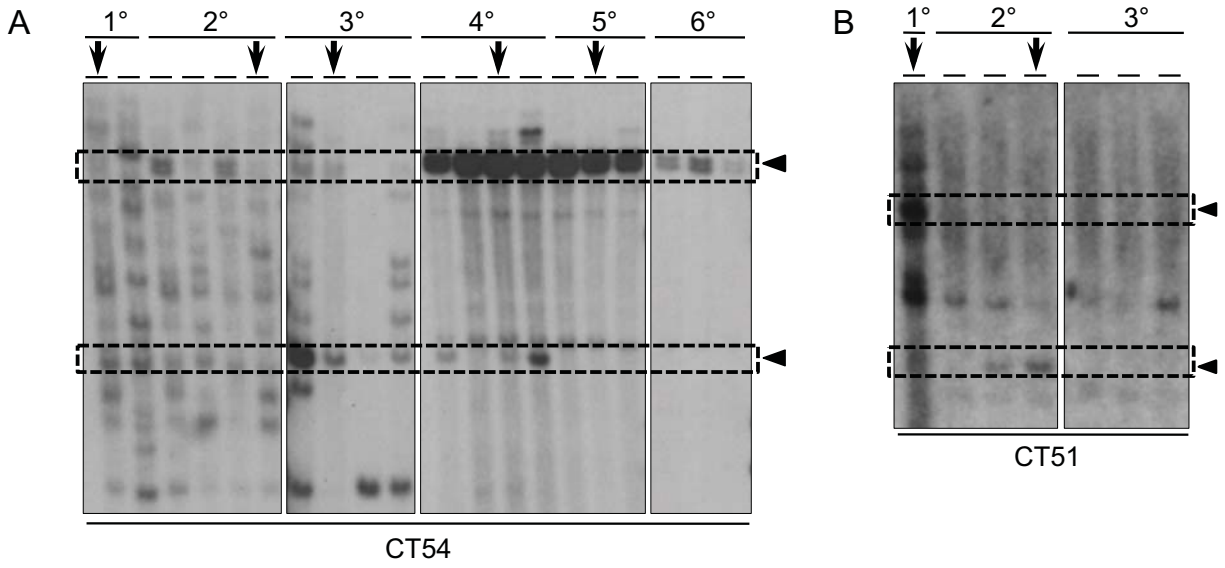

Fig. S11. Clonal behavior of lentivirally marked clones.

Southern blots tracing the integration site pattern of CT54 **(A)** and CT51 **(B)**. Each lane represents the tumor DNA of one mouse; transplant number is depicted above the blot (1°, 2°, 3°, etc.) and the arrow above certain lanes indicates the tumor that was re-injected into the next set of mice. Southern blot band patterns were confirmed by re-digesting samples with a different restriction enzyme.

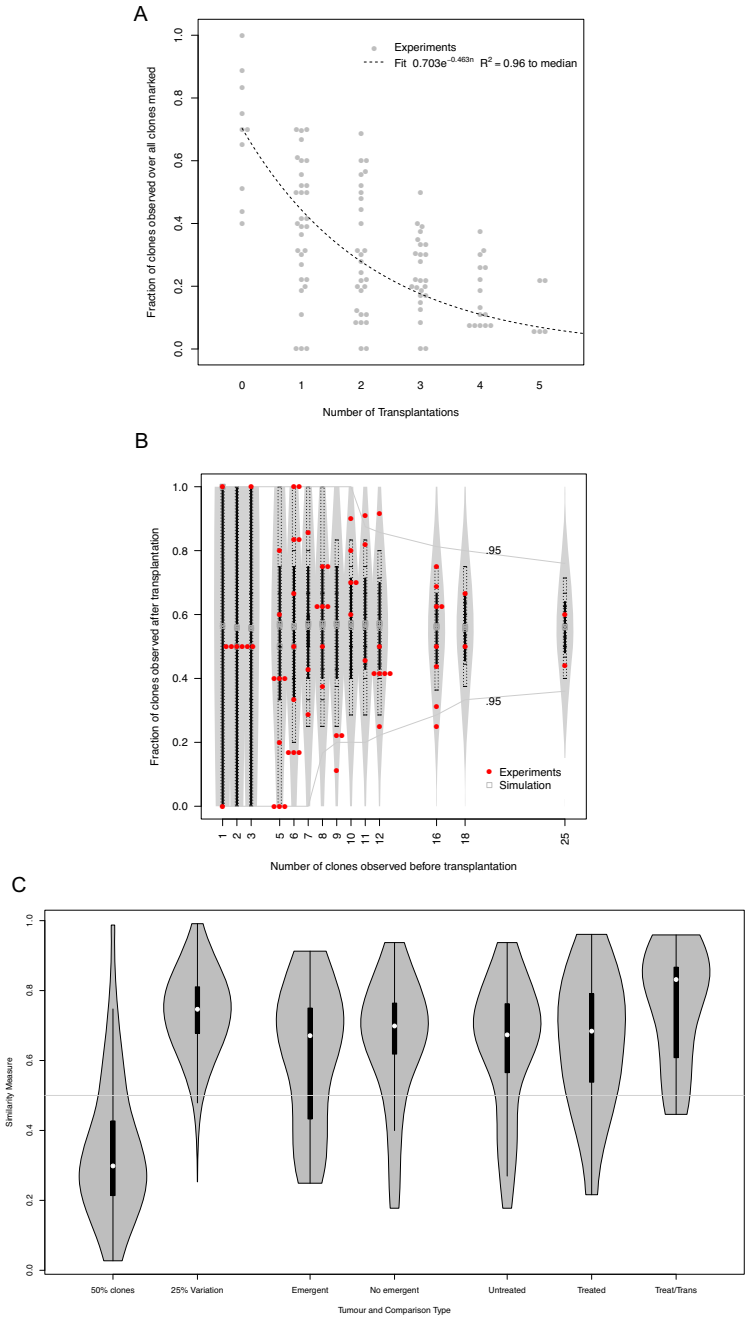

Fig. S12. Mathematical modeling of clonal emergence.

(**A**) Exponential Fit. Data points illustrate fraction of LV clones observed at each transplantation compared to the total number of LV clones observed throughout the serial transplant experiment, with an exponential fit to the median at each transplant. (**B**) Monte-Carlo Simulation. This plot describes the simulated and real dependency between the number of LV clones in a given xenograft

tumor and the fraction of those LV clones observed after transplantation. The simulated distribution is plotted using violin plots. (**C**) Similarity measures using quantitative analysis of LV clones that were successfully retransplanted (conserved LV clones). The similarity measures plot shows the distribution of similarities in terms of conserved LV clone proportions between a given xenograft and its sequential transplants. Two examples are given to illustrate ideal cases and serve as comparison points for the other plots: (1) the '50% LV clones' plot shows the distribution obtained when all LV clones are taken into account, but 50% of them are not present in the transplanted tumor, (2) the '25% Variation' plot shows a simulated distribution when a 25% Gaussian noise is added to the original LV clone proportion vector. The horizontal line at 0.5 indicates the expected value for the comparison of two randomly generated LV clone proportions with all clones present. The 'Emergent' and 'No Emergent' plots compare the similarities of conserved LV clone proportions in tumors that have emergent LV clones (first time Type IV or first time Type V) or not. The 'Untreated,' 'Treated,' and 'Treated/Trans' plots compare the similarities of conserved LV clone proportions in untreated tumors, oxaliplatin treated tumors, and oxaliplatin treated tumors which have been transplanted.

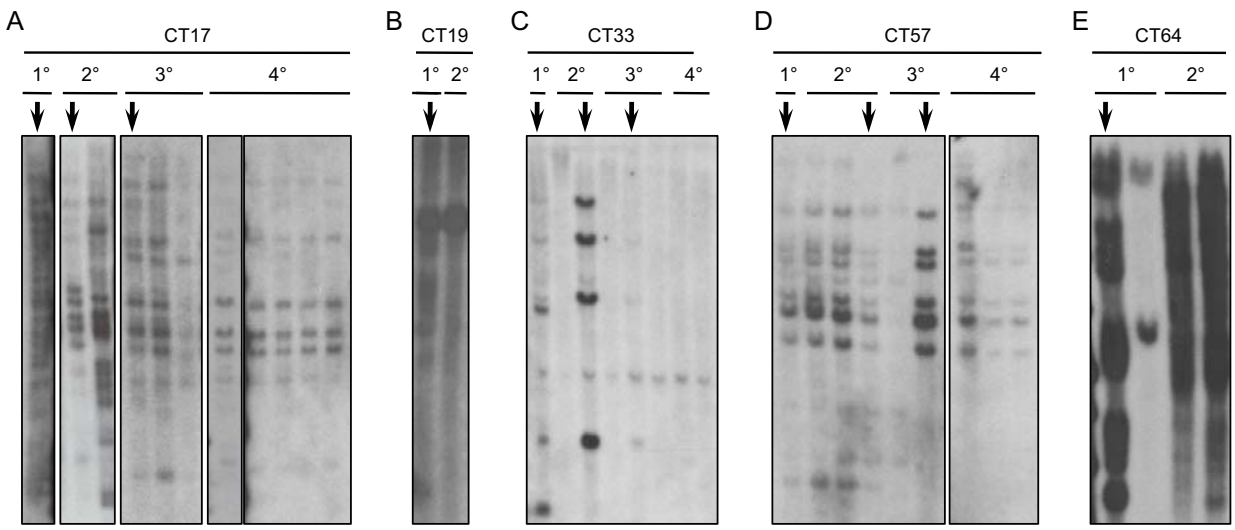

Fig. S13. Integration site analysis by Southern blotting.

(A-E) Southern blots tracing the integration site pattern of different patients over several transplants in mice. Each lane represents the tumor DNA of one mouse; transplant number is depicted above the blot (1°, 2°, 3°, etc.) and the arrow above certain lanes indicates the tumor that was re-injected into the next set of mice. Clonal tracking (CT) numbers, representing different patients samples, are shown above each panel.

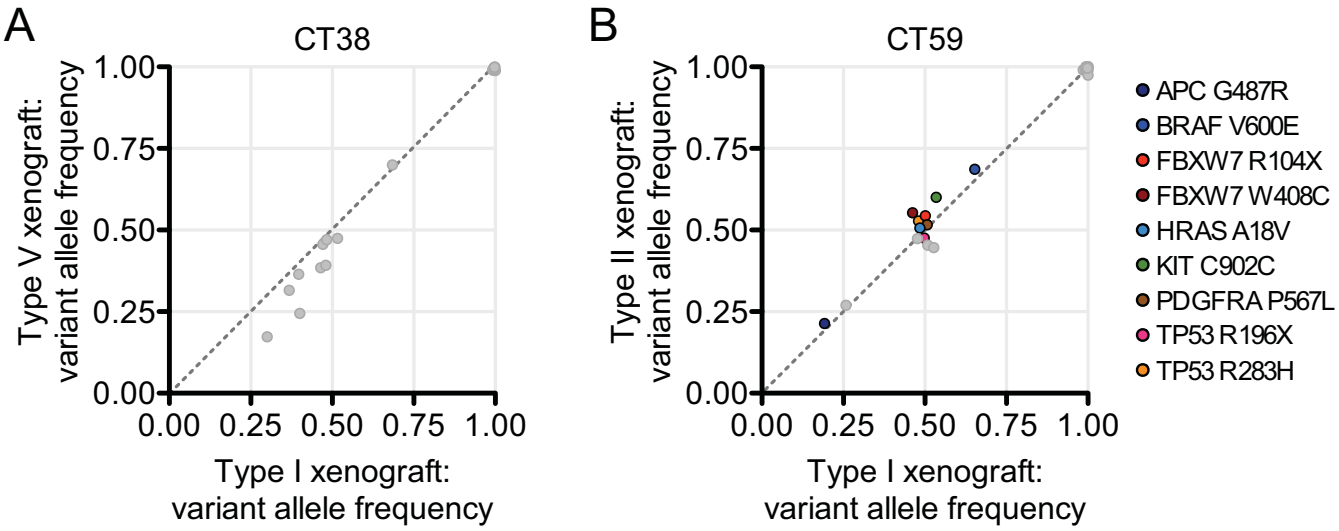

Fig. S14. Variant allele frequency comparisons between single-cell derived LV clones.

GFP-expressing tumor cells from CT38 (**A**) and CT59 (**B**) were separated using fluorescence activated cell sorting and viable cells were injected subcutaneously at varying cell doses in a limiting dilution assay. Tumor DNA was isolated from tumors that were generated at a cell dose, where it was statistically estimated that one cell formed the tumor. DNA was profiled using Southern blotting to confirm the presence of one insertion. Tumors that were confirmed to be generated by one LV clone were subjected to targeted deep sequencing using the RainDance platform. Frequency of both germline (gray) and somatic variants (colored circles) is shown.

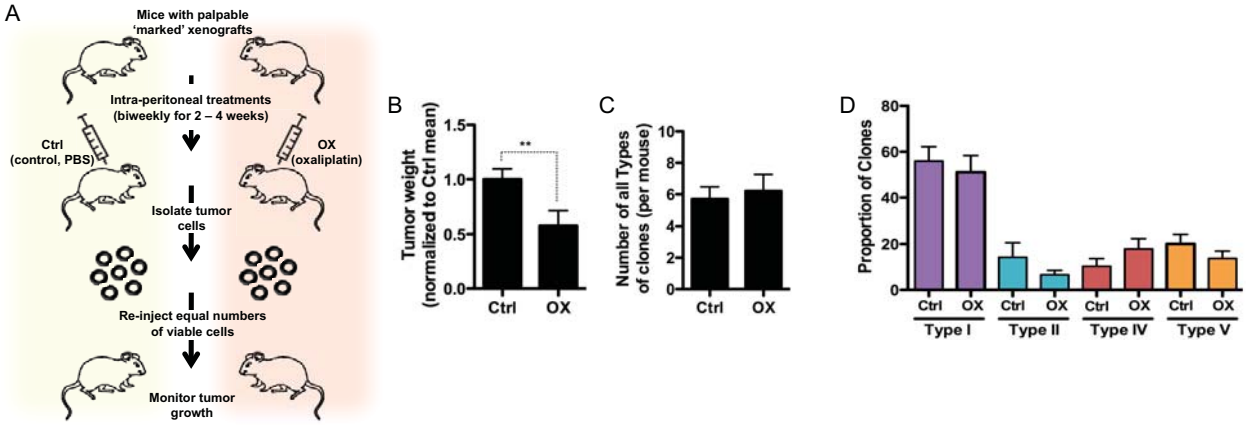

Fig. S15. Variable response of marked clones to oxaliplatin.

(A) Schematic representation of the experimental approach. Xenografts that were used for the initial treatment were obtained from previously transduced cells that had generated tumors in mice and for which the LV clones were defined. From these marked xenografts, cells were re-injected into mice and the chemotherapy experiment was initiated once these tumors were palpable. Mice were either treated with PBS (Ctrl) or oxaliplatin (OX) for 2 to 4 weeks and cells from these 'primary' tumors were re-injected into 'secondary' mice, which did not receive further treatment. **(B)** Tumor weight after administration of oxaliplatin *in vivo*. Tumor weights were normalized to mean tumor weight of Ctrl group and data was pooled from five patient samples, representing 28 Ctrl and 26 OX mice. **(C)** Cumulative number of LV clones per mouse in Ctrl and OX groups immediately following treatment. **(D)** Proportion of LV clone types in primary mice following oxaliplatin treatment.

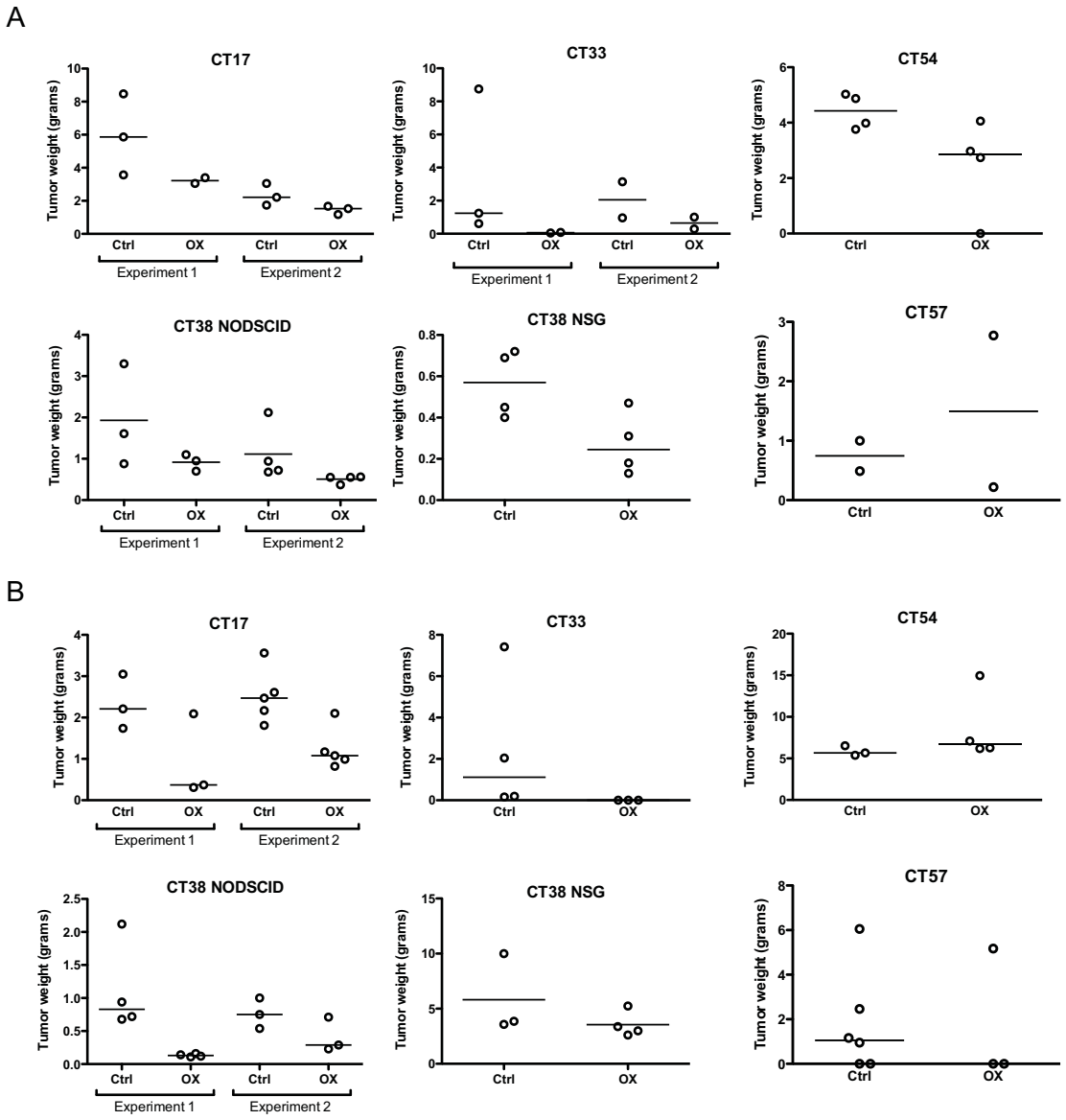

Fig. S16. Oxaliplatin administration reduces tumor size in mice.

(**A**) Graphs displaying tumor weights after the mice were either treated with vehicle (Ctrl) or oxaliplatin (OX) for 2 to 4 weeks. Mice were sacrificed 2 to 5 days after the last OX treatment and the tumor weights were recorded. **(B)** Tumor growth is reduced after re-injection of OX-treated tumors. Graphs are displaying tumor weights in secondary mice that were injected with a previously Ctrl- or OX-treated tumor; the mice did not receive any further treatment. **(A-B)** Each circle represents the data of one mouse and lines represent median tumor weights.

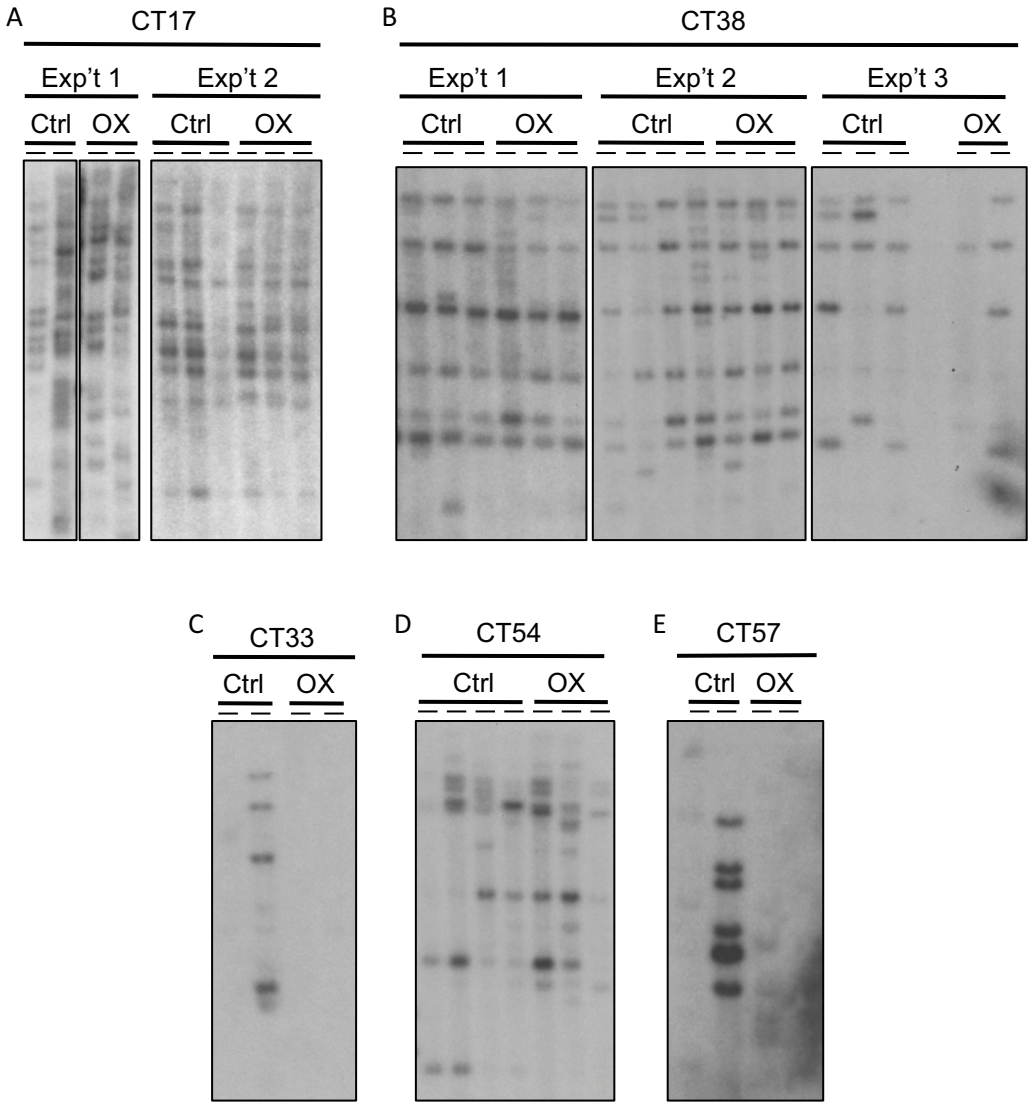

Fig. S17. Clonal distribution after oxaliplatin treatment.

(**A-E**) Southern blots illustrating the clonal behavior observed after oxaliplatin treatment. Mice were sacrificed 2-5 days after the last oxaliplatin treatment and tumor DNA was extracted. Each lane represents the tumor DNA of one mouse.

Table S1. Tumor samples and patient characteristics[1]

Experiment ID	Age	Sex	Tumor site	Stage	Microsatellite status[2]	Prior chemotherapy
CT15	41	M	liver	IV	MSS	FOLFOX
CT17	83	M	liver	IV	MSS	None
CT19	70	M	liver	IV	n.d.[1]	CPT-11, Avastin, Xeloda
CT33	86	F	colon	IIIC	MSS	None
CT38	64	M	colon	III	MSS	None
CT51	66	M	colon	IIIB	MSS	None
CT54	47	F	colon	IIA	MSI-H	None
CT57	79	M	colon	IIA	MSS	None
CT59	69	F	colon	IV	MSI-H	None
CT64	62	M	liver	IV	MSS	FOLFOX

[1] n.d., no data available

[2] MSS, microsatellite stable; MSI-H, microsatellite instability high frequency

Table S2. Engraftment of CRC cells at different sites

Sample	Injection site	No. of cells injected	No. of mice injected	No. of tumors formed
CRC001	Colon	5E+05	1	0
CRC002	Colon	5E+05	1	0
CRC003	Colon	1E+05	3	0
CRC004	Colon	1E+05	3	0
	Liver	1E+05	3	0
CRC005	Colon	2E+06	3	1
	Liver	2E+06	3	0
CRC006	Colon	2E+05	1	0
	Liver	2E+05	1	0
CRC007	Colon	6E+05	1	0
	Liver	6E+05	1	0
CRC008	Colon	1E+06	1	0
	Liver	1E+06	1	0
CRC009	Colon	1E+06	1	0
	Liver	1E+06	1	0
CRC010	Colon	1E+06	2	0
	Liver	1E+06	2	0
CRC011	Colon	1E+06	1	0
	Liver	1E+06	1	0
CRC012	Colon	5E+05	1	0
CRC013	Colon	1E+06	1	0
CRC014	Colon	1E+06	2	0
	Liver	1E+06	2	0

Table S3. Integration sites of lentiviral vectors in human CRC cells

Insertion ID[1]	Insertion locus[2]		Gene locus[3] name (region)
	Chr.	Position	
A_01	10	7803490	KIN (intron)
A_02	10	64571154	EGR2 (3'), ADO (3')
A_03	11	64699177	PPP2R5B (intron)
A_04	9	140536901	EHMT1 (intron)
B_01	1	231070911	TTC13 (intron)
B_02	12	80061572	PAWR (intron)
B_03	15	98510681	ARRDC4 (intron)
B_04	2	148745299	ORC4L (intron)
B_05	22	43359448	PACSIN2 (intron)
C_01	1	78078772	ZZZ3 (intron)
C_02	2	84851618	DNAH6 (exon)
C_03	2	198044186	ANKRD44 (intron)
C_04	6	5141666	LYRM4 (intron)
C_05	6	31379519	MICA (intron), HCP5 (intron)
C_06	8	117776823	UTP23 (5'), EIF3B (5')
D_01	1	78270014	FAM73 (intron)
D_02	1	240010391	CHRM3 (intron)
D_03	2	55790854	SMEK2 (intron)
D_04	8	144876267	SCRIB (intron)
D_05	13	40241324	COG6 (intron)
D_06	17	73785509	UNK (intron)

[1] Insertions identified by two or more independent splinkerette PCR reactions

[2] Human assembly GRCh37

[3] Genes adjacent to the insertions site

Table S4. Listing of copy number segments in paired copy number analysis

Patient ID	Chrom.	Cytoband	Segment start	Segment end	Segment mean (log2)	Copy number	Segment size (kb)	Total # of gene in segment	First 10 genes in segment	Total # of miRNA in segment	First 10 miRNAs in segment
CT38	12	p13.1	13,040,237	13,070,902	-0.842	1.120	31	2	HEBP1, HTR7P1	0	
	18	q12.1	25,154,000	67,230,220	-1.026	1.085	42,076	156	MIR302F, DSC3, DSC2, DSC1, DSG1, DSG4, DSG3, DSG2, TTR, B4GALT6	0	
CT54	No new copy number changes in xenografts										
CT59	1	p35.1	32,935,980	33,161,218	-1.084	0.940	225	7	SYNC, KIAA1522, YARS, S100PBP, FNDC5, HPCA, TMEM54	0	
	1	q31.1	185,610,830	185,913,759	-0.830	1.130	303	0		0	
	2	p25.3	2,772	50,356,406	-0.581	1.411	50,354	283	FAM110C, SH3YL1, ACP1, FAM150B, TMEM18, SNTG2, TPO, PXDN, MYT1L, LOC730811	0	
	2	q33.1	202,313,659	202,874,779	0.759	3.380	561	8	ALS2, CDK15, FZD7, SUMO1, NOP58, SNORD70, SNORD11B, SNORD11	0	
	6	p25.3	94,649	7,341,437	-1.210	1.231	7,247	55	DUSP22, IRF4, EXOC2, HUS1, LOC285768, FOXQ1, FOXF2, FOXC1, GMDS, C6orf195	0	
	6	p22.3	17,161,878	17,286,173	-0.594	1.330	124	0		0	
	6	q24.3	146,456,373	147,024,177	-0.772	1.170	568	3	GRM1, RAB32, C6orf103	0	
	7	q21.13; q21.2; q21.3	89,146,000	158,820,000	0.430	2.831	69,674	544	DPY19L2P4, STEAP1, STEAP2, C7orf63, GTPBP10, CLDN12, CDK14, FZD1, MTERF, AKAP9	3	hsa-mir-1285-1, hsa-mir-653, hsa-mir-489
	16	q22.1	66,915,438	67,932,447	-1.024	0.980	1,017	14	PRMT7, SMPD3, ZFP90, CDH3, CDH1, TMCO7, HAS3, CHTF8, CIRH1A, SNTB2	0	

17	p13.3	514	4,867,000	0.797	3.505	4,866	104	RPH3AL, C17orf97, FAM101B, VPS53, FAM57A, GEMIN4, ELP2P, GLOD4, RNMTL1, NXN	4	hsa-mir-22, hsa-mir-132, hsa-mir-212, hsa-mir-1253
18	q21.31; q21.32	54,218,857	56,626,154	-0.976	1.020	2,407	14	NEDD4L, MIR122, ALPK2, MALT1, ZNF532, LOC390858, SEC11C, GRP, RAX, CPLX4	1	hsa-mir-122
2[a]	p16.3	50,323,000	50,619,000	1.265	3.231	296	1	NRXN1	0	

[a] copy number detected only in 2° tumours 1 and 2

Table S5. SNVs in CT38

Gene	CHR	Location	Position	Type	NCBI Ref	Coding	Protein	RS	Ref. Allele	Var. Allele	Q Score	Variant Allele Frequency (%)													
												Patient Normal	Patient Tumor	1° xenografts				2° xenografts			4° xenografts			4° - Oxaliplatin	
														tm1	tm2	tm3	tm4	tm1	tm2	tm3	tm1	tm2	tm3	tm1	tm2
ANKRD13C	chr1	exon1	70,820,008	synonymous SNV	NM_030816	c.G84A	p.E28E	rs61782675	C	T	115,352	41.9%	50.6%	50.5%	46.4%	45.9%	50.0%	53.5%	43.4%	47.6%	38.0%	48.0%	41.6%	35.4%	48.1%
APOB	chr2	exon4	21,263,900	nonsynonymous SNV	NM_000384	c.C293T	p.T98I	rs1367117	G	A	146,570	45.3%	47.3%	58.4%	47.8%	51.5%	50.0%	46.2%	43.4%	52.4%	49.3%	52.1%	51.8%	47.4%	49.9%
BRCA1	chr17	exon10	41,244,000	nonsynonymous SNV	NM_007300	c.A3548G	p.K1183R	rs16942	T	C	89,126	52.5%	49.8%	49.9%	52.0%	55.6%	43.0%	50.3%	46.6%	47.7%	53.5%	55.7%	52.7%	48.2%	50.1%
BRCA1	chr17	exon10	41,244,435	nonsynonymous SNV	NM_007300	c.A3113G	p.E1038G	rs16941	T	C	172,794	48.6%	51.5%	49.6%	50.2%	43.4%	47.7%	53.8%	49.6%	50.4%	55.0%	44.8%	62.3%	52.7%	52.5%
BRCA1	chr17	exon10	41,244,936	nonsynonymous SNV	NM_007300	c.C2612T	p.P871L	rs799917	G	A	78,551	46.5%	46.9%	50.5%	36.0%	49.9%	43.4%	51.3%	50.3%	55.3%	45.7%	45.5%	48.7%	51.2%	62.0%
BRCA2	chr13	exon10	32,906,729	nonsynonymous SNV	NM_000059	c.A1114C	p.N372H	rs144848	A	C	173,029	48.0%	80.7%	74.2%	87.6%	81.7%	89.8%	93.0%	100.0%	93.9%	80.6%	97.0%	100.0%	71.1%	75.9%
BRCA2	chr13	exon11	32,912,299	synonymous SNV	NM_000059	c.T3807C	p.V1269V	rs543304	T	C	6,741	46.6%	28.4%	24.6%	25.5%	26.4%	11.2%	6.8%	0.0%	10.9%	25.1%	5.6%	1.5%	41.2%	15.2%
C9orf174	chr9	exon2	100,070,351	synonymous SNV	NM_020893	c.G138C	p.S46S	rs12683119	G	C	139,622	48.1%	47.9%	41.4%	51.3%	56.0%	52.8%	51.9%	49.9%	52.1%	45.8%	51.5%	56.6%	50.9%	53.9%
CD3E	chr11	exon3	118,178,007	synonymous SNV	NM_000733	c.C54T	p.G18G	rs4606515	C	T	14,620	51.6%	25.9%	0.3%	0.0%	0.0%	0.0%	0.0%	0.0%	0.0%	0.2%	0.0%	0.0%	0.2%	0.0%
CDH1	chr16	exon13	68,857,441	synonymous SNV	NM_004360	c.T2076C	p.A692A	rs1801552	T	C	671,567	99.7%	99.0%	99.4%	99.8%	99.8%	99.9%	99.6%	99.7%	99.7%	99.5%	99.5%	99.4%	99.5%	98.7%
CDKN2A	chr9	UTR3	21,968,199					rs11515	C	G	140,721	49.5%	45.5%	53.0%	49.6%	52.0%	49.9%	48.1%	51.9%	49.0%	45.0%	49.9%	51.5%	51.8%	53.4%
CSF1R	chr5	exon22	149,433,752	synonymous SNV	NM_005211	c.T2799C	p.G933G	rs41287092	A	G	14,983	46.0%	19.7%	0.5%	0.3%	0.2%	0.8%	0.3%	0.4%	1.0%	0.5%	0.4%	0.2%	0.6%	1.2%
EGFR	chr7	exon20	55,249,063	synonymous SNV	NM_005228	c.G2361A	p.Q787Q	rs1050171	G	A	377,367	51.0%	53.3%	48.9%	52.5%	46.4%	51.0%	42.8%	45.2%	50.3%	47.0%	48.0%	47.7%	49.2%	45.1%
EGFR	chr7	exon23	55,266,417	synonymous SNV	NM_005228	c.T2709C	p.T903T	rs1140475	T	C	395,986	99.9%	99.6%	99.6%	99.6%	99.8%	98.9%	99.8%	99.7%	99.4%	99.6%	99.9%	99.5%	99.7%	99.7%
EGFR	chr7	exon25	55,268,916	synonymous SNV	NM_005228	c.C2982T	p.D994D	rs2293347	C	T	188,203	49.0%	41.4%	49.3%	52.2%	49.4%	50.6%	50.9%	49.9%	50.5%	56.7%	54.0%	47.6%	50.8%	45.8%
FGFR3	chr4	exon12	1,807,894	synonymous SNV	NM_022965	c.G1617A	p.T539T	rs7688609	G	A	417,272	99.0%	99.3%	99.1%	98.9%	98.9%	99.4%	99.4%	100.0%	99.6%	99.6%	99.3%	99.4%	99.6%	98.7%
FGFR3	chr4	exon9	1,806,131	nonsynonymous SNV	NM_001163213	c.T1156C	p.F386L	rs17881656	T	C	122,912	52.7%	56.8%	49.7%	53.7%	40.1%	42.4%	46.4%	44.1%	41.5%	43.5%	49.2%	52.4%	51.2%	44.2%
FGFR3	chr4	intronic	1,806,519					rs3135890	C	T	161,645	47.8%	47.4%	49.0%	47.9%	36.1%	44.0%	51.1%	52.8%	48.7%	49.8%	55.2%	47.6%	47.2%	48.2%
FLT3	chr13	intronic	28,589,267					rs4073630	C	T	145,186	47.7%	46.7%	52.1%	47.7%	50.0%	52.1%	55.5%	46.1%	45.5%	49.8%	58.7%	47.6%	48.5%	47.3%
FLT3	chr13	intronic	28,610,183					rs2491231	A	G	356,334	100.0%	100.0%	99.6%	99.8%	99.7%	99.8%	99.8%	99.6%	100.0%	99.8%	100.0%	99.8%	100.0%	100.0%
GDF9	chr5	intronic	132,198,287					rs254285	C	G	5,942	44.1%	15.5%	0.0%	0.0%	0.0%	0.5%	0.0%	0.0%	0.2%	0.0%	0.4%	0.0%	0.1%	0.4%
HDLBP	chr2	exon10	242,192,848	nonsynonymous SNV	NM_203346	c.A1253G	p.N418S	rs7578199	T	C	359,245	100.0%	99.7%	99.8%	99.8%	99.8%	99.6%	99.8%	100.0%	100.0%	99.6%	99.7%	100.0%	100.0%	99.7%
HEATR2	chr7	exon6	796,430	synonymous SNV	NM_017802	c.C1269T	p.S423S	rs73036225	C	T	197,222	53.7%	49.2%	47.7%	56.6%	46.7%	51.1%	52.3%	40.2%	54.2%	49.5%	52.9%	59.0%	49.0%	48.2%
HIF1A	chr14	intronic	62,213,553					rs10147275	T	G	107,475	31.7%	35.4%	36.9%	25.4%	34.1%	31.6%	36.0%	34.8%	34.0%	37.6%	35.7%	32.2%	33.2%	34.8%
HRAS	chr11	intronic	534,197					rs41258054	C	T	14,040	48.1%	31.8%	0.3%	0.0%	0.3%	0.0%	0.0%	0.5%	0.6%	0.2%	0.0%	0.4%	0.2%	0.0%
IL9	chr5	exon5	135,228,165	nonsynonymous SNV	NM_000590	c.C350T	p.T117M	rs2069885	G	A	408,950	55.3%	86.1%	99.3%	99.6%	99.4%	99.8%	99.8%	99.3%	99.5%	99.0%	99.2%	99.5%	99.4%	99.3%
KIAA0802	chr18	exon6	8,784,723	nonsynonymous SNV	NM_015210	c.A1613G	p.D538G	rs3744979	A	G	369,659	52.2%	82.2%	99.7%	99.9%	99.9%	99.8%	99.5%	100.0%	99.7%	100.0%	99.3%	100.0%	99.7%	99.6%
KRTAP10-10	chr21	exon1	46,057,548	nonsynonymous SNV	NM_181688	c.A214C	p.T72P	rs4818947	A	C	100,333	45.7%	41.7%	48.7%	40.8%	41.9%	44.4%	52.1%	46.9%	48.2%	44.4%	42.9%	43.6%	53.1%	46.1%
KRTAP10-10	chr21	exon1	46,057,590	nonsynonymous SNV	NM_181688	c.A256T	p.T86S	rs9306109	A	T	115,836	46.1%	42.4%	48.7%	41.1%	42.5%	44.9%	51.9%	46.9%	48.3%	44.6%	43.0%	43.7%	53.3%	45.7%
KRTAP19-6	chr21	exon1	31,914,000	synonymous SNV	NM_181612	c.A153T	p.G51G	rs1023364	T	A	8,578	48.8%	27.0%	0.0%	0.0%	0.3%	0.0%	0.0%	0.0%	0.0%	0.0%	0.3%	0.0%	0.0%	0.3%
LDLR	chr19	exon12	11,227,602	synonymous SNV	NM_000527	c.C1773T	p.N591N	rs688	C	T	340,524	99.7%	99.0%	98.5%	99.2%	99.7%	99.4%	99.3%	99.4%	99.7%	99.2%	98.8%	99.4%	99.9%	99.2%
LILRA4	chr19	exon4	54,849,463	synonymous SNV	NM_012276	c.G399A	p.V133V	rs12976217	C	T	157,519	49.7%	46.4%	46.4%	51.8%	49.1%	44.3%	49.7%	46.9%	47.3%	51.9%	52.3%	53.7%	44.7%	52.6%
LILRA4	chr19	exon4	54,849,481	synonymous SNV	NM_012276	c.A381C	p.A127A	rs7256494	T	G	155,445	49.3%	46.3%	46.7%	52.5%	49.3%	44.4%	49.2%	48.6%	47.3%	51.9%	52.3%	54.4%	44.7%	52.4%
LOC57653	chr9	ncRNA	100,070,435					rs2401382	C	T	100,178	47.7%	48.1%	40.7%	51.5%	56.0%	53.0%	51.9%	49.7%	51.1%	46.0%	51.6%	55.9%	50.5%	54.0%
MAST2	chr1	exon29	46,500,613	synonymous SNV	NM_015112	c.T4272C	p.T1424T	rs17855317	T	C	172,978	48.9%	51.7%	46.1%	46.9%	49.0%	53.4%	60.0%	53.7%	51.4%	57.1%	51.7%	47.6%	43.3%	52.3%
MBD4	chr3	exon3	129,155,670	nonsynonymous SNV	NM_003925	c.G817A	p.A273T	rs10342	C	T	375,188	99.9%	99.7%	99.6%	99.4%	99.8%	99.3%	99.2%	100.0%	99.7%	100.0%	99.0%	99.3%	99.7%	99.4%
MLH1	chr3	exon8	37,053,568	nonsynonymous SNV	NM_000249	c.A655G	p.I219V	rs1799977	A	G	115,694	47.8%	48.7%	53.7%	51.9%	43.8%	50.6%	54.7%	45.8%	52.5%	50.6%	56.7%	56.0%	52.1%	52.1%
MLH1	chr3	intronic	37,083,740					rs9876116	A	G	89,330	32.0%	37.1%	34.2%	36.1%	33.6%	36.8%	29.9%	34.1%	40.1%	38.0%	33.2%	41.4%	39.7%	35.9%
MRC1, MRC1L1	chr10	intronic	17,875,857					rs56278466	T	G	145,026	100.0%	100.0%	100.0%	99.8%	99.6%	99.6%	100.0%	99.3%	100.0%	99.2%	100.0%	99.8%	99.7%	99.8%
NF1	chr17	intronic	29,654,876					rs2285894	T	A	127,802	50.8%	47.1%	52.3%	50.8%	45.7%	51.7%	54.7%	54.1%	47.9%	51.2%	51.3%	45.9%	50.2%	49.5%
NOC4L	chr12	exon4	132,631,855	synonymous SNV	NM_024078	c.C375T	p.F125F	rs11543305	C	T	177,916	51.7%	49.5%	48.8%	51.2%	50.3%	48.8%	42.1%	48.4%	46.4%	44.7%	51.5%	44.2%	41.2%	47.6%
NOTCH1	chr9	intronic	139,393,307					rs9632944	A	G	102,294	45.0%	53.0%	50.1%	53.6%	50.1%	52.3%	52.6%	45.2%	47.4%	53.6%	53.2%	49.1%	45.9%	52.4%
OR2D3	chr11	exon1	6,942,726	nonsynonymous SNV	NM_001004684	c.G494C	p.W165S	rs10839659	G	C	177,064	49.1%	73.4%	98.9%	99.6%	100.0%	98.8%	99.3%	99.5%	99.5%	99.2%	99.0%	99.6%	100.0%	98.3%
OR2L3	chr1	exon1	248,224,746	nonsynonymous SNV	NM_001004687	c.G763T	p.V255F	rs6697812	G	T	192,740	49.2%	44.6%	46.1%	45.8%	40.9%	46.7%	58.9%	50.6%	52.4%	49.6%	47.1%	50.0%	47.5%	50.8%
OR2L3	chr1	exon1	248,224,754	synonymous SNV	NM_001004687	c.T771C	p.T257T	rs55893924	T	C	201,627	49.8%	55.2%	53.3%	54.1%	59.1%	52.9%	41.1%	49.2%	47.1%	50.1%	52.5%	49.8%	51.9%	48.1%
OR2Y1	chr5	exon1	180,166,834	synonymous SNV	NM_001001657	c.C225A	p.T75T	rs61737915	G	T	464,053	52.2%	89.7%	99.6%	99.2%	99.6%	99.3%	99.4%	99.2%	99.4%	99.6%	99.1%	99.8%	99.9%	99.5%
OR51B5	chr11	exon1	5,364,450	nonsynonymous SNV	NM_001005567	c.T305C	p.I102T	rs11036912	A	G	242,950	48.0%	72.1%	100.0%	99.9%	99.8%	99.8%	100.0%	99.7%	100.0%	99.6%	99.0%	100.0%	99.8%	99.3%
OR6S1	chr14	exon1	21,109,671	synonymous SNV	NM_001001968	c.T180C	p.P60P	rs11627574	A	G	25,239	49.0%	21.4%	27.6%	20.0%	23.7%	5.1%	10.1%	2.6%	7.0%	22.9%	5.9%	0.3%	36.1%	20.5%
OR6S1	chr14	exon1	21,109,726	nonsynonymous SNV	NM_001001968	c.C125T	p.T42I	rs11622794	G	A	39,772	49.5%	22.0%	28.0%	20.2%	23.5%	5.4%	9.9%	2.6%	6.8%	22.4%	5.6%	0.3%	35.9%	20.7%
PALM	chr19	exon5	731,144	nonsynonymous SNV	NM_001040134	c.A319G	p.T107A	rs1050457	A	G	100,048	51.4%	45.8%	52.4%	46.9%	52.2%	50.0%	45.5%	52.0%	51.4%	47.5%	50.1%	50.6%	43.2%	45.2%
PDGFRA	chr4	exon23	55,161,391	synonymous SNV	NM_006206	c.T3222C	p.D1074D	rs7685117	T	C	286,849	100.0%	99.7%	99.9%	99.7%	100.0%	99.7%	99.4%	100.0%	100.0%	99.5%	99.6%	99.9%	99.8%	99.9%
PDGFRA	chr4	intronic	55,151,711					rs2412559	C	A	332,125	99.8%	99.7%	100.0%	98.2%	99.4%	99.8%	98.9%	99.7%	99.2%	99.2%	98.9%	99.7%	98.8%	99.1%
PDGFRA	chr4	intronic	55,161,254					rs3733540	C	T	352,349	99.5%	99.5%	99.8%	99.7%	99.6%	99.5%	99.6%	99.4%	99.7%	99.7%	99.1%	99.4%	99.7%	99.8%
PIK3CA	chr3	intronic	178,922,274					rs2699896	C	A	132,394	50.4%	42.3%	46.6%	41.6%	47.2%	48.5%	51.3%	54.1%	51.8%	50.7%	50.6%	46.8%	43.8%	48.4%
PLEKHG2	chr19	exon9	39,908,657	nonsynonymous SNV	NM_022835	c.G995T	p.G332V	rs117405645	G	T	34,783	52.7%	54.7%	49.0%	46.3%	55.2%	47.4%	56.3%	55.6%	52.2%	48.6%	46.3%	56.7%	47.5%	47.8%
PML	chr15	exon9	74,336,633	nonsynonymous SNV	NM_033238	c.T1933C	p.F645L	rs5742915	T	C	93,975	49.2%	54.3%	54.2%	48.3%	46.8%	56.6%	55.8%	54.8%	54.6%	50.1%	49.7%	47.2%	41.2%	43.5%
PRIC285	chr20	exon5	62,200,575	synonymous SNV	NM_001037335	c.A1014G	p.S338S	rs1741594	T	C	391,589	99.3%	99.9%	100.0%	99.8%	99.7%	99.8%	99.9%	100.0%	99.9%	99.8%	99.9%	99.8%	99.8%	99.6%
RB1	chr13	intronic	48,919,358					rs198617	T	G	164,689	100.0%	99.6%	99.6%	99.6%	100.0%	100.0%	99.6%	100.0%	100.0%	100.0%	99.7%	99.7%	99.7%	100.0%
RET	chr10	exon13	43,613,843	synonymous SNV	NM_020630	c.G2307T	p.L769L	rs1800861	G	T	387,117	99.9%	99.4%	99.2%	99.2%	99.5%	99.5%	99.7%	99.2%	98.6%	99.6%	99.6%	99.4%	99.5%	99.8%
RET	chr10	intronic	43,608,968					.	G	A	136,210	0.0%	61.5%	66.0%	73.4%	71.5%	76.6%	75.9%	74.5%	66.8%	78.1%	74.5%	68.8%	73.4%	76.7%
SAA1	chr11	exon4	18,291,321	synonymous SNV	NM_199161	c.T288C	p.A96A	rs12218	T	C	189,361	44.1%	76.1%	99.7%	99.6%	99.5%	100.0%	100.0%	99.6%	100.0%	99.5%	98.9%	99.5%	99.7%	99.7%
SACM1L	chr3	exon6	45,754,685	synonymous SNV	NM_014016	c.A540G	p.P180P	rs2271619	A	G	131,801	50.2%	52.5%	51.0%	56.4%	53.6%	52.3%	47.2%	58.2%	51.4%	50.9%	52.0%	56.9%	50.2%	57.0%

SACM1L	chr3	intronic	45,754,749					rs2248991	G	A	78,300	50.1%	46.9%	49.1%	43.3%	46.5%	47.9%	53.4%	42.0%	48.5%	48.9%	48.1%	42.6%	49.7%	43.0%
SCRN3	chr2	exon2	175,263,063	nonsynonymous SNV	NM_024583	c.G52A	p.D18N	rs10497410	G	A	101,020	46.0%	52.0%	53.6%	45.7%	46.2%	53.8%	54.0%	52.2%	50.0%	53.6%	50.0%	52.4%	48.6%	52.3%
SENP6	chr6	exon23	76,425,288	nonsynonymous SNV	NM_001100409	c.A3296G	p.Y1099C	rs9250	A	G	554,196	100.0%	99.7%	100.0%	99.9%	99.9%	99.9%	99.9%	99.9%	99.7%	99.7%	99.7%	99.9%	99.7%	99.3%
SFTPC	chr8	exon5	22,021,517	nonsynonymous SNV	NM_003018	c.G557A	p.S186N	rs1124	G	A	26,108	45.8%	27.8%	35.5%	19.9%	23.8%	17.6%	6.6%	4.1%	7.4%	33.8%	0.6%	0.4%	55.3%	39.4%
SFTPC	chr8	intronic	22,021,388					rs2070687	C	G	93,079	53.3%	72.2%	63.5%	80.1%	76.6%	83.0%	93.0%	95.9%	92.2%	66.3%	97.0%	100.0%	43.9%	60.3%
SMO	chr7	intronic	128,845,018					rs2703091	C	T	289,191	99.5%	100.0%	99.7%	99.8%	99.5%	99.3%	99.5%	99.7%	99.5%	99.7%	97.8%	99.5%	99.5%	99.1%
SMO	chr7	intronic	128,846,469					rs2735842	A	G	528,537	99.8%	100.0%	100.0%	99.6%	99.7%	100.0%	99.9%	100.0%	99.9%	100.0%	99.8%	99.6%	99.8%	99.9%
SPAG11B	chr8	intronic	7,308,729					rs2294141	G	C	175,019	44.0%	29.0%	28.3%	29.3%	31.7%	23.4%	32.0%	27.2%	28.5%	29.3%	25.5%	25.0%	32.8%	27.1%
STK11	chr19	UTR5	1,206,903						T	C	28,052	23.7%	25.2%	27.7%	27.5%	22.7%	23.7%	22.8%	27.1%	30.9%	22.7%	21.7%	21.8%	27.9%	24.6%
SYNE2	chr14	intronic	64,686,207					rs915057	A	G	350,328	100.0%	100.0%	100.0%	99.4%	99.7%	100.0%	99.9%	100.0%	100.0%	99.7%	99.4%	99.5%	99.8%	99.7%
TACC2	chr10	exon3	123,970,530	nonsynonymous SNV	NM_206860	c.T824C	p.V275A	rs2295873	T	C	197,098	44.9%	52.9%	46.1%	52.9%	45.6%	49.2%	51.4%	54.8%	48.8%	43.2%	45.8%	47.4%	40.0%	41.9%
TACC3	chr4	exon4	1,729,953	nonsynonymous SNV	NM_006342	c.G824A	p.C275Y	rs17132047	G	A	63,753	44.7%	54.3%	53.1%	59.1%	61.1%	48.6%	44.3%	44.7%	38.6%	42.5%	43.3%	40.7%	48.2%	52.1%
TACC3	chr4	exon4	1,729,988	nonsynonymous SNV	NM_006342	c.G859A	p.G287S	rs1063743	G	A	66,659	45.9%	56.1%	55.0%	61.2%	62.1%	48.9%	46.0%	46.6%	40.9%	44.2%	44.6%	40.7%	47.8%	53.0%
TECPR2	chr14	exon9	102,901,201	nonsynonymous SNV	NM_001172631	c.A2047G	p.I683V	rs10149146	A	G	212,212	47.5%	46.7%	52.2%	49.2%	52.3%	44.1%	51.3%	50.2%	51.5%	50.5%	47.2%	47.3%	47.9%	52.2%
TP53	chr17	exon4	7,579,472	nonsynonymous SNV	NM_001126114	c.C215G	p.P72R	rs1042522	G	C	239,696	99.8%	99.8%	99.8%	99.8%	99.8%	100.0%	99.5%	100.0%	100.0%	99.6%	99.8%	99.7%	99.3%	99.6%
TP53	chr17	intronic	7,579,801					rs1642785	G	C	50,453	100.0%	100.0%	100.0%	100.0%	100.0%	97.4%	100.0%	100.0%	100.0%	99.3%	100.0%	99.2%	98.6%	99.3%
UBQLN3	chr11	exon2	5,529,139	synonymous SNV	NM_017481	c.A1650G	p.A550A	rs2234456	T	C	8,966	47.6%	31.7%	0.2%	0.0%	0.4%	0.0%	1.2%	0.0%	0.6%	0.2%	0.2%	0.0%	0.7%	0.6%
USP34	chr2	exon53	61,468,761	synonymous SNV	NM_014709	c.A6711G	p.K2237K	rs72884996	T	C	75,307	54.3%	58.6%	49.7%	42.3%	47.4%	46.8%	53.9%	50.6%	45.1%	59.0%	48.2%	60.4%	48.0%	53.4%

Table S6. SNVs in CT54

Gene	CHR	Location	Position	Type	NCBI Ref	Coding	Protein	RS	Ref. Allele	Var. Allele	Q Score	Variant Allele Frequency (%)															
												Patient Normal	Patient Tumor	1° xenografts			2° xenografts				5° xenografts			5° - Oxaliplatin			
														tm1	tm2	tm3	tm1	tm2	tm3	tm4	tm1	tm2	tm3	tm1	tm2	tm3	tm4
APC	chr5	exon12	112,162,854	synonymous SNV	NM_000038	c.T1458C	p.Y486Y	rs2229992	T	C	513,636	99.9%	99.7%	98.9%	100.0%	99.6%	99.8%	100.0%	99.5%	99.9%	99.6%	99.6%	99.8%	99.9%	99.6%	100.0%	99.8%
APC	chr5	exon16	112,176,325	synonymous SNV	NM_000038	c.G5034A	p.G1678G	rs42427	G	A	586,953	99.7%	99.5%	99.3%	99.9%	99.4%	99.5%	99.4%	99.6%	99.7%	99.5%	98.8%	99.5%	99.7%	99.9%	98.9%	99.4%
APC	chr5	exon6	112,116,592	stopgain SNV	NM_000038	c.C637T	p.R213X		C	T	124,604	0.4%	30.1%	48.7%	51.0%	53.4%	42.8%	47.3%	49.7%	46.7%	42.0%	51.1%	46.0%	52.6%	44.8%	45.9%	53.9%
BRCA1	chr17	exon10	41,244,936	nonsynonymous SNV	NM_007300	c.C2612T	p.P871L	rs799917	G	A	7,802	29.6%	0.0%	0.0%	0.0%	0.0%	16.2%	26.7%	23.9%	19.2%	47.5%	29.8%	25.0%	23.0%	36.5%	27.6%	22.4%
BRCA2	chr13	exon25	32,968,851	synonymous SNV	NM_000059	c.A9282C	p.S3094S		A	C	1,816	8.3%	0.0%	0.0%	0.0%	0.0%	8.0%	6.6%	7.5%	6.3%	6.7%	5.9%	5.8%	7.1%	7.4%	8.7%	7.8%
BRCA2	chr13	UTR5	32,890,572					rs1799943	G	A	134,405	51.3%	0.0%	0.0%	0.0%	0.0%	54.0%	53.8%	50.3%	45.0%	51.5%	49.5%	51.0%	47.8%	49.0%	55.8%	45.2%
CDH1	chr16	exon10	68,849,464	nonsynonymous SNV	NM_004360	c.T1367C	p.V456A		T	C	45,159	0.1%	0.4%	0.8%	0.2%	0.5%	0.3%	0.3%	0.2%	0.1%	15.1%	13.9%	22.5%	29.8%	26.4%	31.5%	23.1%
CDH1	chr16	exon14	68,862,114	nonsynonymous SNV	NM_004360	c.A2202C	p.R734S		A	C	185,290	63.5%	0.1%	0.1%	0.2%	0.2%	63.5%	50.2%	52.8%	43.3%	62.4%	61.5%	55.4%	55.1%	50.7%	58.5%	64.8%
CDH1	chr16	exon13	68,857,441	synonymous SNV	NM_004360	c.T2076C	p.A692A	rs1801552	T	C	372,621	46.0%	47.1%	51.2%	51.8%	51.0%	45.1%	44.6%	47.5%	44.2%	48.0%	46.9%	48.8%	47.2%	50.4%	46.0%	47.9%
CDH1	chr16	intronic	68,771,372					rs3743674	C	T	128,653	99.5%	100.0%	99.6%	100.0%	99.1%	97.9%	99.6%	98.7%	100.0%	100.0%	99.2%	100.0%	100.0%	99.5%	98.6%	100.0%
CDH1	chr16	intronic	68,771,380						C	T	1,769	4.8%	19.6%	21.3%	17.5%	21.8%	3.2%	3.5%	7.2%	4.5%	3.1%	2.4%	1.8%	3.5%	5.4%	3.2%	3.2%
CDH1	chr16	intronic	68,842,480					rs33963999	G	C	222,159	51.8%	54.0%	48.9%	48.8%	49.5%	48.0%	50.6%	48.9%	45.2%	46.8%	44.9%	51.8%	47.8%	55.0%	51.7%	53.9%
EGFR	chr7	exon17	55,240,810	nonsynonymous SNV	NM_005228	c.A2054T	p.E685V		A	T	178,924	36.2%	0.0%	0.0%	0.0%	0.3%	35.5%	31.0%	33.9%	29.4%	34.9%	32.7%	38.6%	33.9%	30.0%	34.1%	30.9%
EGFR	chr7	exon17	55,240,803	synonymous SNV	NM_005228	c.C2047T	p.L683L	rs55669340	C	T	332,780	49.7%	44.0%	47.0%	55.1%	50.1%	47.6%	49.3%	52.5%	47.8%	42.3%	48.2%	47.0%	53.5%	46.7%	49.0%	47.5%
EGFR	chr7	exon20	55,249,063	synonymous SNV	NM_005228	c.G2361A	p.Q787Q	rs1050171	G	A	426,152	49.8%	48.5%	53.9%	53.8%	52.8%	49.6%	50.3%	47.0%	52.6%	53.2%	50.1%	54.8%	45.6%	54.0%	51.6%	46.5%
FGFR1	chr8	exon13	38,274,863	stopgain SNV	NM_001174064	c.A1594T	p.K532X		T	A	141	4.8%	0.0%	0.2%	0.0%	0.2%	5.8%	7.1%	5.6%	6.1%	5.2%	4.6%	5.7%	6.3%	2.4%	5.1%	5.4%
FGFR1	chr8	exon13	38,274,868	nonsynonymous SNV	NM_001174064	c.A1589G	p.K530R		T	C	18,500	0.2%	44.4%	39.3%	42.6%	38.2%	0.0%	0.3%	0.1%	0.0%	0.2%	0.2%	0.1%	0.0%	0.1%	0.1%	0.1%
FGFR2	chr10	exon5	123,298,158	synonymous SNV	NM_001144915	c.A429G	p.V143V	rs1047100	T	C	589,641	100.0%	99.7%	100.0%	99.8%	99.4%	99.9%	99.7%	99.9%	99.9%	99.9%	100.0%	100.0%	100.0%	99.9%	99.8%	99.6%
FGFR3	chr4	exon12	1,807,894	synonymous SNV	NM_022965	c.G1617A	p.T539T	rs7688609	G	A	597,549	99.8%	99.7%	100.0%	99.8%	99.5%	99.1%	99.3%	99.1%	99.9%	99.8%	99.7%	99.9%	99.7%	99.2%	99.3%	99.8%
FLT3	chr13	exon8	28,623,594	synonymous SNV	NM_004119	c.A963C	p.A321A		T	G	3,410	7.1%	0.0%	0.1%	0.0%	0.0%	8.9%	4.8%	7.9%	5.2%	8.2%	8.8%	6.1%	7.2%	4.8%	6.8%	7.5%
FLT3	chr13	exon20	28,592,664	synonymous SNV	NM_004119	c.A2481C	p.I827I		T	G	11,282	8.4%	0.0%	0.0%	0.0%	0.0%	12.1%	9.4%	11.5%	5.3%	12.6%	11.5%	10.3%	10.7%	3.1%	8.6%	10.8%
FLT3	chr13	intronic	28,589,267					rs4073630	C	T	540,800	99.9%	99.2%	99.0%	99.8%	99.8%	100.0%	99.7%	100.0%	99.5%	99.9%	99.9%	99.2%	99.6%	99.5%	99.7%	99.6%
FLT3	chr13	intronic	28,610,183					rs2491231	A	G	567,945	99.9%	99.8%	100.0%	99.5%	100.0%	100.0%	99.9%	100.0%	99.8%	100.0%	99.6%	100.0%	100.0%	99.9%	100.0%	99.9%
JAK2	chr9	exon6	5,050,706	synonymous SNV	NM_004972	c.C489T	p.H163H	rs10429491	C	T	542,211	99.8%	99.3%	99.7%	98.8%	98.2%	99.7%	99.8%	100.0%	99.4%	99.7%	99.6%	100.0%	99.7%	99.9%	99.8%	99.5%
MET	chr7	exon17	116,418,845	nonsynonymous SNV	NM_001127500	c.G3410A	p.G1137E		G	A	112	0.1%	6.0%	8.0%	5.7%	10.6%	0.0%	0.0%	0.0%	0.0%	0.0%	0.0%	0.0%	0.0%	0.1%	0.0%	0.1%
MLH1	chr3	exon8	37,053,568	nonsynonymous SNV	NM_000249	c.A655G	p.I219V	rs1799977	A	G	55,697	39.6%	50.1%	46.0%	49.7%	48.2%	35.0%	40.3%	37.6%	36.9%	32.1%	34.5%	35.6%	43.3%	36.3%	39.7%	34.0%
MLH1	chr3	intronic	37,083,740					rs9876116	A	G	439,668	99.8%	99.4%	99.5%	100.0%	99.5%	99.2%	99.7%	99.7%	99.9%	99.8%	99.9%	99.5%	99.8%	99.8%	100.0%	99.8%
MSH2	chr2	exon13	47,703,584	nonsynonymous SNV	NM_000251	c.T2084G	p.V695G		T	G	130,173	0.1%	61.7%	90.5%	63.0%	82.6%	43.3%	46.3%	47.9%	50.6%	50.3%	55.6%	54.9%	56.1%	48.9%	55.0%	47.3%
MSH2	chr2	exon13	47,703,583	nonsynonymous SNV	NM_000251	c.G2083T	p.V695L		G	T	159,208	0.0%	61.3%	90.5%	62.8%	82.8%	43.4%	46.4%	47.4%	50.6%	50.0%	55.5%	54.6%	55.6%	48.6%	54.9%	47.1%
MSH2	chr2	exon13	47,703,523	stopgain SNV	NM_000251	c.A2023T	p.K675X		A	T	168,500	0.2%	10.3%	9.4%	36.7%	17.3%	56.0%	52.8%	51.3%	49.1%	49.6%	43.6%	44.6%	43.7%	50.9%	44.6%	51.8%
NF1	chr17	exon4	29,490,352	nonsynonymous SNV	NM_001042492	c.G437A	p.S146N		G	A	25,290	12.6%	0.0%	0.0%	0.0%	0.0%	9.7%	12.1%	11.8%	8.7%	12.0%	12.5%	10.1%	12.4%	7.3%	10.9%	11.7%
NF1	chr17	intronic	29,654,876					rs2285894	T	A	247,813	51.0%	45.6%	55.5%	44.0%	46.3%	53.8%	56.2%	53.1%	52.0%	43.9%	46.3%	46.0%	48.9%	47.7%	49.3%	56.1%
PDGFRA	chr4	exon23	55,161,391	synonymous SNV	NM_006206	c.T3222C	p.D1074D	rs7685117	T	C	359,253	100.0%	99.7%	99.4%	99.8%	99.9%	99.8%	99.8%	100.0%	99.3%	99.8%	99.6%	99.6%	99.7%	100.0%	99.7%	99.6%
PDGFRA	chr4	exon22	55,156,588	nonsynonymous SNV	NM_006206	c.G2989A	p.E997K		G	A	104	3.7%	0.2%	0.2%	0.0%	0.2%	6.4%	7.2%	4.6%	4.2%	6.5%	5.5%	5.1%	5.8%	4.1%	5.1%	5.6%
PDGFRA	chr4	exon23	55,161,302	nonsynonymous SNV	NM_006206	c.T3133C	p.S1045P		T	C	4,194	10.9%	0.7%	0.5%	0.8%	0.6%	7.9%	7.9%	6.5%	7.1%	9.0%	7.9%	6.5%	6.6%	8.3%	8.2%	7.9%
PIK3CA	chr3	exon21	178,952,085	nonsynonymous SNV	NM_006218	c.A3140G	p.H1047R	rs121913279	A	G	190,418	0.6%	0.0%	39.9%	42.3%	58.0%	42.0%	44.5%	50.8%	43.8%	47.2%	50.7%	50.4%	47.0%	46.9%	51.6%	44.9%
PIK3CA	chr3	intronic	178,922,274					rs2699896	C	A	300,155	99.8%	99.5%	99.3%	100.0%	99.5%	99.8%	99.2%	99.4%	99.4%	98.6%	99.0%	99.6%	99.4%	99.8%	100.0%	99.5%
RB1	chr13	exon16	48,954,376	nonsynonymous SNV	NM_000321	c.C1497A	p.S499R		C	A	175	2.2%	0.0%	0.0%	0.0%	0.0%	5.5%	5.5%	2.9%	3.8%	3.5%	4.0%	7.0%	5.2%	2.4%	3.8%	6.6%
RB1	chr13	intronic	48,919,358					rs198617	T	G	376,268	99.9%	99.7%	100.0%	99.7%	99.7%	99.9%	99.8%	99.9%	99.8%	100.0%	99.8%	99.8%	99.7%	100.0%	99.7%	99.9%
RB1	chr13	intronic	48,916,895					rs520342	C	T	156,530	47.5%	0.0%	0.0%	0.0%	0.0%	46.9%	49.2%	50.2%	46.4%	48.8%	48.1%	51.0%	54.5%	49.9%	54.4%	48.5%
SMAD4	chr18	exon12	48,604,803	nonsynonymous SNV	NM_005359	c.C1625T	p.T542I		C	T	539	0.1%	0.1%	0.2%	1.3%	0.6%	4.1%	4.3%	9.1%	5.1%	0.0%	3.8%	0.3%	0.0%	0.2%	0.2%	0.0%
SMO	chr7	exon6	128,846,413	nonsynonymous SNV	NM_005631	c.T1249G	p.Y417D		T	G	221	5.7%	0.0%	0.1%	0.0%	0.0%	5.7%	4.0%	2.8%	2.5%	4.4%	5.6%	2.9%	4.1%	0.0%	4.0%	7.6%
STK11	chr19	UTR5	1,206,903						T	C	9,980	0.6%	25.4%	26.6%	24.3%	30.1%	0.4%	0.0%	0.3%	1.2%	0.5%	0.0%	0.3%	0.4%	0.1%	0.2%	0.2%
TP53	chr17	exon4	7,577,076	nonsynonymous SNV	NM_001126115	c.A466C	p.N156H		T	G	6,864	0.0%	9.8%	10.5%	6.7%	11.2%	0.1%	0.0%	0.1%	0.0%	0.0%	0.0%	0.0%	0.1%	0.0%	0.0%	0.0%
TP53	chr17	exon4	7,579,472	nonsynonymous SNV	NM_001126114	c.C215G	p.P72R	rs1042522	G	C	394,647	44.7%	47.7%	52.1%	43.0%	51.7%	45.6%	46.9%	49.0%	48.4%	47.3%	45.8%	50.7%	47.4%	49.1%	48.1%	46.1%
TP53	chr17	intronic	7,579,801					rs1642785	G	C	131,658	47.5%	49.8%	39.5%	55.4%	50.2%	44.7%	51.3%	40.7%	41.7%	45.3%	40.6%	45.7%	47.1%	47.6%	42.9%	49.0%

Table S7. SNVs in CT59

Gene	CHR	Location	Position	Type	NCBI Ref	Coding	Protein	RS	Ref. Allele	Var. Allele	Q Score	Variant Allele Frequency (%)								
												Patient Normal	Patient Tumor	1° xenografts				2° xenografts		
														tm1	tm2	tm3	tm4	tm1	tm2	tm3
AAAS	chr12	exon5	53,708,910	synonymous SNV	NM_015665	c.T414C	p.D138D	rs11540353	A	G	103,607	51.6%	49.9%	45.5%	49.6%	46.1%	46.1%	45.8%	46.5%	44.9%
AMT	chr3	exon8	49,455,330	synonymous SNV	NM_000481	c.G954A	p.R318R	rs11715915	C	T	129,223	48.5%	57.5%	44.2%	45.9%	47.9%	51.9%	49.9%	57.2%	53.0%
APC	chr5	intronic	112,136,892						T	C	3,441	12.7%	16.7%	11.8%	13.2%	11.6%	15.7%	15.1%	16.8%	20.2%
APC	chr5	exon16	112,176,559	synonymous SNV	NM_000038	c.T5268G	p.S1756S	rs866006	T	G	136,160	100.0%	100.0%	99.6%	99.6%	100.0%	99.7%	100.0%	99.9%	100.0%
APC	chr5	exon12	112,162,855	nonsynonymous SNV	NM_000038	c.G1459A	p.G487R		G	A	49,868	0.0%	13.4%	63.1%	50.8%	56.1%	49.8%	55.8%	47.4%	48.6%
APC	chr5	exon12	112,162,854	synonymous SNV	NM_000038	c.T1458C	p.Y486Y	rs2229992	T	C	135,746	100.0%	100.0%	99.6%	100.0%	100.0%	99.7%	100.0%	100.0%	100.0%
APC	chr5	exon16	112,177,171	synonymous SNV	NM_000038	c.G5880A	p.P1960P	rs465899	G	A	220,648	99.5%	99.7%	100.0%	99.5%	99.5%	99.7%	99.9%	99.4%	99.2%
APC	chr5	exon16	112,176,325	synonymous SNV	NM_000038	c.G5034A	p.G1678G	rs42427	G	A	185,369	99.6%	99.3%	99.1%	99.7%	99.8%	98.1%	99.3%	99.0%	100.0%
APEH	chr3	exon9	49,714,225	synonymous SNV	NM_001640	c.T852C	p.Y284Y	rs1131095	T	C	116,749	51.0%	48.5%	51.1%	49.5%	40.8%	48.7%	49.8%	47.4%	50.0%
APOB	chr2	exon4	21,263,900	nonsynonymous SNV	NM_000384	c.C293T	p.T98I	rs1367117	G	A	103,923	46.6%	42.6%	66.3%	58.3%	75.9%	69.2%	93.9%	96.1%	85.9%
BMPR1A	chr10	intronic	88,659,754					rs148331454	A	G	113,705	46.5%	45.1%	61.9%	49.6%	50.0%	56.5%	48.7%	51.2%	53.7%
BRAF	chr7	exon15	140,453,136	nonsynonymous SNV	NM_004333	c.T1799A	p.V600E	rs113488022	A	T	145,650	0.1%	43.3%	56.7%	58.5%	55.0%	58.0%	69.3%	66.2%	60.9%
BRCA2	chr13	exon11	32,912,299	synonymous SNV	NM_000059	c.T3807C	p.V1269V	rs543304	T	C	22,993	55.0%	52.8%	41.8%	51.3%	48.7%	52.8%	57.0%	56.9%	50.5%
BRCA2	chr13	exon10	32,906,729	nonsynonymous SNV	NM_000059	c.A1114C	p.N372H	rs144848	A	C	103,710	43.5%	45.3%	46.5%	45.4%	52.6%	48.5%	50.8%	50.3%	45.8%
BSN	chr3	exon5	49,689,210	nonsynonymous SNV	NM_003458	c.G2221A	p.A741T	rs34762726	G	A	91,590	52.2%	50.1%	49.8%	47.1%	44.2%	48.8%	54.1%	47.3%	48.2%
C18orf26	chr18	exon1	52,258,548	nonsynonymous SNV	NM_173629	c.T113C	p.V38A	rs35428499	T	C	68,874	51.7%	55.0%	48.6%	53.1%	50.7%	50.0%	51.6%	51.6%	50.3%
C9orf174	chr9	exon2	100,070,351	synonymous SNV	NM_020893	c.G138C	p.S46S	rs12683119	G	C	197,464	100.0%	99.9%	99.1%	100.0%	99.8%	99.6%	100.0%	100.0%	99.7%
CAV3	chr3	exon1	8,775,589	synonymous SNV	NM_001234	c.C27T	p.L9L	rs1974763	C	T	123,792	53.2%	48.1%	48.6%	53.1%	47.9%	46.3%	45.1%	46.2%	46.5%
CD3E	chr11	exon3	118,178,007	synonymous SNV	NM_000733	c.C54T	p.G18G	rs4606515	C	T	127,591	47.0%	43.5%	48.5%	47.8%	55.5%	52.9%	49.2%	47.4%	50.4%
CDH1	chr16	intronic	68,771,372					rs3743674	C	T	109,665	99.8%	99.4%	99.5%	99.6%	99.7%	99.7%	100.0%	99.1%	99.7%
CDH1	chr16	exon13	68,857,441	synonymous SNV	NM_004360	c.T2076C	p.A692A	rs1801552	T	C	207,194	45.3%	53.1%	99.5%	99.4%	99.1%	97.8%	99.3%	99.2%	99.4%
CDKN2A	chr9	UTR3	21,968,199					rs11515	C	G	203,106	99.6%	99.9%	99.6%	99.2%	99.3%	99.7%	99.7%	99.8%	99.9%
CNOT1	chr16	exon9	58,616,984	synonymous SNV	NM_206999	c.A909G	p.G303G	rs17854029	T	C	254,452	99.9%	99.9%	100.0%	100.0%	99.7%	100.0%	100.0%	99.8%	100.0%
COQ6	chr14	exon4	74,424,938	synonymous SNV	NM_182480	c.T345C	p.H115H	rs3180946	T	C	204,071	99.7%	99.5%	100.0%	100.0%	99.5%	100.0%	100.0%	99.7%	99.6%
CSF1R	chr5	exon9	149,449,827	nonsynonymous SNV	NM_005211	c.G1237A	p.G413S	rs34951517	C	T	71,085	58.1%	50.3%	48.8%	45.4%	52.6%	44.8%	49.1%	60.4%	52.5%
DTX2	chr7	exon9	76,132,898	synonymous SNV	NM_001102594	c.T1545C	p.G515G	rs17855260	T	C	114,999	54.7%	49.4%	49.1%	46.0%	53.3%	46.8%	44.8%	52.0%	49.2%
EGFR	chr7	intronic	55,220,407						G	A	80	0.7%	0.0%	0.0%	0.8%	0.2%	0.0%	0.0%	0.0%	0.0%
EGFR	chr7	intronic	55,220,406						C	T	37	0.0%	0.0%	1.0%	0.0%	0.0%	0.9%	0.3%	0.0%	0.2%
EGFR	chr7	intronic	55,220,408						C	T	56	0.2%	0.0%	0.3%	0.3%	0.2%	0.3%	0.0%	0.5%	0.0%
EGFR	chr7	exon23	55,266,417	synonymous SNV	NM_005228	c.T2709C	p.T903T	rs1140475	T	C	246,278	99.6%	99.6%	99.9%	99.7%	99.8%	99.7%	99.7%	99.8%	99.9%
EGFR	chr7	exon20	55,249,063	synonymous SNV	NM_005228	c.G2361A	p.Q787Q	rs1050171	G	A	537,876	99.6%	99.5%	99.4%	98.8%	99.4%	99.3%	99.4%	99.4%	99.3%
EPHA8	chr1	intronic	22,919,951						G	A	173	0.3%	1.3%	0.0%	0.7%	0.5%	1.1%	0.5%	0.6%	0.7%
FBXW7	chr4	exon3	153,268,144	stopgain SNV	NM_001013415	c.C310T	p.R104X		G	A	87,009	0.2%	22.2%	50.5%	45.2%	46.9%	51.1%	53.1%	45.9%	51.0%
FBXW7	chr4	exon9	153,247,224	nonsynonymous SNV	NM_001013415	c.G1224T	p.W408C		C	A	173,859	0.0%	16.6%	49.0%	56.1%	53.7%	46.2%	50.5%	51.2%	51.1%
FGFR2	chr10	exon6	123,298,158	synonymous SNV	NM_001144917	c.A696G	p.V232V	rs1047100	T	C	120,948	53.3%	51.0%	54.8%	45.8%	48.3%	53.6%	49.2%	53.5%	47.7%
FGFR3	chr4	intronic	1,806,519					rs3135890	C	T	117,478	52.4%	47.5%	49.6%	52.7%	55.1%	45.3%	51.6%	47.9%	51.8%
FGFR3	chr4	intronic	1,805,593					rs3135886	G	C	105,315	48.8%	45.8%	50.2%	45.9%	49.4%	53.1%	53.2%	49.2%	46.4%
FGFR3	chr4	exon12	1,807,894	synonymous SNV	NM_022965	c.G1617A	p.T539T	rs7688609	G	A	264,982	99.6%	99.7%	99.8%	99.6%	99.6%	99.5%	99.3%	99.5%	99.2%
FLT3	chr13	exon11	28,610,134	stopgain SNV	NM_004119	c.T1356A	p.C452X		A	T	83,692	0.0%	21.3%	50.7%	55.2%	52.2%	57.5%	48.9%	46.6%	49.6%
FLT3	chr13	intronic	28,610,183					rs2491231	A	G	228,020	99.9%	100.0%	100.0%	99.7%	100.0%	99.9%	99.9%	100.0%	100.0%
GDF9	chr5	intronic	132,198,287					rs254285	C	G	159,930	99.9%	100.0%	100.0%	99.8%	100.0%	100.0%	99.9%	99.5%	100.0%
GDF9	chr5	exon2	132,198,199	synonymous SNV	NM_005260	c.C447T	p.T149T	rs254286	G	A	113,013	48.3%	53.9%	58.8%	49.2%	49.2%	45.9%	53.1%	50.6%	55.2%
GRK4	chr4	intronic	3,009,435						T	C	31	0.0%	9.9%	0.0%	1.3%	0.0%	2.7%	2.4%	0.0%	1.0%
HIF1A	chr14	intronic	62,213,553					rs10147275	T	G	74,870	36.1%	37.6%	34.2%	36.7%	32.1%	32.7%	34.6%	32.5%	38.7%
HIF1A	chr14	intronic	62,213,626						A	G	1,427	0.2%	0.4%	0.1%	0.5%	0.4%	11.9%	0.4%	1.0%	0.5%
HRAS	chr11	exon2	534,270	nonsynonymous SNV	NM_176795	c.C53T	p.A18V		G	A	15,536	0.4%	9.3%	14.5%	20.8%	13.0%	21.4%	14.0%	23.8%	18.1%
IL9	chr5	exon5	135,228,165	nonsynonymous SNV	NM_000590	c.C350T	p.T117M	rs2069885	G	A	133,385	46.8%	52.6%	54.9%	50.0%	51.9%	42.5%	44.2%	47.0%	49.9%
IP6K2	chr3	exon6	48,725,707	synonymous SNV	NM_001005909	c.G1280A	p.X427X	rs1048940	C	T	84,756	46.0%	55.0%	48.9%	45.8%	49.6%	46.6%	48.4%	49.6%	48.4%
JAK2	chr9	exon6	5,050,706	synonymous SNV	NM_004972	c.C489T	p.H163H	rs10429491	C	T	109,383	100.0%	100.0%	98.9%	99.4%	99.1%	99.8%	99.6%	99.2%	99.2%
KIF6	chr6	exon7	39,563,863	synonymous SNV	NM_145027	c.G813A	p.K271K	rs7738892	C	T	113,933	53.1%	46.0%	58.0%	46.4%	46.8%	48.4%	51.8%	46.1%	46.5%
KIT	chr4	exon20	55,603,362	synonymous SNV	NM_001093772	c.C2706T	p.C902C		C	T	78,478	0.1%	20.6%	50.5%	45.7%	46.0%	39.1%	50.0%	53.9%	48.0%

KIT	chr4	exon10	55,593,481	synonymous SNV	NM_001093772	c.A1626G	p.K542K	rs55986963	A	G	99,296	52.3%	52.8%	42.7%	56.7%	54.7%	49.6%	47.2%	45.8%	50.7%
KRTAP19-6	chr21	exon1	31,914,000	synonymous SNV	NM_181612	c.A153T	p.G51G	rs1023364	T	A	68,750	48.0%	34.9%	53.0%	46.9%	43.5%	44.9%	48.3%	43.9%	43.3%
KRTAP19-6	chr21	exon1	31,914,093	synonymous SNV	NM_181612	c.T60C	p.G20G		A	G	73,848	0.6%	14.7%	53.1%	47.1%	43.8%	45.5%	49.0%	44.1%	44.6%
LDLR	chr19	exon12	11,227,602	synonymous SNV	NM_001195798	c.C1773T	p.N591N	rs688	C	T	103,814	42.6%	46.1%	49.7%	48.0%	52.2%	49.9%	48.3%	49.0%	52.8%
LOC57653	chr9	ncRNA	100,070,435					rs2401382	C	T	122,142	99.7%	99.3%	99.1%	99.2%	99.8%	100.0%	98.9%	99.8%	99.7%
MBD4	chr3	exon3	129,155,670	nonsynonymous SNV	NM_003925	c.G817A	p.A273T	rs10342	C	T	121,285	49.1%	45.3%	49.4%	47.2%	47.8%	54.5%	49.9%	54.2%	52.0%
MET	chr7	exon17	116,418,845	nonsynonymous SNV	NM_001127500	c.G3410A	p.G1137E		G	A	2,170	10.9%	9.3%	11.8%	11.4%	11.5%	10.4%	8.7%	11.8%	11.6%
MET	chr7	exon20	116,435,768	synonymous SNV	NM_001127500	c.C3912T	p.D1304D	rs41736	C	T	369,805	99.0%	98.4%	99.2%	99.5%	99.5%	99.8%	99.7%	99.6%	99.5%
MST1	chr3	exon18	49,721,532	nonsynonymous SNV	NM_020998	c.C2107T	p.R703C	rs3197999	G	A	67,608	52.8%	48.6%	53.5%	57.8%	44.4%	51.1%	50.3%	44.4%	47.7%
NEO1	chr15	exon19	73,564,881	synonymous SNV	NM_002499	c.C2943T	p.S981S	rs1131854	C	T	105,238	52.8%	46.6%	51.2%	58.9%	47.6%	55.0%	46.7%	51.7%	43.9%
NF1	chr17	exon35	29,588,752	nonsynonymous SNV	NM_001042492	c.G4601A	p.R1534Q		G	A	39	0.0%	0.0%	0.3%	0.0%	0.5%	0.0%	0.4%	0.2%	0.3%
NF1	chr17	intronic	29,654,876					rs2285894	T	A	201,624	99.4%	98.1%	99.2%	99.0%	99.8%	99.5%	99.0%	99.2%	99.1%
NLRP1	chr17	exon3	5,485,367	nonsynonymous SNV	NM_001033053	c.T464A	p.L155H	rs12150220	A	T	30,659	44.6%	54.4%	52.5%	47.6%	48.1%	49.8%	58.6%	50.2%	53.0%
NOTCH1	chr9	intronic	139,401,504					rs3124596	G	A	30,878	99.7%	98.8%	99.3%	99.4%	98.9%	98.7%	99.5%	99.1%	99.4%
OLFM2	chr19	exon4	9,968,139	nonsynonymous SNV	NM_058164	c.C380T	p.T127M	rs11556087	G	A	104,142	47.8%	46.8%	45.0%	51.8%	43.7%	46.8%	49.3%	47.0%	47.9%
OR10A4	chr11	exon1	6,898,495	nonsynonymous SNV	NM_207186	c.T617C	p.L206P	rs2595453	T	C	138,718	54.5%	49.3%	45.2%	51.7%	54.3%	48.0%	50.8%	52.2%	47.5%
OR2L3	chr1	exon1	248,224,754	synonymous SNV	NM_001004687	c.T771C	p.T257T	rs55893924	T	C	125,821	53.1%	45.3%	31.6%	33.3%	32.8%	34.5%	34.3%	37.4%	34.1%
OR51B5	chr11	exon1	5,364,450	nonsynonymous SNV	NM_001005567	c.T305C	p.I102T	rs11036912	A	G	115,602	50.7%	45.7%	53.7%	49.6%	50.7%	46.6%	48.1%	40.3%	46.4%
PALM	chr19	exon5	731,144	nonsynonymous SNV	NM_001040134	c.A319G	p.T107A	rs1050457	A	G	73,708	55.0%	53.9%	57.1%	54.8%	44.9%	58.9%	42.3%	49.7%	49.3%
PDGFRA	chr4	intronic	55,133,936					rs28489067	C	T	14,802	47.9%	27.3%	0.2%	0.6%	0.7%	0.1%	0.0%	0.0%	0.1%
PDGFRA	chr4	intronic	55,133,959					rs28650939	C	T	90,908	50.1%	46.8%	48.2%	45.9%	47.6%	50.2%	51.9%	44.2%	46.5%
PDGFRA	chr4	exon7	55,133,806	nonsynonymous SNV	NM_006206	c.G1019C	p.R340P	rs77524207	G	C	117	0.8%	0.4%	1.3%	1.1%	0.7%	0.4%	0.6%	0.9%	0.5%
PDGFRA	chr4	exon23	55,161,391	synonymous SNV	NM_006206	c.T3222C	p.D1074D	rs7685117	T	C	181,173	99.9%	99.9%	99.5%	99.4%	99.9%	99.7%	99.9%	99.9%	99.7%
PDGFRA	chr4	intronic	55,161,254					rs3733540	C	T	100,884	51.1%	45.7%	52.9%	52.6%	50.9%	49.2%	49.0%	52.3%	53.2%
PDGFRA	chr4	exon18	55,152,040	synonymous SNV	NM_006206	c.C2472T	p.V824V	rs2228230	C	T	74,318	49.3%	52.9%	51.1%	52.9%	50.4%	58.1%	41.0%	48.1%	53.3%
PDGFRA	chr4	intronic	55,129,831					rs55947416	C	T	95,274	51.6%	43.6%	46.5%	53.6%	48.1%	49.4%	46.7%	45.8%	47.4%
PDGFRA	chr4	intronic	55,151,711					rs2412559	C	A	244,189	99.8%	99.7%	98.8%	99.7%	99.4%	99.4%	99.7%	99.5%	99.7%
PDGFRA	chr4	exon10	55,139,771	nonsynonymous SNV	NM_006206	c.T1432C	p.S478P	rs35597368	T	C	81,976	39.3%	44.2%	46.7%	45.4%	44.2%	44.6%	46.8%	40.4%	44.6%
PDGFRA	chr4	exon12	55,141,054	nonsynonymous SNV	NM_006206	c.C1700T	p.P567L		C	T	115,220	0.3%	24.0%	45.2%	47.8%	56.3%	51.5%	48.6%	43.6%	54.2%
PIK3CA	chr3	intronic	178,922,274					rs2699896	C	A	187,038	99.6%	97.3%	99.7%	99.5%	99.5%	99.2%	99.2%	100.0%	99.5%
PLEKHG2	chr19	exon9	39,908,574	synonymous SNV	NM_022835	c.C912T	p.T304T	rs35466645	C	T	32,696	54.4%	44.8%	39.2%	58.2%	45.9%	58.2%	49.9%	55.3%	52.5%
PLEKHG2	chr19	exon5	39,907,036	synonymous SNV	NM_022835	c.C528T	p.A176A	rs2277743	C	T	169,263	99.7%	99.7%	99.8%	99.7%	99.5%	99.8%	99.5%	99.3%	99.5%
PRIC285	chr20	exon5	62,200,575	synonymous SNV	NM_001037335	c.A1014G	p.S338S	rs1741594	T	C	217,459	99.9%	99.9%	99.8%	99.7%	99.7%	99.7%	99.8%	99.6%	99.9%
PSG9	chr19	exon4	43,763,059	nonsynonymous SNV	NM_002784	c.G938A	p.R313Q	rs12977717	C	T	93,368	54.8%	55.3%	62.3%	60.8%	60.2%	47.2%	56.0%	46.8%	57.5%
RB1	chr13	intronic	49,051,481					rs77317605	T	A	33,607	99.1%	100.0%	98.1%	100.0%	98.8%	100.0%	100.0%	98.9%	99.1%
RB1	chr13	intronic	48,919,358					rs198617	T	G	82,809	100.0%	100.0%	100.0%	100.0%	100.0%	100.0%	99.7%	100.0%	100.0%
RET	chr10	exon13	43,613,843	synonymous SNV	NM_020975	c.G2307T	p.L769L	rs1800861	G	T	249,557	99.7%	99.1%	99.1%	99.6%	99.6%	99.6%	99.7%	99.3%	99.9%
ROGDI	chr16	exon6	4,849,705	synonymous SNV	NM_024589	c.G414A	p.T138T	rs11553876	C	T	121,590	50.9%	51.1%	56.7%	46.7%	48.5%	46.5%	50.6%	43.3%	51.9%
RUNX1	chr21	exon4	36,206,719	nonsynonymous SNV	NM_001001890	c.A712G	p.S238G		T	C	83	7.2%	7.8%	12.2%	8.7%	7.9%	7.4%	8.5%	8.3%	7.6%
SACM1L	chr3	intronic	45,754,749					rs2248991	G	A	138,507	99.0%	99.3%	100.0%	99.1%	99.3%	99.5%	99.8%	99.8%	99.7%
SENP6	chr6	exon23	76,425,288	nonsynonymous SNV	NM_001100409	c.A3296G	p.Y1099C	rs9250	A	G	409,665	99.9%	99.7%	99.5%	99.9%	99.9%	99.9%	99.8%	100.0%	100.0%
SFTPC	chr8	exon5	22,021,530	synonymous SNV	NM_003018	c.C570T	p.G190G		C	T	48	0.0%	0.5%	0.0%	0.0%	0.0%	0.0%	0.1%	0.0%	0.5%
SFTPC	chr8	intronic	22,021,388					rs2070687	C	G	72,398	49.6%	51.7%	57.5%	45.1%	53.1%	45.0%	53.1%	52.2%	46.2%
SMARCAD1	chr4	exon10	95,186,055	synonymous SNV	NM_020159	c.A1479G	p.Q493Q	rs2306802	A	G	293,086	100.0%	100.0%	99.8%	100.0%	99.9%	99.9%	100.0%	99.9%	99.9%
SMO	chr7	intronic	128,845,018					rs2703091	C	T	223,271	99.8%	99.4%	99.5%	99.6%	100.0%	99.8%	99.7%	98.7%	98.9%
SMO	chr7	intronic	128,846,469					rs2735842	A	G	412,884	99.9%	99.4%	99.8%	99.6%	99.9%	100.0%	99.9%	99.9%	99.7%
STK11	chr19	UTR5	1,206,903						T	C	17,231	26.0%	23.5%	25.5%	25.3%	21.8%	29.7%	23.1%	25.0%	28.4%
SYNE2	chr14	exon3	64,686,125	synonymous SNV	NM_182910	c.G381T	p.L127L	rs35648226	G	T	65,587	45.8%	48.0%	46.9%	46.9%	58.1%	49.1%	51.7%	42.1%	46.9%
SYNE2	chr14	intronic	64,686,207					rs915057	A	G	95,715	46.2%	48.9%	46.6%	46.8%	58.1%	49.6%	51.9%	42.4%	47.7%
TACC2	chr10	exon6	123,970,465	synonymous SNV	NM_206861	c.G963A	p.T321T		G	A	190	0.2%	0.0%	0.0%	0.1%	0.1%	1.0%	0.0%	0.6%	0.1%
TECPR2	chr14	exon9	102,901,201	nonsynonymous SNV	NM_001172631	c.A2047G	p.I683V	rs10149146	A	G	135,622	51.3%	52.5%	47.0%	54.1%	46.2%	48.7%	55.7%	45.6%	50.6%
TP53	chr17	intronic	7,579,801					rs1642785	G	C	47,855	97.5%	99.6%	97.8%	99.4%	99.0%	99.2%	99.4%	98.1%	100.0%
TP53	chr17	intronic	7,577,457						G	A	131	9.5%	8.6%	9.3%	5.8%	5.9%	7.4%	7.5%	7.3%	7.0%
TP53	chr17	exon4	7,579,472	nonsynonymous SNV	NM_001126114	c.C215G	p.P72R	rs1042522	G	C	266,809	99.4%	99.7%	99.9%	99.9%	99.6%	99.9%	99.9%	99.8%	99.8%
TP53	chr17	exon8	7,577,076	nonsynonymous SNV	NM_001126114	c.A862C	p.N288H		T	G	4,437	9.2%	9.2%	4.5%	4.9%	5.6%	4.3%	6.8%	5.8%	4.6%
TP53	chr17	exon8	7,577,090	nonsynonymous SNV	NM_001126114	c.G848A	p.R283H		C	T	101,569	0.2%	20.8%	48.9%	43.4%	45.9%	48.2%	49.1%	40.8%	48.9%

TP53	chr17	exon5	7,578,430	nonsynonymous SNV	NM_001126114	c.A500C	p.Q167P		T	G	79,720	49.2%	60.7%	62.2%	63.5%	61.1%	65.7%	60.9%	61.7%	59.9%
TP53	chr17	exon6	7,578,263	stopgain SNV	NM_001126114	c.C586T	p.R196X		G	A	83,674	0.0%	13.7%	33.4%	41.1%	35.7%	38.9%	35.4%	37.0%	32.9%
TRAK2	chr2	exon5	202,264,156	nonsynonymous SNV	NM_015049	c.G424A	p.V142I	rs13022344	C	T	274,054	99.7%	100.0%	99.7%	99.7%	99.5%	99.6%	99.5%	99.7%	99.7%
UBQLN1	chr9	exon10	86,278,913	synonymous SNV	NM_013438	c.G1494A	p.S498S	rs2781004	C	T	103,755	51.7%	47.4%	41.3%	50.0%	49.8%	53.6%	47.1%	52.9%	52.1%
USP19	chr3	exon2	49,156,473	nonsynonymous SNV	NM_001199162	c.G106C	p.D36H	rs11552724	C	G	83,816	55.1%	54.9%	48.3%	50.4%	44.6%	44.7%	45.6%	43.3%	47.7%
USP4	chr3	exon5	49,362,369	synonymous SNV	NM_199443	c.G591A	p.K197K	rs56038006	C	T	112,461	49.0%	45.2%	53.2%	41.7%	54.3%	49.7%	47.4%	53.8%	49.6%

Table S8. Somatically aquired SNVs in CT38 as determined by exome sequencing

Gene	Chr	Exon	Pos	Type	NCBI Ref	Coding	Protein	Ref. Allele	Var. Allele	Q Score	Variant Allele Frequency (%)							
											Patient Normal	Patient Tumor	1° xenografts		2° xenografts		4° xenografts	
													tm1	tm2	tm1	tm2	tm1	tm2
ABCA13	chr7	exon17	48312208	nonsynonymous SNV	NM_152701	c.G2945T	p.G982V	G	T	34,926	0.2%	36.4%	52.1%	46.8%	52.7%	52.3%	46.8%	47.5%
ABCA2	chr9	intronic	139914664					C	T	12,322	0.0%	30.9%	44.2%	47.8%	46.2%	50.3%	50.0%	47.5%
ABCG1	chr21	intronic	43704605					G	A	16,104	0.0%	33.5%	42.1%	52.7%	48.7%	47.6%	36.7%	48.8%
ABI3BP	chr3	intronic	100484940					C	A	2,535	0.0%	39.5%	51.4%	58.6%	21.4%	57.1%	41.7%	46.7%
ABL1	chr9	exon11	133759719	nonsynonymous SNV	NM_005157	c.T2042C	p.F681S	T	C	36,051	0.3%	34.5%	50.1%	52.3%	48.5%	51.7%	48.2%	49.4%
ACOX2	chr3	exon3	58520136	nonsynonymous SNV	NM_003500	c.C274T	p.R92W	G	A	12,108	0.0%	36.1%	33.5%	45.3%	45.8%	42.2%	29.4%	41.4%
ACSF3	chr16	ncRNA	89220672					G	A	19,271	0.5%	31.5%	54.7%	52.4%	45.1%	51.3%	45.9%	46.3%
ACTN2	chr1	intronic	236891098					G	A	36,866	0.2%	34.9%	50.2%	52.6%	49.8%	47.6%	55.2%	44.3%
ADAMTS1	chr21	exon1	28216984	nonsynonymous SNV	NM_006988	c.C290T	p.A97V	G	A	25,934	0.3%	36.7%	50.6%	50.3%	56.3%	45.6%	37.8%	55.5%
ADAMTS19	chr5	intronic	128862362					T	A	1,022	0.0%	46.2%	35.7%	NoCall	57.9%	NoCall	NoCall	NoCall
ADAMTSL1	chr9	intronic	18718637					G	A	6,434	0.0%	30.1%	58.0%	42.5%	57.8%	56.1%	51.9%	51.1%
ADD2	chr2	intronic	70933831					C	T	8,716	0.0%	50.8%	100.0%	100.0%	100.0%	100.0%	100.0%	94.1%
ADRB1	chr10	exon1	115804827	synonymous SNV	NM_000684	c.G936A	p.S312S	G	A	9,384	0.0%	36.1%	38.5%	48.1%	40.6%	43.2%	43.6%	39.4%
AGMO	chr7	exon8	15430364	nonsynonymous SNV	NM_001004320	c.G754T	p.A252S	C	A	11,890	0.0%	32.8%	45.5%	40.3%	41.1%	47.5%	37.5%	54.2%
AIM1L	chr1	intronic	26663887					G	A	37,802	0.0%	56.2%	100.0%	100.0%	99.4%	99.3%	100.0%	100.0%
ALK	chr2	intronic	29450181					C	T	14,583	0.0%	33.1%	42.2%	43.6%	48.9%	45.8%	50.0%	41.1%
AP1M1	chr19	intronic	16344156					G	A	5,602	0.0%	24.7%	58.2%	48.7%	54.2%	56.7%	55.6%	32.1%
AP3D1	chr19	exon28	2109148	nonsynonymous SNV	NM_003938	c.G3223A	p.D1075N	C	T	35,046	0.0%	35.9%	35.5%	44.4%	51.7%	43.5%	28.8%	42.3%
AP4E1	chr15	exon18	51289708	nonsynonymous SNV	NM_007347	c.G2532T	p.K844N	G	T	32,290	0.0%	32.5%	46.9%	48.3%	49.1%	49.2%	45.9%	46.5%
APC	chr5	exon16	112175197	synonymous SNV	NM_000038	c.G3906A	p.L1302L	G	A	45,340	0.0%	57.8%	100.0%	100.0%	100.0%	100.0%	100.0%	100.0%
APC	chr5	exon16	112175198	stopgain SNV	NM_000038	c.C3907T	p.Q1303X	C	T	44,976	0.0%	56.8%	100.0%	100.0%	99.5%	99.4%	100.0%	100.0%
APC	chr5	exon16	112175202	nonsynonymous SNV	NM_000038	c.T3911A	p.I1304K	T	A	49,126	0.0%	57.6%	100.0%	100.0%	99.5%	100.0%	100.0%	100.0%
ARHGAP32	chr11	exon22	128840436	nonsynonymous SNV	NM_001142685	c.G4630A	p.A1544T	C	T	46,129	0.0%	46.2%	100.0%	99.3%	98.3%	99.5%	99.4%	100.0%
ARHGAP40	chr20	exon9	37267961	nonsynonymous SNV	NM_001164431	c.G1208T	p.R403M	G	T	31,983	0.0%	22.7%	30.1%	31.2%	34.1%	30.9%	35.1%	32.2%
ARHGEF10	chr8	intronic	1874495					C	T	10,896	0.0%	32.9%	49.1%	50.8%	51.2%	54.1%	44.4%	50.0%
ARR3	chrX	intronic	69496633					G	C	17,648	0.0%	68.0%	61.5%	81.5%	93.8%	90.9%	55.4%	86.0%
ATAD2B	chr2	intronic	24008732					G	C	3,351	0.0%	29.0%	26.1%	42.2%	41.8%	48.3%	19.4%	47.1%
ATG9B	chr7	intronic	150720503					G	A	44,348	0.0%	37.9%	46.5%	47.0%	47.3%	47.8%	44.7%	45.9%
AXIN1	chr16	intronic	339426					G	A	19,359	0.3%	35.0%	40.5%	44.9%	47.8%	41.4%	35.9%	45.2%
B3GAT2	chr6	exon1	71666064	synonymous SNV	NM_080742	c.C69T	p.L23L	G	A	34,343	0.2%	29.7%	36.8%	41.4%	50.5%	46.7%	29.2%	49.7%
B4GALT6	chr18	intronic	29210851					G	A	24,083	0.0%	71.2%	100.0%	100.0%	100.0%	100.0%	100.0%	100.0%
BCL11B	chr14	exon4	99640863	synonymous SNV	NM_138576	c.G2310A	p.T770T	C	T	14,022	0.0%	37.1%	58.6%	48.7%	59.6%	62.6%	53.6%	57.4%
BPIL3	chr20	intronic	31623630					C	T	39,308	0.0%	54.1%	66.2%	66.1%	61.7%	64.0%	59.3%	63.0%
BRS3	chrX	intronic	135572742					T	G	19,678	0.0%	64.8%	100.0%	100.0%	100.0%	100.0%	100.0%	100.0%
C12orf48	chr12	exon11	102589752	stopgain SNV	NM_017915	c.A1423T	p.R475X	A	T	5,838	0.0%	33.0%	38.8%	41.7%	49.2%	45.5%	32.9%	46.8%
C13orf40	chr13	exon4	103388035	synonymous SNV	NM_001146197	c.A15012G	p.P5004P	T	C	29,603	0.3%	34.1%	48.0%	50.1%	49.2%	46.8%	51.4%	44.8%
C13orf40	chr13	exon4	103390783	synonymous SNV	NM_001146197	c.C12264T	p.C4088C	G	A	33,770	0.2%	29.6%	46.2%	49.0%	46.6%	51.4%	42.4%	47.2%
C19orf53	chr19	intergenic	13899760					C	A	5,964	0.0%	11.1%	41.5%	38.3%	54.2%	49.4%	35.0%	54.5%
C7	chr5	upstream	40909301					G	C	1,065	0.0%	52.6%	72.7%	NoCall	NoCall	NoCall	NoCall	NoCall
C7orf42	chr7	intronic	66418120					G	C	6,754	0.0%	32.4%	42.9%	39.3%	41.5%	45.3%	28.8%	42.3%
C8orf38	chr8	UTR5	96037230					C	G	4,664	0.0%	20.9%	56.3%	45.3%	39.7%	31.3%	48.3%	60.5%
C9orf142	chr9	intronic	139887178					C	T	10,457	0.0%	26.8%	29.0%	51.8%	53.4%	43.8%	33.1%	48.9%
C9orf86	chr9	exon13	139734238	synonymous SNV	NM_024718	c.C1851T	p.P617P	C	T	42,402	0.2%	39.1%	51.4%	50.9%	47.0%	47.4%	48.6%	55.6%
CACNA1B	chr9	UTR3	141016616					C	T	4,654	0.0%	22.2%	34.7%	48.5%	49.0%	57.4%	45.1%	73.9%
CACNA1H	chr16	intronic	1259817					C	T	1,718	0.0%	37.5%	33.3%	43.8%	42.1%	50.0%	54.5%	55.0%
CADPS2	chr7	intronic	121960479					T	C	18,809	0.0%	33.2%	55.4%	55.0%	48.1%	48.0%	53.6%	50.6%
CAMK2A	chr5	intronic	149624682					G	A	15,764	0.0%	33.8%	50.5%	52.7%	47.9%	45.9%	51.0%	58.2%
CARD11	chr7	intronic	2949845					G	A	13,003	0.5%	29.3%	46.9%	41.1%	51.5%	49.7%	44.4%	56.3%
CBLN1	chr16	intronic	49314819					G	C	11,820	0.0%	24.9%	32.4%	46.9%	53.2%	41.8%	39.8%	50.0%
CCDC162	chr6	intergenic	109661825					C	G	292	0.0%	27.7%	0.0%	0.0%	0.0%	0.0%	0.0%	0.0%
CD163	chr12	exon11	7637803	nonsynonymous SNV	NM_004244	c.G2668A	p.V890M	C	T	38,545	0.0%	35.7%	53.2%	50.3%	49.1%	49.4%	58.5%	45.4%
CDC14B	chr9	intronic	99296589					A	C	11,822	0.0%	32.8%	56.6%	46.2%	50.6%	51.4%	47.7%	54.7%
CDC27	chr17	intronic	45259162					G	A	4,348	2.0%	47.9%	42.0%	50.0%	31.4%	54.3%	37.9%	54.1%
CENPE	chr4	intronic	104069927					C	T	12,290	0.0%	32.5%	24.1%	39.0%	49.6%	44.7%	30.0%	43.2%
CES2	chr16	ncRNA	66976396					G	A	11,485	0.0%	31.8%	31.7%	43.7%	43.8%	50.0%	41.7%	46.9%
CHRNA4	chr20	intronic	61986918					G	A	24,102	0.0%	51.1%	68.8%	59.9%	60.0%	66.4%	58.9%	57.3%

CHRNA9	chr4	upstream	40337179					G	C	2,963	0.0%	35.5%	21.9%	55.2%	47.2%	57.1%	59.3%	61.1%
CHST8	chr19	exon4	34263103	nonsynonymous SNV	NM_022467	c.C410T	p.P137L	C	T	36,581	0.0%	32.5%	49.3%	47.5%	48.8%	48.1%	54.0%	47.5%
COL1A2	chr7	intronic	94024506					C	T	20,807	0.0%	28.3%	43.5%	50.3%	47.5%	45.5%	44.1%	52.6%
COL22A1	chr8	intronic	139610924					G	A	10,051	0.0%	37.7%	52.9%	48.9%	49.0%	46.0%	58.1%	39.2%
COL25A1	chr4	exon20	109784484	synonymous SNV	NM_198721	c.C1143T	p.P381P	G	A	22,520	0.0%	36.7%	66.9%	53.4%	55.5%	48.1%	59.5%	49.6%
COL5A1	chr9	intronic	137687341					C	T	9,603	0.0%	35.9%	44.9%	54.4%	39.2%	47.4%	58.4%	42.9%
COL5A1	chr9	intronic	137714737					G	A	20,730	0.0%	33.3%	57.0%	52.2%	50.8%	50.0%	63.0%	51.3%
COL5A2	chr2	intronic	189923763					C	T	8,690	0.9%	32.7%	48.9%	46.3%	51.0%	50.7%	43.3%	51.1%
COL6A6	chr3	exon7	130292935	nonsynonymous SNV	NM_001102608	c.G3113A	p.R1038Q	G	A	16,895	0.0%	29.5%	49.0%	42.0%	49.7%	40.9%	47.7%	48.4%
CRHBP	chr5	exon7	76264618	nonsynonymous SNV	NM_001882	c.C877T	p.R293C	C	T	6,205	0.0%	34.7%	46.8%	43.9%	46.3%	45.8%	49.3%	40.4%
CRMP1	chr4	intergenic	5961304					G	A	27,485	0.3%	33.7%	61.5%	52.4%	52.3%	53.4%	51.2%	55.2%
CSMD1	chr8	intronic	3057229					C	T	6,197	0.0%	30.9%	50.8%	41.2%	51.9%	53.4%	41.2%	53.3%
CSMD3	chr8	intronic	113504553					T	C	7,378	0.0%	27.1%	60.9%	54.0%	52.8%	39.3%	56.1%	64.5%
CUEDC1	chr17	intronic	55950478					C	T	1,194	0.0%	25.0%	NoCall	41.2%	41.2%	50.0%	NoCall	NoCall
CUL1	chr7	intronic	148495155					G	A	3,684	0.0%	21.1%	40.3%	46.6%	51.1%	47.2%	54.5%	50.0%
DBC1	chr9	exon8	121929828	nonsynonymous SNV	NM_014618	c.G1820A	p.R607Q	C	T	48,667	0.1%	32.3%	48.7%	48.6%	45.6%	48.8%	47.6%	33.3%
DLG4	chr17	intronic	7095566					G	C	2,427	0.0%	33.3%	71.4%	NoCall	93.3%	NoCall	NoCall	100.0%
DLG5	chr10	exon30	79554674	nonsynonymous SNV	NM_004747	c.C5479T	p.R1827W	G	A	24,723	0.0%	37.1%	53.0%	51.0%	48.3%	54.8%	50.9%	48.7%
DMD	chrX	exon59	31496332	nonsynonymous SNV	NM_004009	c.C8816T	p.T2939M	G	A	27,246	0.0%	70.9%	100.0%	100.0%	100.0%	100.0%	100.0%	100.0%
DNAH17	chr17	intronic	76522639					C	A	13,956	0.0%	41.5%	36.0%	50.2%	51.6%	46.2%	28.4%	42.7%
DNAJC1	chr10	intronic	22055097					C	G	9,261	0.0%	30.6%	49.4%	51.3%	43.0%	47.7%	49.1%	53.2%
DOCK2	chr5	intronic	169309350					T	C	5,182	0.0%	29.3%	61.8%	55.0%	52.5%	58.3%	63.6%	48.6%
DOCK9	chr13	intronic	99497897					C	T	1,811	0.0%	28.6%	42.3%	45.5%	45.5%	46.7%	55.0%	37.5%
DONSON	chr21	exon4	34957011	nonsynonymous SNV	NM_017613	c.C670G	p.P224A	G	C	16,059	0.0%	31.6%	44.2%	42.5%	44.4%	49.4%	43.8%	51.4%
DPP10	chr2	UTR5	115200093					A	G	11,393	0.0%	34.1%	34.8%	41.3%	53.0%	44.9%	32.9%	57.8%
DTNB	chr2	intronic	25602372					C	T	24,881	0.0%	29.5%	46.4%	48.4%	49.4%	44.9%	48.0%	49.0%
E2F1	chr20	intronic	32268039					G	A	13,450	0.0%	23.1%	23.3%	24.1%	31.5%	25.3%	20.4%	28.5%
E2F5	chr8	intronic	86118373					C	A	11,755	0.0%	32.7%	46.2%	49.1%	57.4%	50.0%	51.3%	56.0%
ECI1	chr16	intronic	2294703					C	T	8,011	0.0%	34.0%	47.0%	48.0%	49.4%	40.4%	30.0%	41.3%
EFHB	chr3	intronic	19930392					A	G	1,486	0.0%	28.0%	40.0%	43.8%	39.1%	50.0%	42.9%	70.0%
EIF3A	chr10	intronic	120820943					A	T	5,045	0.0%	31.2%	47.3%	54.5%	56.9%	44.4%	47.2%	36.4%
EPHB1	chr3	exon10	134898739	synonymous SNV	NM_004441	c.T1797A	p.T599T	T	A	12,162	0.0%	27.1%	45.8%	46.9%	48.8%	41.7%	43.9%	45.9%
ETNK1	chr12	UTR3	22797278					G	A	12,598	0.0%	27.0%	53.2%	49.0%	38.6%	58.0%	49.2%	34.9%
EVI2A,NF1	chr17	intronic	29647362					A	T	85	1.4%	11.8%	3.5%	7.0%	1.6%	8.5%	5.2%	8.5%
FAM102B	chr1	intronic	109148925					C	G	11,276	0.0%	35.1%	45.5%	42.2%	45.8%	51.5%	45.7%	55.6%
FAM124B	chr2	exon1	225266130	nonsynonymous SNV	NM_001122779	c.T356C	p.L119P	A	G	19,084	0.8%	25.7%	45.8%	50.0%	46.7%	45.7%	38.9%	51.1%
FAM154A	chr9	intronic	19028153					G	A	9,385	0.0%	30.4%	47.1%	42.7%	48.4%	33.0%	44.3%	60.0%
FAM181B	chr11	UTR3	82443179					A	G	2,889	0.0%	45.0%	100.0%	100.0%	100.0%	100.0%	NoCall	100.0%
FAM19A1	chr3	exon3	68466481	nonsynonymous SNV	NM_213609	c.G170A	p.R57H	G	A	5,288	0.0%	39.1%	45.5%	39.3%	59.6%	39.0%	44.0%	54.2%
FAM73B	chr9	intronic	131830204					G	T	25,181	0.0%	30.3%	33.0%	41.2%	50.4%	44.1%	30.0%	50.4%
FAM84A	chr2	exon2	14774879	nonsynonymous SNV	NM_145175	c.T776G	p.F259C	T	G	49,858	0.2%	33.0%	52.5%	49.3%	44.3%	49.2%	52.9%	49.7%
FAT2	chr5	exon22	150886928	nonsynonymous SNV	NM_001447	c.G12304A	p.E4102K	C	T	54,203	0.0%	33.1%	51.6%	52.7%	50.7%	47.3%	48.9%	41.8%
FBN2	chr5	intronic	127625753					C	T	10,687	0.0%	31.7%	57.9%	48.4%	54.3%	63.6%	37.5%	50.8%
FER1L5	chr2	intronic	97327324					G	A	39,870	0.0%	35.4%	50.2%	48.3%	46.5%	46.0%	50.4%	49.7%
FER1L6	chr8	exon11	124992845	nonsynonymous SNV	NM_001039112	c.G1204A	p.A402T	G	A	28,064	0.3%	30.5%	50.6%	49.8%	41.1%	44.5%	45.8%	45.8%
FERD3L	chr7	UTR5	19185003					G	T	40,317	0.3%	28.0%	46.7%	52.5%	46.8%	49.0%	50.1%	48.6%
FGD1	chrX	intronic	54475104					G	A	34,876	0.0%	67.9%	100.0%	100.0%	100.0%	100.0%	100.0%	100.0%
FGF9	chr13	intergenic	23279210					T	A	20,816	0.0%	37.1%	41.2%	42.0%	46.7%	36.5%	33.7%	48.7%
FLJ46257	chr22	ncRNA	48025102					C	T	32,321	0.0%	51.1%	99.4%	100.0%	99.2%	100.0%	100.0%	100.0%
FLT4	chr5	intronic	180050730					C	T	15,090	0.4%	23.0%	47.5%	47.1%	39.9%	47.5%	49.5%	43.4%
FMO5	chr1	intronic	146675402					G	T	952	0.0%	22.8%	0.7%	0.0%	0.0%	0.0%	0.0%	0.0%
GAD2	chr10	intronic	26505879					C	T	11,319	0.9%	29.7%	32.9%	45.7%	50.4%	50.0%	34.6%	49.4%
GADD45G	chr9	exon3	92220649	stopgain SNV	NM_006705	c.C223T	p.Q75X	C	T	47,870	0.1%	37.0%	46.0%	50.8%	49.9%	43.7%	51.6%	51.9%
GCKR	chr2	intronic	27721007					T	C	9,134	0.0%	26.5%	48.3%	44.0%	47.6%	43.2%	44.1%	51.2%
GIGYF2	chr2	intronic	233661048					G	A	2,092	0.0%	25.0%	26.5%	46.3%	41.2%	53.8%	60.0%	43.8%
GMIP	chr19	splicing	19745833					C	T	42,827	0.0%	33.1%	48.5%	48.5%	47.8%	53.2%	50.0%	49.5%
GML	chr8	intronic	143921693					G	A	4,798	0.0%	37.5%	56.0%	54.5%	50.0%	48.8%	63.3%	27.8%
GNAT3	chr7	exon8	80088168	nonsynonymous SNV	NM_001102386	c.C884G	p.T295R	G	C	10,927	0.0%	35.9%	29.8%	40.1%	46.8%	46.7%	27.6%	50.4%
GOLGA2B	chr12	ncRNA	100552526					C	A	717	0.0%	22.3%	0.0%	0.7%	0.0%	0.0%	0.0%	0.0%
GPR141	chr7	downstream	37781203					G	A	2,533	1.5%	30.6%	43.3%	33.3%	47.1%	47.8%	34.8%	38.5%
GPRC5B	chr16	intronic	19873332					A	G	189	0.0%	12.0%	0.0%	0.0%	0.0%	0.0%	0.0%	0.0%

GRK4	chr4	intronic	3037295					C	T	5,122	0.0%	20.3%	72.3%	50.0%	50.9%	54.8%	46.2%	47.4%
GRM7	chr3	intronic	7735189					G	A	11,198	0.0%	27.7%	36.7%	47.2%	48.9%	46.8%	45.1%	46.3%
GRM8	chr7	ncRNA	126409752					T	C	10,282	0.0%	30.1%	50.9%	49.2%	60.6%	59.3%	44.6%	54.0%
GUK1	chr1	intronic	228333006					G	A	7,865	0.0%	36.3%	47.8%	44.3%	52.5%	43.7%	48.2%	61.4%
H3F3B	chr17	intronic	73775519					C	A	1,115	0.0%	22.2%	41.7%	36.4%	53.8%	66.7%	NoCall	NoCall
HCK	chr20	exon9	30674489	synonymous SNV	NM_001172131	c.G828A	p.S276S	G	A	25,149	0.0%	49.3%	63.3%	63.3%	63.2%	61.3%	62.1%	58.3%
HDAC6	chrX	exon25	48681883	nonsynonymous SNV	NM_006044	c.C3074T	p.S1025L	C	T	49,359	0.4%	67.3%	99.6%	100.0%	99.5%	100.0%	100.0%	100.0%
HEATR6	chr17	intronic	58145100					G	A	31,831	0.0%	36.3%	52.0%	48.0%	48.3%	47.4%	48.5%	50.8%
HEXDC	chr17	intronic	80400030					G	A	11,185	0.0%	33.1%	51.9%	50.0%	48.8%	45.4%	48.8%	49.0%
HOXA2	chr7	exon2	27141071	synonymous SNV	NM_006735	c.C405T	p.I135I	G	A	32,291	0.0%	33.0%	49.3%	49.3%	47.9%	47.1%	41.2%	47.3%
HSD3B2	chr1	intergenic	120016239					G	T	1,632	0.0%	60.0%	40.0%	32.0%	36.8%	26.7%	58.8%	60.0%
HTR2A	chr13	exon3	47409499	nonsynonymous SNV	NM_001165947	c.C637T	p.R213W	G	A	35,801	0.0%	33.0%	49.1%	48.4%	44.4%	52.1%	49.7%	45.0%
HYAL1	chr3	intronic	50338394					A	C	58	0.0%	12.1%	3.6%	13.8%	10.2%	6.3%	11.4%	5.1%
IGDCC4	chr15	intronic	65685926					A	C	22,058	2.2%	32.4%	51.2%	48.7%	51.7%	48.1%	46.3%	42.5%
IGF2BP3	chr7	intronic	23353426					T	C	1,722	0.0%	23.8%	58.3%	69.2%	58.8%	57.1%	NoCall	NoCall
IGFBP4	chr17	exon4	38612760	synonymous SNV	NM_001552	c.G702A	p.G234G	G	A	17,719	0.0%	35.3%	48.4%	51.7%	51.7%	48.9%	44.1%	49.4%
IKBKAP	chr9	exon34	111640933	stopgain SNV	NM_003640	c.G3670T	p.E1224X	C	A	16,669	0.0%	35.4%	36.4%	37.6%	45.6%	47.9%	34.5%	41.0%
INF2	chr14	intronic	105181426					G	A	3,024	0.0%	36.4%	41.4%	61.1%	34.1%	44.4%	45.5%	52.4%
INTS1	chr7	intronic	1511545					G	A	2,015	0.0%	34.4%	56.3%	57.1%	50.0%	57.7%	57.1%	36.4%
INTS1	chr7	exon39	1515693	nonsynonymous SNV	NM_001080453	c.G5393A	p.R1798H	C	T	29,384	0.0%	35.4%	51.3%	53.1%	48.0%	52.4%	49.6%	48.6%
INTS9	chr8	ncRNA	28670889					C	T	8,964	0.0%	68.1%	76.8%	94.7%	100.0%	97.6%	72.7%	95.2%
ITGAX	chr16	intronic	31391742					C	T	31,818	0.0%	35.8%	40.4%	47.4%	44.2%	47.7%	45.6%	42.7%
ITGB2	chr21	intronic	46319913					G	A	1,660	0.0%	31.0%	54.5%	46.2%	50.0%	63.2%	50.0%	18.2%
IVL	chr1	intronic	152881903					C	T	3,035	0.0%	30.8%	48.4%	55.3%	40.5%	45.2%	27.3%	47.1%
KCNA6	chr12	exon1	4920057	nonsynonymous SNV	NM_002235	c.G850A	p.A284T	G	A	40,811	0.2%	39.2%	51.6%	47.6%	52.4%	46.0%	42.8%	50.5%
KCNH4	chr17	intronic	40318151					C	T	1,839	0.0%	29.0%	40.0%	42.9%	50.0%	34.6%	22.2%	60.0%
KCNIP4	chr4	exon3	20852237	nonsynonymous SNV	NM_147182	c.C31G	p.L11V	G	C	3,656	0.0%	48.5%	61.5%	90.3%	95.8%	84.2%	58.3%	86.4%
KCNT1	chr9	intronic	138678419					C	T	30,420	0.0%	34.8%	47.5%	46.8%	44.8%	45.7%	53.7%	43.4%
KCNU1	chr8	UTR5	36641863					A	G	22,511	0.0%	31.1%	43.4%	48.0%	54.7%	49.3%	38.0%	50.0%
KDM4B	chr19	intronic	5071271					C	T	13,659	0.0%	32.2%	47.2%	48.5%	52.3%	48.3%	55.7%	52.3%
KIAA0368	chr9	intronic	114202936					A	C	4,201	0.0%	29.4%	34.1%	60.0%	41.7%	39.6%	29.6%	37.5%
KIAA0368	chr9	intronic	114202953					C	A	3,094	0.0%	30.4%	43.8%	57.1%	38.5%	46.7%	34.8%	38.1%
KIF23	chr15	exon8	69718418	synonymous SNV	NM_138555	c.A744G	p.Q248Q	A	G	12,859	0.6%	33.3%	52.1%	50.3%	54.9%	47.5%	56.1%	39.2%
KIT	chr4	upstream	55523939					G	C	3,630	0.8%	27.7%	25.0%	34.8%	44.9%	40.2%	23.8%	42.9%
KLRF2	chr12	splicing	10037632					G	A	14,899	0.0%	30.9%	50.0%	47.4%	49.5%	49.1%	53.1%	50.4%
KRI1	chr19	exon10	10670548	stopgain SNV	NM_023008	c.A883T	p.K295X	T	A	1,642	0.0%	22.7%	0.0%	0.0%	0.0%	0.0%	0.0%	0.0%
KRT222	chr17	intronic	38812913					G	C	111	0.0%	9.3%	0.0%	0.0%	0.0%	0.0%	0.0%	0.0%
KRT76	chr12	intronic	53165352					G	A	2,160	0.0%	34.2%	55.6%	69.2%	50.0%	15.0%	41.7%	58.8%
KRT78	chr12	intronic	53238167					C	T	9,999	0.5%	33.8%	29.9%	42.0%	54.7%	32.1%	34.7%	43.1%
KRTAP22-1	chr21	exon1	31973445	nonsynonymous SNV	NM_181620	c.C6A	p.S2R	C	A	16,646	0.0%	51.2%	100.0%	98.9%	100.0%	100.0%	100.0%	100.0%
LAMC3	chr9	intronic	133947026					G	A	11,997	0.0%	32.0%	52.8%	49.2%	40.7%	50.0%	45.3%	57.5%
LAMTOR3	chr4	ncRNA	100803259					A	G	12,612	0.0%	36.2%	67.8%	50.3%	44.3%	54.5%	57.6%	40.9%
LATS2	chr13	exon5	21557682	synonymous SNV	NM_014572	c.C2163T	p.A721A	G	A	61,943	0.0%	31.4%	50.4%	48.4%	47.9%	51.1%	48.7%	54.1%
LDB1	chr10	intronic	103869531					G	A	44,702	0.0%	52.2%	100.0%	99.6%	99.4%	100.0%	98.7%	100.0%
LEPREL1	chr3	UTR5	189838817					C	T	1,797	0.0%	32.6%	25.0%	36.4%	56.5%	50.0%	31.6%	NoCall
LOC100130274	chr8	intronic	144789824					G	A	11,559	0.0%	38.5%	56.8%	61.0%	43.2%	50.3%	53.8%	55.6%
LOC340515	chr9	upstream	93345070					C	T	2,754	0.0%	56.3%	45.0%	58.6%	34.6%	59.3%	50.0%	52.4%
LOC389493	chr7	intergenic	56373096					A	C	8,079	0.0%	32.1%	54.0%	48.5%	51.4%	45.6%	53.8%	43.4%
LPHN3	chr4	exon3	62542613	synonymous SNV	NM_015236	c.C339A	p.T113T	C	A	8,178	0.0%	19.8%	28.4%	44.1%	49.3%	56.9%	44.5%	63.5%
LRFN4,PC	chr11	intronic	66626924					C	T	30,753	0.0%	51.4%	100.0%	100.0%	100.0%	100.0%	100.0%	100.0%
LRP1B	chr2	intronic	140992108					G	A	2,350	0.0%	43.9%	43.5%	52.0%	48.1%	58.3%	40.0%	50.0%
LRP1B	chr2	exon82	141079621	nonsynonymous SNV	NM_018557	c.T12551C	p.L4184P	A	G	6,712	0.0%	23.0%	47.5%	57.1%	54.7%	52.0%	43.5%	40.8%
LRP1B	chr2	exon76	141110629	nonsynonymous SNV	NM_018557	c.G11543T	p.C3848F	C	A	14,020	0.0%	26.0%	50.0%	44.5%	44.7%	47.3%	48.9%	50.0%
LRRC16A	chr6	upstream	25279403					C	T	4,250	0.0%	27.4%	43.9%	42.1%	49.1%	40.0%	45.7%	56.3%
LY6E	chr8	intronic	144102525					G	A	38,801	0.0%	33.1%	38.4%	42.2%	52.4%	45.7%	38.6%	47.3%
MALAT1	chr11	ncRNA	65266460					T	G	16,983	0.0%	49.4%	100.0%	100.0%	100.0%	100.0%	98.6%	100.0%
MANEA	chr6	intronic	96053461					T	C	3,309	0.0%	33.3%	31.8%	51.1%	58.5%	42.1%	44.8%	33.3%
MASP1	chr3	exon11	186953538	synonymous SNV	NM_139125	c.C2121T	p.Y707Y	G	A	36,644	0.2%	50.9%	77.2%	89.6%	97.5%	86.5%	75.5%	95.3%
MARCH7	chr2	intronic	160605422					C	T	8,520	0.0%	36.9%	41.1%	42.2%	47.4%	43.8%	51.7%	52.8%
MC1R	chr16	exon1	89986144	nonsynonymous SNV	NM_002386	c.C478T	p.R160W	C	T	51,516	0.0%	36.0%	39.0%	50.5%	48.3%	48.8%	45.7%	51.7%
MCM4	chr8	intronic	48878981					C	G	22,139	0.0%	29.6%	40.2%	37.8%	56.5%	36.5%	35.0%	51.6%

MCPH1	chr8	intronic	6338221					C	T	23,547	0.0%	34.0%	37.9%	44.4%	45.3%	45.2%	43.0%	37.8%
MED15	chr22	intergenic	20993536					C	A	3,960	0.0%	40.0%	100.0%	100.0%	100.0%	100.0%	100.0%	NoCall
MGRN1	chr16	intronic	4732782					C	T	6,017	0.0%	29.7%	34.2%	47.2%	50.0%	56.8%	39.6%	47.7%
MICALL2	chr7	exon6	1484672	nonsynonymous SNV	NM_182924	c.C1034T	p.P345L	G	A	36,456	0.0%	32.8%	47.5%	49.7%	47.5%	47.9%	49.5%	43.7%
MIR518A2	chr19	upstream	54242575					G	A	3,810	0.0%	39.6%	25.0%	34.5%	44.4%	42.9%	40.7%	42.9%
MLL	chr11	intronic	118391724					G	A	4,872	0.0%	61.5%	100.0%	100.0%	100.0%	100.0%	100.0%	100.0%
MMEL1	chr1	intronic	2526711					G	A	20,491	0.0%	31.7%	50.4%	45.1%	45.4%	51.3%	42.9%	54.5%
MOCOS	chr18	intergenic	33854078					G	A	1,181	0.0%	33.9%	0.0%	1.9%	0.0%	0.0%	0.0%	0.0%
MORC2	chr22	UTR5	31364184					C	A	5,425	0.0%	53.8%	100.0%	100.0%	100.0%	100.0%	94.7%	100.0%
MRPS21	chr1	exon3	150280647	synonymous SNV	NM_031901	c.G249A	p.P83P	G	A	3,138	0.0%	24.2%	48.6%	48.1%	48.6%	52.6%	57.1%	41.7%
MSC	chr8	exon1	72756170	nonsynonymous SNV	NM_005098	c.G244A	p.G82S	C	T	47,771	0.0%	30.7%	45.6%	47.2%	49.4%	47.7%	50.0%	39.4%
MUC16	chr19	intronic	9002359					C	T	10,278	0.0%	39.2%	52.3%	54.6%	52.1%	46.5%	51.5%	65.7%
MUC16	chr19	intronic	9007948					C	T	13,811	0.0%	30.1%	54.4%	50.6%	34.3%	48.4%	39.8%	37.7%
MXD3	chr5	UTR3	176732862					C	T	22,928	0.0%	33.8%	57.9%	49.2%	45.5%	53.1%	58.6%	44.6%
MYEF2	chr15	intronic	48451173					G	A	12,831	0.5%	9.1%	33.3%	42.9%	49.7%	48.4%	42.7%	55.7%
MYH10	chr17	exon37	8383839	nonsynonymous SNV	NM_005964	c.G5176A	p.A1726T	C	T	22,576	0.2%	34.6%	51.6%	48.0%	43.3%	47.5%	51.6%	46.2%
MYL2	chr12	intronic	111350836					C	T	18,263	0.0%	34.2%	45.1%	49.8%	46.8%	45.3%	40.0%	52.3%
NAALADL2	chr3	intronic	174935823					T	C	12,230	0.0%	35.0%	51.4%	59.2%	60.2%	51.8%	47.4%	55.9%
NCDN	chr1	exon5	36029010	synonymous SNV	NM_014284	c.C1593T	p.T531T	C	T	19,753	0.0%	33.7%	46.7%	49.2%	50.5%	48.6%	45.0%	48.9%
NDST3	chr4	UTR3	119177005					G	A	11,846	0.0%	48.5%	65.2%	62.4%	50.5%	54.5%	65.8%	48.2%
NDUFA10	chr2	intronic	240913239					G	A	10,145	0.0%	45.5%	55.3%	44.2%	47.3%	59.0%	50.0%	37.0%
NDUFAF4	chr6	intronic	97345524					C	A	6,794	0.0%	45.5%	50.0%	44.8%	38.9%	45.2%	46.2%	43.4%
NEO1	chr15	intronic	73428136					C	A	4,246	0.0%	29.1%	37.0%	39.7%	42.9%	18.8%	35.6%	34.3%
NEUROG3	chr10	UTR3	71331945					G	C	32,676	0.2%	33.3%	43.7%	45.0%	48.1%	43.0%	43.4%	49.5%
NID1	chr1	exon16	236144994	synonymous SNV	NM_002508	c.G3144A	p.A1048A	C	T	17,983	0.0%	29.2%	49.5%	51.3%	53.0%	47.5%	44.8%	55.1%
NID1	chr1	intronic	236212518					G	A	5,407	0.0%	43.5%	44.4%	42.7%	48.0%	52.8%	43.3%	37.1%
NLRP8	chr19	intronic	56463542					C	T	2,693	0.0%	47.2%	52.2%	50.0%	61.1%	43.5%	59.1%	42.9%
NONE	chrM	intergenic	711					G	A	164,663	0.0%	80.6%	87.0%	86.2%	84.7%	84.3%	82.8%	83.8%
NONE	chrM	intergenic	3680					T	C	197,721	0.3%	77.9%	84.0%	87.2%	85.0%	83.2%	81.8%	82.9%
NONE	chrM	intergenic	14161					G	A	16,009	0.0%	11.6%	15.8%	17.5%	17.1%	18.1%	16.4%	14.4%
NONE	chrM	intergenic	14488					T	C	11,063	0.2%	7.7%	16.3%	15.8%	13.2%	16.3%	9.4%	12.0%
NOP16	chr5	intronic	175812171					G	C	2,336	0.0%	27.3%	0.0%	0.0%	0.0%	0.0%	0.0%	0.0%
NRBP1	chr2	intronic	27657883					G	A	1,631	0.3%	23.9%	0.0%	0.0%	0.0%	0.0%	0.0%	0.0%
NRP2	chr2	exon9	206607971	nonsynonymous SNV	NM_201267	c.G1336T	p.A446S	G	T	24,491	0.0%	30.9%	47.3%	44.9%	47.6%	46.4%	41.3%	38.3%
NUPL1	chr13	intronic	25910115					A	T	8,098	0.0%	29.4%	27.0%	43.7%	37.2%	33.3%	31.4%	43.6%
OR8U1,OR8U8	chr11	exon1	56143373	nonsynonymous SNV	NM_001013356	c.A274C	p.I92L	A	C	32,811	0.2%	47.2%	61.0%	80.8%	95.1%	84.3%	54.5%	94.1%
P2RX2	chr12	exon10	133198359	nonsynonymous SNV	NM_016318	c.C1145T	p.P382L	C	T	40,396	0.0%	30.2%	45.4%	42.3%	49.8%	49.0%	42.5%	49.7%
PAH	chr12	exon3	103288570	synonymous SNV	NM_000277	c.A295C	p.R99R	T	G	20,438	0.0%	34.6%	54.6%	47.3%	51.2%	52.3%	59.1%	56.6%
PBRM1	chr3	exon5	52692256	nonsynonymous SNV	NM_018165	c.C604T	p.R202C	G	A	10,900	0.0%	33.9%	48.1%	47.4%	41.5%	48.0%	38.0%	43.4%
PCBP3	chr21	intronic	47315817					C	T	855	0.0%	17.6%	47.4%	41.7%	23.1%	46.7%	NoCall	NoCall
PCDHGA2	chr5	exon1	140720765	nonsynonymous SNV	NM_032009	c.G2227A	p.V743M	G	A	28,525	0.2%	35.9%	42.9%	40.9%	48.6%	46.8%	41.3%	48.2%
PCDHGA7	chr5	exon1	140762754	synonymous SNV	NM_032087	c.C288T	p.C96C	C	T	21,127	0.0%	31.9%	39.0%	39.6%	47.1%	46.4%	43.4%	45.5%
PCDHGB7	chr5	exon1	140797814	nonsynonymous SNV	NM_018927	c.G388A	p.A130T	G	A	22,387	0.0%	29.5%	37.1%	47.1%	50.2%	50.9%	40.4%	46.9%
PCGF3	chr4	intronic	728675					C	T	21,623	0.0%	31.3%	15.5%	33.3%	47.6%	36.9%	30.7%	40.5%
PDE1B	chr12	intronic	54963474					G	A	19,453	0.0%	33.1%	50.5%	53.7%	50.3%	50.5%	49.4%	50.8%
PDIA5;PDIA5	chr3	exon5	122821598	synonymous SNV	NM_006810	c.G342A	p.Q114Q	G	A	8,025	1.0%	30.5%	45.1%	43.8%	40.3%	55.4%	47.8%	46.6%
PHGDH	chr1	exon7	120277989	nonsynonymous SNV	NM_006623	c.A715G	p.I239V	A	G	28,776	0.0%	32.0%	44.6%	44.9%	43.1%	49.1%	46.4%	50.0%
PIK3C3	chr18	intronic	39613595					T	G	4,103	0.0%	71.4%	100.0%	100.0%	93.8%	100.0%	NoCall	100.0%
PLA2G4A	chr1	exon7	186880516	nonsynonymous SNV	NM_024420	c.C553T	p.R185C	C	T	15,333	0.0%	32.0%	39.7%	42.4%	41.6%	43.1%	44.9%	43.9%
PLA2G4A	chr1	intronic	186909083					A	C	18,947	0.0%	28.0%	51.0%	48.0%	51.5%	42.4%	51.2%	50.6%
PLCZ1	chr12	intronic	18837339					A	G	3,612	0.0%	29.4%	43.9%	38.7%	46.3%	60.7%	43.5%	40.0%
PLK1;PLK1	chr16	exon8	23700559	nonsynonymous SNV	NM_005030	c.G1271A	p.G424E	G	A	46,665	0.0%	30.3%	35.7%	44.0%	47.4%	48.8%	37.5%	49.2%
PLXNA4	chr7	exon10	131895838	nonsynonymous SNV	NM_020911	c.C2162T	p.T721M	G	A	23,299	0.0%	33.2%	52.2%	48.4%	52.3%	43.7%	43.8%	46.9%
PNMAL2	chr19	exon1	46998126	synonymous SNV	NM_020709	c.C597T	p.D199D	G	A	60,213	0.1%	34.1%	50.8%	47.5%	50.6%	49.5%	49.1%	46.1%
POC1B	chr12	ncRNA	89894063					A	C	5,029	0.0%	32.8%	36.7%	42.6%	43.3%	39.6%	45.8%	36.2%
POLR3E	chr16	intronic	22340088					A	T	8,856	0.0%	35.7%	59.8%	45.8%	51.6%	49.5%	50.0%	41.9%
PRICKLE4	chr6	intronic	41753665					G	A	4,687	0.0%	25.9%	46.9%	38.6%	54.5%	47.0%	44.4%	45.5%
PRSS36	chr16	intronic	31153467					T	C	10,385	0.0%	36.3%	64.2%	50.0%	53.8%	39.0%	51.1%	48.5%
PRSS45	chr3	intergenic	46852987					C	A	2,597	0.0%	31.8%	43.2%	43.2%	46.9%	30.0%	41.7%	50.0%
PRUNE2	chr9	exon8	79320884	synonymous SNV	NM_015225	c.C6306T	p.S2102S	G	A	48,811	0.0%	34.9%	47.1%	47.5%	48.7%	47.9%	43.1%	51.3%
PTGS1	chr9	intronic	125141465					C	T	3,305	0.0%	38.6%	48.8%	40.0%	40.0%	64.3%	48.1%	30.0%

PYCRL	chr8	intronic	144688334					C	T	31,988	0.0%	32.3%	54.9%	52.7%	52.4%	53.5%	47.9%	43.9%
RAB3IP	chr12	intergenic	70330107					C	A	43,213	0.1%	36.2%	36.9%	42.6%	50.8%	39.9%	33.1%	42.9%
RALGPS1	chr9	intronic	129812630					C	T	14,910	0.5%	37.6%	52.6%	55.5%	52.0%	50.4%	36.8%	49.1%
RAPGEF3	chr12	intronic	48134319					A	G	18,804	0.0%	32.5%	47.7%	49.8%	51.6%	47.5%	48.5%	43.4%
RASAL1	chr12	intronic	113568903					G	A	22,320	0.3%	37.4%	51.6%	48.3%	52.2%	47.2%	56.2%	42.7%
RASSF3	chr12	intronic	65088445					G	A	3,468	0.0%	26.5%	49.2%	36.2%	34.5%	54.3%	34.5%	48.4%
RBFOX1	chr16	intronic	7629665					T	A	307	0.0%	10.8%	0.0%	0.0%	0.0%	0.0%	0.0%	0.0%
RBM19	chr12	intronic	114403832					A	C	26,335	0.0%	30.2%	39.1%	42.1%	42.5%	44.7%	34.7%	38.0%
REC8	chr14	intronic	24649186					C	T	60,987	0.0%	59.0%	77.9%	88.9%	97.8%	88.8%	76.2%	95.3%
RET	chr10	intronic	43608968					G	A	4,252	2.6%	32.6%	47.2%	54.8%	46.7%	56.8%	56.9%	47.2%
RNF112	chr17	intronic	19315633					C	T	3,049	0.0%	30.2%	29.3%	36.6%	56.0%	36.5%	40.0%	NoCall
RPN2	chr20	intronic	35826548					C	T	14,976	0.0%	49.4%	69.6%	68.6%	65.7%	57.1%	62.3%	51.2%
RYR1	chr19	exon28	38964317	nonsynonymous SNV	NM_000540	c.G4066A	p.A1356T	G	A	17,508	0.0%	41.0%	48.2%	53.5%	48.0%	48.7%	55.6%	45.0%
SARS	chr1	intronic	109770850					G	A	11,461	0.0%	34.1%	47.7%	47.7%	58.5%	45.5%	49.3%	54.8%
SCAF1	chr19	intronic	50158341					C	T	6,832	1.1%	40.0%	40.9%	43.2%	52.4%	51.3%	48.9%	63.6%
SCYL2	chr12	intronic	100729376					T	G	11,149	0.0%	30.5%	47.7%	43.3%	49.5%	49.3%	55.2%	56.5%
SEC16A	chr9	exon18	139352017	nonsynonymous SNV	NM_014866	c.C5429A	p.S1810Y	G	T	31,422	0.0%	27.9%	47.7%	43.4%	47.2%	45.7%	46.4%	50.3%
SHANK3	chr22	intronic	51153165					G	T	7,408	0.0%	58.5%	100.0%	100.0%	100.0%	100.0%	100.0%	100.0%
SLC16A3	chr17	exon3	80194746	nonsynonymous SNV	NM_004207	c.C365T	p.T122M	C	T	21,775	0.0%	34.6%	32.3%	43.4%	50.4%	41.8%	34.1%	44.9%
SLC1A7	chr1	intronic	53557985					C	T	2,062	0.0%	42.9%	55.6%	60.0%	53.8%	50.0%	35.3%	58.8%
SLC35A1	chr6	upstream	88182586					T	A	17,246	0.0%	23.8%	38.6%	37.8%	39.7%	42.5%	42.3%	32.8%
SLC3A1	chr2	exon10	44547675	nonsynonymous SNV	NM_000341	c.C1955T	p.T652M	C	T	28,882	0.2%	28.2%	46.6%	47.9%	48.6%	50.5%	46.8%	50.3%
SLC45A4	chr8	intronic	142228062					C	T	26,140	0.0%	37.0%	47.6%	49.6%	45.8%	47.0%	40.4%	50.4%
SLC46A2	chr9	exon1	115652325	nonsynonymous SNV	NM_033051	c.G637A	p.V213M	C	T	45,411	0.0%	33.4%	50.1%	49.3%	50.7%	48.5%	50.8%	46.1%
SLC5A1	chr22	ncRNA	32479348					T	C	1,623	0.0%	33.3%	NoCall	100.0%	100.0%	NoCall	NoCall	NoCall
SLC5A6	chr2	ncRNA	27427870					G	A	35,829	0.0%	35.1%	45.2%	45.6%	45.9%	49.9%	47.2%	43.1%
SMC5	chr9	splicing	72933880					G	A	3,795	0.0%	25.4%	34.0%	38.2%	42.6%	42.9%	44.4%	36.8%
SNX24	chr5	intronic	122301307					G	A	7,955	0.0%	37.4%	32.2%	37.3%	57.0%	45.8%	34.8%	62.0%
SNX8	chr7	UTR3	2292774					G	A	14,661	0.0%	33.2%	33.0%	49.0%	42.6%	45.3%	33.9%	43.7%
SOS1	chr2	intronic	39222212					G	A	6,163	0.0%	22.7%	43.4%	49.3%	48.3%	34.8%	57.6%	48.3%
SPEG	chr2	upstream	220299580					C	T	10,592	0.0%	29.7%	52.8%	50.9%	59.5%	54.2%	50.8%	48.9%
SPICE1	chr3	intronic	113221958					C	G	2,779	0.0%	11.7%	30.6%	33.3%	36.8%	41.0%	27.7%	34.0%
SPOCK3	chr4	intronic	168041089					C	T	5,733	0.0%	29.2%	67.9%	50.0%	48.1%	34.0%	55.3%	43.8%
SPON1	chr11	intronic	14281838					C	A	190	0.0%	38.1%	0.0%	7.1%	0.0%	NoCall	NoCall	NoCall
SSTR4	chr20	exon1	23016578	nonsynonymous SNV	NM_001052	c.G458A	p.R153H	G	A	153,022	0.1%	50.7%	65.0%	65.7%	65.3%	65.1%	62.1%	67.8%
SSU72	chr1	intronic	1479516					A	G	9,318	0.0%	27.3%	34.9%	38.9%	47.3%	41.3%	28.3%	49.3%
ST3GAL5	chr2	intronic	86090211					G	A	5,701	0.0%	35.1%	54.5%	50.0%	49.2%	47.2%	52.9%	42.3%
STK31	chr7	exon4	23757195	nonsynonymous SNV	NM_032944	c.C177G	p.N59K	C	G	5,230	1.9%	28.8%	41.1%	37.1%	50.0%	45.1%	26.7%	52.0%
SULT1C2	chr2	intronic	108922123					T	C	11,442	0.0%	40.1%	48.2%	53.2%	41.9%	56.4%	50.5%	52.4%
SV2B	chr15	UTR3	91836118					G	A	1,428	0.0%	46.4%	33.3%	35.7%	61.5%	20.0%	66.7%	NoCall
SYNE2	chr14	intronic	64468993					C	T	2,377	0.0%	28.6%	41.2%	31.0%	55.2%	45.2%	45.8%	50.0%
SYT17	chr16	intronic	19234115					T	A	2,766	0.0%	26.1%	67.7%	42.4%	51.7%	61.5%	47.4%	76.5%
TBX6	chr16	exon5	30100112	synonymous SNV	NM_004608	c.C670A	p.R224R	G	T	51,904	0.0%	35.6%	35.6%	47.8%	50.4%	49.9%	41.0%	44.3%
TEAD4	chr12	intronic	3147299					G	C	23,482	0.0%	32.5%	51.0%	45.6%	44.0%	49.2%	48.8%	47.2%
TECPR2	chr14	exon17	102931496	nonsynonymous SNV	NM_001172631	c.G3659A	p.S1220N	G	A	18,254	0.0%	30.9%	47.8%	51.2%	42.3%	40.6%	43.8%	50.0%
TEX14	chr17	intronic	56708039					T	A	7,365	0.0%	41.8%	52.9%	50.0%	40.5%	43.7%	68.6%	51.4%
TGM3	chr20	intronic	2312967					C	T	23,235	0.0%	26.9%	31.0%	37.5%	35.5%	29.0%	34.2%	34.2%
TMEM149	chr19	exon5	36230512	nonsynonymous SNV	NM_024660	c.C737T	p.A246V	G	A	28,475	0.0%	30.3%	48.0%	49.9%	43.1%	49.2%	49.3%	53.6%
TMEM154	chr4	UTR3	153549557					G	A	2,422	0.0%	36.4%	58.8%	68.0%	48.0%	70.0%	53.8%	50.0%
TMEM194B	chr2	intronic	191390147					G	A	5,797	0.0%	31.1%	58.3%	48.7%	40.8%	50.0%	47.5%	51.2%
TMEM235	chr17	UTR5	76227519					G	A	15,606	0.0%	35.2%	45.3%	42.4%	47.8%	37.7%	46.5%	49.2%
TMEM8A	chr16	exon3	427569	nonsynonymous SNV	NM_021259	c.G316T	p.A106S	C	A	23,922	0.6%	37.8%	40.4%	46.8%	53.5%	47.7%	45.3%	46.7%
TOP2B	chr3	intronic	25679853					A	G	8,821	0.0%	27.3%	45.3%	48.8%	46.2%	41.0%	40.2%	50.0%
TRIL	chr7	UTR3	28995112					C	T	18,802	0.0%	28.6%	42.7%	50.4%	42.1%	45.2%	53.7%	56.4%
TRIL	chr7	UTR3	28995174					C	T	26,486	0.3%	35.3%	42.0%	43.8%	45.6%	49.1%	59.6%	43.5%
TRIML1	chr4	intronic	189064777					G	A	3,653	0.0%	26.2%	65.4%	54.3%	64.7%	40.6%	62.5%	47.1%
TRMT1	chr19	exon12	13218573	nonsynonymous SNV	NM_017722	c.C1498T	p.R500C	G	A	24,094	0.0%	35.1%	48.8%	49.1%	50.9%	46.6%	47.6%	37.9%
TTBK2	chr15	exon4	43132587	stopgain SNV	NM_173500	c.C262T	p.R88X	G	A	21,421	0.0%	55.9%	99.0%	100.0%	96.0%	97.5%	96.0%	84.5%
TTN	chr2	exon155	179438056	nonsynonymous SNV	NM_133437	c.G46184A	p.R15395H	C	T	36,378	0.2%	33.0%	46.5%	45.2%	46.7%	45.6%	49.1%	54.5%
TTN	chr2	exon71	179489340	synonymous SNV	NM_133437	c.G18048A	p.G6016G	C	T	18,012	0.0%	32.9%	36.7%	38.3%	43.1%	29.6%	31.9%	37.2%
TULP3	chr12	intronic	3000266					C	G	6,761	0.0%	31.8%	46.1%	49.0%	49.3%	44.7%	40.6%	42.9%

TYR	chr11	upstream	88910985					T	C	17,329	0.0%	56.4%	100.0%	100.0%	100.0%	100.0%	100.0%	100.0%
UGGT1	chr2	ncRNA	128922271					A	T	22,772	0.0%	38.7%	49.6%	49.0%	48.4%	47.5%	46.7%	42.7%
UHRF1BP1	chr6	UTR5	34759881					A	G	1,080	1.6%	10.3%	0.0%	16.9%	13.0%	7.0%	0.0%	28.3%
UHRF1BP1	chr6	UTR5	34759884					G	C	1,481	2.3%	10.0%	0.0%	17.6%	13.3%	6.3%	1.9%	28.0%
UNK	chr17	intronic	73814962					T	C	22,007	0.0%	33.8%	27.6%	39.8%	46.6%	44.8%	32.9%	52.0%
USP25	chr21	exon12	17197364	nonsynonymous SNV	NM_013396	c.C1288A	p.Q430K	C	A	3,019	0.0%	41.2%	25.0%	41.2%	48.8%	50.0%	33.3%	40.6%
USP37	chr2	intronic	219394561					A	G	9,138	0.0%	34.3%	44.1%	44.9%	39.6%	50.0%	54.2%	55.2%
VPS13B	chr8	splicing	100520141					T	A	29,493	0.3%	28.9%	48.8%	51.2%	49.8%	50.9%	62.1%	53.8%
WBP2	chr17	upstream	73851586					A	C	8,072	0.0%	36.3%	62.3%	44.8%	45.2%	47.8%	46.0%	52.9%
WDFY4	chr10	exon9	49939538	nonsynonymous SNV	NM_020945	c.C1513T	p.R505W	C	T	30,293	0.0%	34.5%	54.5%	49.8%	48.3%	47.0%	53.0%	53.0%
WDFY4	chr10	intronic	49995011					G	A	8,384	0.0%	30.9%	52.7%	47.0%	62.8%	47.3%	50.0%	48.1%
WDR34	chr9	intronic	131399661					G	A	1,925	0.0%	43.3%	38.9%	47.6%	50.0%	54.2%	38.5%	NoCall
WDR64	chr1	intergenic	241995707					G	A	4,551	0.0%	31.4%	32.8%	61.5%	44.9%	37.5%	50.8%	40.0%
ZBTB41	chr1	intronic	197141251					C	A	3,093	0.0%	17.9%	34.0%	38.6%	50.0%	21.1%	36.4%	46.5%
ZBTB5	chr9	exon2	37441885	nonsynonymous SNV	NM_014872	c.G664T	p.G222W	C	A	48,968	0.1%	33.9%	38.7%	48.0%	49.3%	40.5%	27.6%	47.2%
ZNF320	chr19	intergenic	53418645					A	G	276	1.7%	10.3%	12.1%	6.9%	10.5%	4.9%	9.2%	7.7%

Table S9. Non-synonymous SNVs preferentially expressed in one of two 1° recipients (recipient was used for further transplantation) and detected in subsequent transplants

Gene	Chr	Exon	Pos	NCBI Ref	Coding	Protein	Ref. Allele	Var. Allele	Variant Allele Frequency (%)							
									Patient Normal	Patient Tumor	1° xenografts		2° xenografts		4° xenografts	
											tm1	tm2	tm1	tm2	tm1	tm2
APBA1	chr9	exon2	72131594	NM_001163	c.G533C	p.G178A	C	G	0.0%	0.0%	1.7%	8.1%	4.3%	13.1%	8.9%	25.4%

Table S10. Non-synonymous SNVs preferentially expressed in one of two 2° recipients (recipient was used for further transplantation) and detected in subsequent transplants

Gene	Chr	Exon	Pos	NCBI Ref	Coding	Protein	Ref. Allele	Var. Allele	Variant Allele Frequency (%)							
									Patient Normal	Patient Tumor	1° xenografts		2° xenografts		4° xenografts	
											tm1	tm2	tm1	tm2	tm1	tm2
AHI1	chr6	exon24	135644434	NM_017651	c.A3194G	p.N1065S	T	C	0.0%	0.0%	0.5%	1.0%	1.3%	9.8%	6.2%	15.0%
ANKHD1	chr5	exon15	139876775	NM_017747	c.T2916G	p.D972E	T	G	0.0%	0.0%	0.7%	1.9%	1.6%	13.0%	6.8%	16.7%
APP	chr21	exon7	27372413	NM_000484	c.C950T	p.A317V	G	A	0.6%	0.0%	1.0%	0.5%	1.3%	5.5%	5.4%	14.4%
BMP5	chr6	exon4	55638918	NM_021073	c.A956G	p.N319S	T	C	0.0%	0.0%	1.6%	1.3%	1.8%	15.8%	7.3%	6.7%
C1QTNF3	chr5	exon1	34043117	NM_181435	c.A114C	p.K38N	T	G	0.0%	0.0%	1.1%	1.1%	1.1%	6.0%	6.6%	18.2%
C1QTNF3	chr5	exon1	34043124	NM_181435	c.G107C	p.R36T	A	G	0.2%	0.0%	1.2%	1.2%	1.1%	5.7%	5.3%	14.1%
C1R	chr12	exon3	7242770	NM_001733	c.G306C	p.K102N	C	G	0.0%	0.0%	1.8%	1.6%	1.7%	9.1%	5.5%	16.9%
C1R	chr12	exon3	7242771	NM_001733	c.A305G	p.K102R	T	C	0.0%	0.0%	1.8%	1.6%	1.7%	9.1%	5.5%	16.8%
C9orf93	chr9	exon24	15874567	NM_173550	c.G3506C	p.S1169T	G	C	0.0%	0.0%	0.6%	0.9%	1.4%	8.4%	5.6%	13.7%
C9orf93	chr9	exon24	15874557	NM_173550	c.T3496A	p.S1166T	T	A	0.0%	0.6%	0.7%	1.0%	1.5%	6.8%	5.6%	13.1%
C9orf93	chr9	exon24	15874554	NM_173550	c.T3493C	p.W1165R	T	C	0.0%	0.0%	0.7%	1.0%	1.5%	7.0%	5.1%	13.3%
CCDC85A	chr2	exon4	56599605	NM_001080433	c.A1444T	p.T482S	A	T	0.9%	0.4%	1.3%	1.6%	1.1%	7.5%	9.9%	21.7%
CHSY3	chr5	exon3	129521281	NM_175856	c.C2446A	p.L816I	C	A	0.0%	0.0%	0.8%	0.7%	1.4%	6.8%	5.2%	14.4%
CSGALNACT2	chr10	exon2	43651159	NM_018590	c.T562G	p.L188V	T	G	0.0%	0.0%	1.4%	0.8%	1.6%	5.3%	5.0%	18.5%
CSGALNACT2	chr10	exon2	43651193	NM_018590	c.A596C	p.E199A	A	C	0.0%	0.0%	1.5%	1.2%	1.4%	10.5%	6.0%	14.8%
FAM5C	chr1	exon2	190423956	NM_199051	c.C65T	p.A22V	G	A	0.0%	0.0%	0.2%	1.7%	2.0%	6.7%	8.4%	16.1%
FNIP1	chr5	exon13	131013443	NM_133372	c.A1472G	p.D491G	T	C	0.0%	0.0%	0.8%	1.5%	2.0%	5.1%	7.0%	9.6%
GLUD2	chrX	exon1	120182856	NM_012084	c.T1318C	p.F440L	T	C	0.0%	0.0%	0.4%	1.1%	1.9%	7.8%	6.3%	22.1%
GOT1	chr10	exon6	101163577	NM_002079	c.A697G	p.N233D	T	C	0.0%	0.0%	0.0%	0.0%	1.6%	5.1%	7.5%	19.0%
GPR98	chr5	exon31	89986745	NM_032119	c.C6838T	p.L2280F	C	T	0.0%	0.0%	1.0%	0.3%	1.5%	6.2%	6.3%	17.6%
GPR98	chr5	exon31	89986731	NM_032119	c.C6824T	p.T2275I	C	T	0.0%	0.0%	1.7%	0.2%	1.5%	6.7%	6.4%	17.0%
HEPACAM	chr11	exon3	124793682	NM_152722	c.A652G	p.M218V	T	C	0.0%	0.0%	1.9%	1.2%	1.8%	10.1%	7.2%	16.0%
HMBOX1	chr8	exon4	28827905	NM_024567	c.G369T	p.E123D	G	T	0.0%	0.0%	1.3%	0.7%	1.2%	5.0%	5.1%	19.0%
KCNH7	chr2	exon7	163291885	NM_173162	c.C1756A	p.Q586K	G	T	0.0%	0.0%	0.5%	1.0%	1.5%	5.1%	5.1%	15.9%
KIAA1429	chr8	exon8	95538788	NM_183009	c.G1684A	p.V562I	C	T	0.0%	0.0%	0.3%	1.0%	1.1%	6.9%	5.0%	14.8%
LRRC7	chr1	exon20	70509755	NM_020794	c.A3974T	p.H1325L	A	T	0.0%	0.0%	0.8%	0.9%	1.5%	6.0%	5.8%	10.5%
MAP1A	chr15	exon4	43814365	NM_002373	c.C694G	p.P232A	C	G	0.0%	0.2%	1.3%	0.7%	0.9%	6.8%	5.9%	18.6%
MB21D2	chr3	exon1	192635604	NM_178496	c.A26G	p.N9S	T	C	0.0%	0.0%	0.0%	1.2%	1.1%	7.7%	5.7%	19.6%
MLL2	chr12	exon31	49434586	NM_003482	c.A6967G	p.T2323A	T	C	0.0%	0.0%	1.5%	1.1%	0.9%	5.6%	6.3%	13.8%
MLLT10	chr10	exon9	21959510	NM_001195626	c.A928G	p.T310A	A	G	0.0%	0.0%	0.0%	1.6%	1.4%	7.3%	6.2%	10.6%
MRPS9	chr2	exon7	105706382	NM_182640	c.G580C	p.V194L	G	C	0.0%	0.0%	1.7%	0.8%	1.4%	15.1%	6.5%	17.3%
MTERF	chr7	exon3	91503660	NM_006980	c.G448A	p.V150M	C	T	0.0%	0.0%	1.0%	0.8%	0.6%	5.4%	5.6%	16.9%
MTERF	chr7	exon3	91503657	NM_006980	c.A451G	p.T151A	T	C	0.2%	0.0%	1.0%	0.9%	0.6%	5.3%	5.2%	17.0%
MYH9	chr22	exon27	36691074	NM_002473	c.G3534C	p.E1178D	C	G	0.4%	0.0%	0.6%	0.4%	0.9%	7.1%	5.8%	20.2%
MYO1E	chr15	exon24	59453335	NM_004998	c.G2722A	p.V908I	C	T	0.5%	0.0%	1.1%	1.7%	0.9%	6.4%	5.9%	14.2%
MYST3	chr8	exon8	41834696	NM_001099413	c.T1193C	p.V398A	A	G	0.0%	0.0%	1.8%	1.2%	0.9%	6.5%	5.9%	15.5%
NFX1	chr9	exon16	33351619	NM_002504	c.C2486T	p.T829M	C	T	0.0%	0.0%	1.4%	1.3%	1.9%	5.9%	5.7%	18.8%
NKRF	chrX	exon3	118725102	NM_017544	c.A286T	p.I96F	T	A	0.3%	0.0%	1.0%	1.2%	2.0%	7.2%	5.9%	11.1%
NSD1	chr5	exon2	176563005	NM_022455	c.T901C	p.S301P	T	C	0.0%	0.3%	1.5%	1.5%	1.5%	8.8%	6.8%	17.1%
NSD1	chr5	exon2	176562966	NM_022455	c.A862C	p.T288P	A	C	0.0%	0.0%	1.5%	1.0%	1.4%	6.2%	5.7%	15.2%
NSD1	chr5	exon2	176562960	NM_022455	c.A856C	p.T286P	A	C	0.0%	0.3%	1.8%	1.2%	1.8%	5.5%	5.2%	14.3%
PHF10	chr6	exon11	170105283	NM_133325	c.A1351G	p.M451V	T	C	0.0%	0.0%	1.4%	0.8%	1.2%	8.6%	7.2%	20.7%
PKD2L1	chr10	exon9	102054351	NM_016112	c.C1600A	p.R534S	G	T	0.2%	0.3%	0.5%	1.3%	1.8%	6.8%	8.5%	20.6%
PKDCC	chr2	exon1	42275890	NM_138370	c.T551C	p.V184A	T	C	0.0%	0.0%	1.9%	0.9%	1.0%	5.3%	5.2%	13.5%
PPM1B	chr2	exon2	44428491	NM_177968	c.A153C	p.E51D	A	C	0.0%	0.0%	1.3%	1.2%	1.9%	8.0%	5.8%	22.1%
PPM1B	chr2	exon2	44428492	NM_177968	c.G154A	p.D52N	G	A	0.0%	0.0%	1.5%	1.5%	1.9%	8.1%	5.8%	22.3%

PPP1CC	chr12	exon5	111160461	NM_002710	c.G563A	p.R188Q	C	T	0.0%	0.0%	1.8%	1.0%	0.9%	7.3%	6.7%	9.8%
RBBP5	chr1	exon13	205064043	NM_005057	c.G1546A	p.A516T	C	T	0.0%	0.0%	1.2%	0.8%	1.6%	6.4%	6.7%	20.0%
RBFOX1	chr16	exon8	7680656	NM_145892	c.C788G	p.A263G	C	G	0.0%	0.3%	1.5%	1.2%	1.9%	5.2%	6.4%	15.8%
RBM46	chr4	exon5	155749119	NM_144979	c.A1502C	p.Y501S	A	C	0.0%	0.0%	1.7%	0.2%	0.7%	7.9%	6.1%	12.8%
RBM46	chr4	exon5	155749130	NM_144979	c.G1513A	p.G505S	G	A	0.0%	0.0%	1.7%	0.2%	1.0%	5.9%	6.0%	11.5%
RNF139	chr8	exon2	125499506	NM_007218	c.G1616A	p.R539H	G	A	0.0%	0.0%	1.8%	1.3%	1.3%	7.4%	5.3%	12.4%
RNF170	chr8	exon7	42711442	NM_001160223	c.C637T	p.L213F	G	A	0.0%	0.0%	1.0%	0.7%	2.0%	6.8%	6.2%	12.9%
SFRS18	chr6	exon12	99848900	NM_032870	c.A1934C	p.Q645P	T	G	0.0%	0.0%	1.4%	1.4%	1.4%	5.2%	6.7%	22.8%
SFRS18	chr6	exon12	99848905	NM_032870	c.T1929G	p.D643E	A	C	0.1%	0.0%	1.4%	1.6%	1.7%	6.3%	6.2%	21.6%
SFRS18	chr6	exon5	99858781	NM_032870	c.A337G	p.T113A	T	C	0.0%	0.0%	1.5%	1.9%	2.0%	6.6%	7.2%	15.1%
SRCAP	chr16	exon26	30740334	NM_006662	c.A5706T	p.E1902D	A	T	0.0%	0.0%	1.6%	1.7%	1.7%	7.9%	5.9%	15.9%
TIAM1	chr21	exon29	32493039	NM_003253	c.C4423G	p.P1475A	G	C	0.2%	0.0%	0.0%	1.4%	1.1%	5.1%	6.0%	22.1%
TSSK2	chr22	exon1	19119120	NM_053006	c.G208C	p.G70R	G	C	0.1%	0.1%	1.0%	0.9%	1.6%	5.8%	5.4%	18.4%
TTN	chr2	exon44	179622425	NM_133432	c.A10384T	p.T3462S	T	A	0.0%	0.0%	1.0%	0.3%	1.5%	6.5%	5.8%	16.2%
TTN	chr2	exon186	179400376	NM_003319	c.C73771T	p.P24591S	G	A	0.0%	0.0%	1.5%	0.2%	1.9%	8.4%	5.0%	12.0%
USP38	chr4	exon1	144106873	NM_032557	c.T270G	p.H90Q	T	G	0.0%	0.0%	1.9%	2.0%	1.7%	6.1%	5.6%	14.0%
VDAC3	chr8	exon7	42259355	NM_001135694	c.G376C	p.V126L	G	C	0.0%	0.0%	1.2%	1.2%	1.8%	5.8%	5.1%	14.4%
ZAK	chr2	exon12	174086046	NM_133646	c.A1156G	p.I386V	A	G	0.0%	0.0%	1.8%	1.7%	1.0%	6.9%	6.3%	20.9%
ZCCHC11	chr1	exon11	52947166	NM_015269	c.C1777G	p.Q593E	G	C	0.0%	0.0%	2.0%	1.1%	1.7%	13.2%	7.1%	15.8%
ZEB1	chr10	exon7	31810640	NM_030751	c.A2377G	p.I793V	A	G	0.0%	0.0%	0.9%	0.3%	0.3%	5.1%	5.7%	16.3%
ZNF148	chr3	exon4	125032353	NM_021964	c.T132G	p.D44E	A	C	0.2%	0.0%	0.4%	0.7%	1.0%	6.9%	5.2%	13.8%

Table S11. Non-synonymous SNVs preferentially expressed in one of two 4° recipients

Gene	Chr	Exon	Pos	NCBI Ref	Coding	Protein	Ref. Allele	Var. Allele	Variant Allele Frequency (%)							
									Patient Normal	Patient Tumor	1° xenografts		2° xenografts		4° xenografts	
											tm1	tm2	tm1	tm2	tm1	tm2
ABCA2	chr9	exon16	139912088	NM_001606	c.C2273G	p.P758R	G	C	0.0%	0.0%	0.0%	0.2%	0.6%	1.2%	1.9%	12.7%
ABCA2	chr9	exon16	139912070	NM_001606	c.C2291T	p.P764L	G	A	0.0%	0.0%	0.0%	0.3%	0.8%	1.2%	1.6%	13.0%
ABCC10	chr6	exon18	43415527	NM_001198934	c.C3811G	p.Q1271E	C	G	0.0%	0.0%	1.1%	0.0%	0.6%	0.4%	1.5%	10.4%
ADORA2A	chr22	exon2	24829500	NM_000675	c.A128T	p.Y43F	A	T	0.2%	0.0%	0.2%	0.1%	1.4%	1.9%	1.3%	13.9%
AGAP3	chr7	exon13	150837197	NM_031946	c.A1798G	p.T600A	A	G	0.0%	0.4%	0.4%	0.9%	0.5%	0.9%	1.4%	9.6%
ANKRD17	chr4	exon21	73984466	NM_198889	c.G3374C	p.G1125A	C	G	0.0%	0.0%	0.0%	0.2%	1.1%	1.4%	1.4%	12.4%
ANKRD17	chr4	exon21	73984467	NM_198889	c.G3373A	p.G1125S	C	T	0.2%	0.0%	0.0%	0.2%	1.1%	1.4%	1.4%	12.1%
ANKS1A	chr6	exon11	34985259	NM_015245	c.G1433A	p.R478Q	G	A	0.0%	0.0%	0.4%	0.3%	0.4%	1.5%	2.0%	11.0%
ANKS1A	chr6	exon11	34985264	NM_015245	c.A1438G	p.S480G	A	G	0.0%	0.3%	0.3%	0.3%	0.4%	1.1%	2.0%	11.8%
ANKS1A	chr6	exon11	34985270	NM_015245	c.A1444G	p.S482G	A	G	0.0%	0.0%	0.3%	0.3%	0.3%	1.7%	1.9%	11.6%
ANLN	chr7	exon4	36445961	NM_018685	c.T659C	p.F220S	T	C	0.0%	0.0%	0.0%	0.0%	0.6%	1.7%	1.0%	11.3%
ANLN	chr7	exon4	36445952	NM_018685	c.A650G	p.N217S	A	G	0.0%	0.0%	0.0%	0.0%	0.6%	1.1%	0.8%	11.1%
ATXN7	chr3	exon6	63968053	NM_001177387	c.C944T	p.P315L	C	T	0.0%	0.0%	0.4%	0.6%	1.5%	0.8%	0.0%	11.7%
ATXN7	chr3	exon6	63968052	NM_001177387	c.C943A	p.P315T	C	A	0.0%	0.3%	0.7%	0.6%	1.5%	0.8%	0.0%	11.7%
ATXN7L3B	chr12	exon1	74932048	NM_001136262	c.G156C	p.E52D	G	C	0.0%	0.0%	0.0%	0.7%	0.8%	1.8%	1.3%	15.8%
BCL9	chr1	exon8	147090839	NM_004326	c.C878G	p.A293G	C	G	0.0%	0.0%	0.6%	0.5%	0.8%	1.4%	1.1%	11.4%
BCL9	chr1	exon8	147090823	NM_004326	c.T862C	p.S288P	T	C	0.1%	0.0%	0.7%	0.7%	1.0%	1.7%	1.9%	12.2%
BSDC1	chr1	exon6	32844408	NM_001143888	c.C496G	p.Q166E	G	C	0.0%	0.0%	0.4%	1.3%	2.0%	1.4%	0.5%	12.3%
BTN1A1	chr6	exon7	26508991	NM_001732	c.G1170T	p.E390D	G	T	0.0%	0.0%	0.0%	0.0%	0.7%	1.1%	1.6%	13.0%
BTN1A1	chr6	exon7	26508959	NM_001732	c.A1138G	p.M380V	A	G	0.0%	0.0%	0.0%	0.0%	0.7%	1.0%	1.4%	10.3%
C10orf2	chr10	exon1	102748268	NM_021830	c.A301T	p.S101C	A	T	0.0%	0.0%	0.3%	0.0%	1.9%	1.3%	0.5%	12.0%
C2orf68	chr2	exon2	85838865	NM_001013649	c.T152C	p.V51A	A	G	0.0%	0.0%	0.6%	0.9%	1.2%	1.7%	0.0%	14.3%
C3orf21	chr3	exon2	194947519	NM_152531	c.C571T	p.H191Y	G	A	0.0%	0.0%	0.8%	0.3%	0.9%	2.0%	1.3%	14.1%
CA7	chr16	exon2	66881047	NM_005182	c.C155T	p.S52F	C	T	0.0%	0.0%	0.7%	0.2%	0.3%	1.4%	1.9%	12.6%
CACNA1G	chr17	exon32	48697095	NM_198396	c.T5731G	p.W1911G	T	G	0.2%	0.0%	1.0%	0.7%	2.0%	1.3%	2.0%	14.5%
CAMK2G	chr10	exon18	75576812	NM_172170	c.T1293A	p.D431E	C	T	0.0%	0.0%	0.5%	0.7%	0.3%	1.8%	1.1%	9.9%
CAMK2G	chr10	exon18	75576815	NM_172173	c.T1248A	p.F416L	C	T	0.0%	0.0%	0.5%	0.8%	0.3%	1.8%	1.1%	10.5%
CAMTA1	chr1	exon9	7725113	NM_015215	c.T2506G	p.S836A	T	G	0.0%	0.0%	0.6%	0.2%	0.5%	1.8%	0.9%	14.3%
CCDC85A	chr2	exon5	56603005	NM_001080433	c.G1507C	p.A503P	G	C	0.0%	0.0%	0.2%	0.3%	0.5%	1.5%	1.5%	13.7%
CCDC85A	chr2	exon5	56603026	NM_001080433	c.G1528A	p.A510T	G	A	0.0%	0.0%	0.4%	0.1%	0.5%	1.5%	1.2%	10.6%
CCDC85A	chr2	exon5	56602997	NM_001080433	c.C1499T	p.P500L	C	T	0.0%	0.0%	0.2%	0.1%	0.5%	1.5%	1.5%	13.3%
CCDC85A	chr2	exon5	56602985	NM_001080433	c.G1487A	p.S496N	G	A	0.0%	0.2%	0.2%	0.3%	0.6%	1.2%	1.2%	13.9%
CELSR3	chr3	exon2	48694314	NM_001407	c.G4216A	p.A1406T	C	T	0.0%	0.0%	0.0%	0.0%	0.9%	0.9%	1.7%	16.5%
CRY2	chr11	exon6	45889208	NM_001127457	c.C604T	p.L202F	C	T	0.0%	0.0%	0.5%	0.2%	0.0%	1.3%	1.1%	13.6%
DCAF7	chr17	exon7	61666444	NM_005828	c.A940G	p.R314G	A	G	0.0%	0.0%	0.9%	0.0%	0.3%	1.8%	2.0%	11.8%
DCAF8	chr1	exon13	160188183	NM_015726	c.A1608C	p.Q536H	T	G	0.0%	0.0%	0.2%	0.2%	1.0%	1.9%	1.9%	10.2%
DCHS1	chr11	exon19	6646457	NM_003737	c.C7118T	p.A2373V	G	A	0.0%	0.0%	0.5%	0.2%	1.6%	1.7%	1.5%	12.0%
DCHS1	chr11	exon21	6645358	NM_003737	c.G7549A	p.A2517T	C	T	0.0%	0.0%	0.5%	0.2%	1.1%	0.8%	0.7%	12.4%
DCHS1	chr11	exon21	6645366	NM_003737	c.G7541C	p.S2514T	C	G	0.0%	0.0%	0.4%	0.3%	1.0%	0.8%	0.7%	11.8%
DGKG	chr3	exon21	185906068	NM_001080744	c.A1943C	p.N648T	T	G	0.0%	0.0%	0.2%	0.3%	1.9%	1.1%	1.6%	13.1%
DHCR24	chr1	exon1	55352678	NM_014762	c.C115T	p.L39F	G	A	0.0%	0.0%	0.0%	0.0%	1.5%	1.5%	1.3%	16.9%
DIO3	chr14	exon1	102028017	NM_001362	c.C184T	p.L62F	C	T	0.0%	0.0%	0.1%	0.0%	1.2%	0.5%	0.2%	9.7%
DNAH1	chr3	exon66	52427395	NM_015512	c.A10520T	p.Y3507F	A	T	0.0%	0.0%	0.1%	0.1%	0.4%	0.7%	1.9%	11.8%
DNAH17	chr17	exon66	76447714	NM_173628	c.A10571G	p.K3524R	T	C	0.3%	0.0%	1.9%	1.0%	0.4%	1.2%	1.6%	10.3%
DNAJB12	chr10	exon1	74114715	NM_001002762	c.G43C	p.V15L	C	G	0.2%	0.0%	0.4%	0.3%	1.9%	1.4%	2.0%	11.8%
DNHD1	chr11	exon14	6555170	NM_144666	c.C2765T	p.A922V	C	T	0.0%	0.0%	0.0%	0.2%	0.4%	1.0%	0.8%	11.8%

DNHD1	chr11	exon14	6555212	NM_144666	c.A2807G	p.K936R	A	G	0.0%	0.0%	0.0%	0.2%	0.4%	1.3%	1.6%	14.8%
DNHD1	chr11	exon14	6555205	NM_144666	c.A2800G	p.M934V	A	G	0.0%	0.0%	0.0%	0.2%	0.4%	1.3%	1.6%	14.8%
DNHD1	chr11	exon14	6555194	NM_144666	c.G2789A	p.R930Q	G	A	0.1%	0.0%	0.0%	0.2%	0.4%	1.3%	1.6%	13.6%
DSTYK	chr1	exon3	205138309	NM_015375	c.A1306G	p.T436A	T	C	0.0%	0.0%	0.5%	0.0%	0.3%	1.1%	0.9%	11.1%
EFNB3	chr17	exon2	7611407	NM_001406	c.G254A	p.G85E	G	A	0.0%	0.0%	1.0%	0.2%	0.5%	1.9%	1.5%	14.9%
EPN3	chr17	exon6	48617648	NM_017957	c.T932C	p.L311P	T	C	0.0%	0.0%	0.3%	0.1%	1.6%	1.5%	1.6%	13.4%
EPN3	chr17	exon6	48617654	NM_017957	c.C938T	p.P313L	C	T	0.0%	0.0%	0.3%	0.1%	1.3%	1.1%	1.6%	12.7%
EPN3	chr17	exon6	48617639	NM_017957	c.T923C	p.V308A	T	C	0.0%	0.0%	0.3%	0.2%	1.6%	1.5%	1.6%	13.6%
FAM120C	chrX	exon14	54107807	NM_017848	c.G2926A	p.G976S	C	T	0.0%	0.0%	0.9%	0.5%	0.0%	1.8%	1.7%	13.9%
FAM155A	chr13	exon1	108518518	NM_001080396	c.G427A	p.G143S	C	T	0.0%	0.0%	0.6%	0.0%	1.7%	0.6%	1.6%	11.5%
FAM159A	chr1	exon1	53099181	NM_001042693	c.A16T	p.T6S	A	T	0.0%	0.0%	0.0%	0.0%	0.0%	1.1%	1.1%	18.3%
FBXO32	chr8	exon7	124518778	NM_058229	c.T688G	p.L230V	A	C	0.0%	0.0%	0.6%	0.5%	0.6%	1.3%	1.3%	10.3%
FBXO42	chr1	exon10	16577563	NM_018994	c.G1756A	p.G586S	C	T	0.2%	0.0%	0.3%	0.8%	0.4%	2.0%	1.2%	12.3%
FGFR2	chr10	exon2	123353298	NM_001144918	c.G34T	p.V12L	C	A	0.0%	0.1%	0.0%	0.6%	0.5%	0.9%	1.1%	14.0%
FIP1L1	chr4	exon12	54294205	NM_001134937	c.A984C	p.E328D	A	C	0.1%	0.0%	1.2%	0.4%	1.0%	1.0%	1.6%	11.2%
FLNB	chr3	exon1	57994478	NM_001457	c.T187C	p.Y63H	T	C	0.0%	0.0%	0.0%	0.1%	0.7%	0.7%	0.5%	11.5%
FMNL1	chr17	exon3	43309791	NM_005892	c.G271C	p.V91L	G	C	0.2%	0.0%	0.2%	0.1%	1.0%	0.7%	0.8%	12.9%
FNDC1	chr6	exon10	159650912	NM_032532	c.G1246C	p.D416H	G	C	0.2%	0.0%	0.6%	0.1%	0.2%	1.9%	1.4%	10.1%
FNDC1	chr6	exon10	159651028	NM_032532	c.G1362A	p.M454I	G	A	0.3%	0.0%	0.0%	0.0%	0.0%	0.9%	1.4%	12.0%
FNDC1	chr6	exon10	159650906	NM_032532	c.C1240T	p.P414S	C	T	0.0%	0.0%	0.4%	0.1%	0.2%	1.9%	1.4%	10.0%
FRMD4B	chr3	exon1	69434992	NM_015123	c.A149G	p.Q50R	T	C	0.0%	0.0%	0.0%	0.3%	1.2%	1.0%	1.0%	11.6%
GALNT6	chr12	exon7	51754582	NM_007210	c.T1090G	p.S364A	A	C	0.0%	0.0%	0.4%	0.3%	0.8%	1.4%	1.3%	11.7%
GAS1	chr9	exon1	89561133	NM_002048	c.A562G	p.T188A	T	C	0.0%	0.2%	0.8%	0.4%	1.4%	1.9%	1.0%	11.4%
GDF6	chr8	exon1	97172613	NM_001001557	c.G308A	p.R103K	C	T	0.0%	0.0%	1.0%	0.3%	0.0%	0.9%	1.8%	11.3%
GLB1L	chr2	exon4	220107549	NM_024506	c.C331A	p.L111I	G	T	0.0%	0.0%	0.2%	0.2%	0.3%	0.8%	0.5%	11.7%
GLB1L	chr2	exon4	220107548	NM_024506	c.T332A	p.L111Q	A	T	0.0%	0.0%	0.0%	0.2%	0.3%	0.8%	0.7%	11.7%
GOLGA3	chr12	exon3	133393214	NM_001172557	c.G318C	p.K106N	C	G	0.0%	0.0%	0.0%	0.7%	1.2%	1.6%	1.6%	13.3%
GORASP1	chr3	exon3	39144284	NM_031899	c.G233A	p.R78K	C	T	0.0%	0.0%	0.7%	0.5%	0.0%	0.6%	1.7%	10.1%
GPER	chr7	exon2	1131722	NM_001505	c.C358G	p.H120D	C	G	0.1%	0.0%	0.6%	0.2%	1.0%	1.0%	1.3%	12.5%
GPER	chr7	exon2	1131729	NM_001505	c.G365A	p.R122Q	G	A	0.1%	0.1%	1.3%	0.4%	1.1%	1.5%	1.1%	13.0%
GPR135	chr14	exon1	59931001	NM_022571	c.A944C	p.N315T	T	G	0.1%	0.1%	0.1%	0.3%	1.0%	1.1%	0.9%	11.2%
GPR135	chr14	exon1	59931005	NM_022571	c.G940A	p.V314M	C	T	0.1%	0.0%	0.1%	0.4%	1.0%	1.1%	0.9%	11.6%
GPR27	chr3	exon1	71804065	NM_018971	c.G865A	p.V289I	G	A	0.0%	0.0%	0.3%	0.2%	1.7%	1.1%	1.3%	14.4%
GPR6	chr6	exon1	110301345	NM_005284	c.C1030T	p.L344F	C	T	0.0%	0.0%	0.1%	0.0%	0.4%	0.5%	1.5%	13.0%
GREB1	chr2	exon26	11770131	NM_014668	c.A4507G	p.I1503V	A	G	0.0%	0.0%	0.0%	0.2%	1.6%	0.6%	1.9%	12.4%
GREB1	chr2	exon26	11770111	NM_014668	c.A4487G	p.Y1496C	A	G	0.3%	0.1%	0.0%	0.4%	1.6%	0.6%	1.6%	10.0%
GREB1L	chr18	exon26	19088200	NM_001142966	c.A4490G	p.K1497R	A	G	0.0%	0.0%	1.3%	0.6%	0.0%	0.9%	1.1%	11.5%
GRM8	chr7	exon2	126883135	NM_001127323	c.G124C	p.V42L	C	G	0.0%	0.0%	0.2%	0.3%	0.2%	1.6%	1.5%	10.6%
HAPLN2	chr1	exon4	156593656	NM_021817	c.A143G	p.H48R	A	G	0.0%	0.0%	0.0%	0.0%	0.4%	1.0%	0.6%	12.6%
HCFC1	chrX	exon19	153218245	NM_005334	c.G4662C	p.E1554D	C	G	0.0%	0.0%	0.7%	0.3%	1.0%	1.2%	0.0%	11.3%
HCFC1	chrX	exon19	153218276	NM_005334	c.C4631A	p.P1544Q	G	T	0.0%	0.0%	0.4%	0.6%	1.5%	0.8%	0.0%	11.5%
HERPUD2	chr7	exon9	35673415	NM_022373	c.G1106C	p.G369A	C	G	0.0%	0.0%	0.5%	0.4%	1.1%	2.0%	1.3%	12.7%
HGF	chr7	exon7	81372738	NM_001010933	c.C781A	p.Q261K	G	T	0.0%	0.0%	1.8%	0.0%	0.7%	1.4%	1.9%	13.2%
HMX2	chr10	exon1	124908007	NM_005519	c.T113C	p.V38A	T	C	0.0%	0.0%	0.0%	0.0%	0.3%	0.6%	0.9%	11.9%
HNRNPUL2	chr11	exon7	62489628	NM_001079559	c.T1320G	p.C440W	T	C	0.2%	0.2%	0.6%	1.2%	1.9%	1.4%	0.4%	12.2%
HNRNPUL2	chr11	exon10	62487586	NM_001079559	c.G1689T	p.L563F	G	A	0.0%	0.0%	0.2%	0.0%	0.9%	1.3%	1.1%	10.7%
HRH2	chr5	exon1	175110481	NM_022304	c.G245T	p.C82F	G	T	0.0%	0.1%	0.1%	0.1%	0.4%	0.5%	0.2%	11.0%
HRH2	chr5	exon1	175110498	NM_022304	c.A262C	p.K88Q	A	C	0.0%	0.0%	0.1%	0.0%	0.6%	1.0%	0.4%	12.7%
HSPA12A	chr10	exon12	118434525	NM_025015	c.G1795A	p.V599I	C	T	0.0%	0.0%	0.2%	0.5%	1.1%	1.3%	1.6%	11.4%
IGFBP4	chr17	exon1	38600219	NM_001552	c.C232A	p.L78M	C	A	0.0%	0.0%	0.8%	0.0%	1.4%	1.4%	1.4%	12.5%
ITPRIPL1	chr2	exon3	96992989	NM_001008949	c.A620G	p.Q207R	A	G	0.0%	0.0%	0.0%	0.0%	1.5%	1.2%	1.8%	11.7%
ITPRIPL1	chr2	exon3	96992895	NM_001008949	c.G526A	p.V176I	G	A	0.0%	0.0%	0.5%	0.3%	1.3%	0.6%	1.4%	10.5%

JAK1	chr1	exon8	65330584	NM_002227	c.G1062T	p.E354D	C	A	0.0%	0.0%	0.0%	0.6%	1.0%	1.5%	1.0%	13.0%
JAK1	chr1	exon8	65330579	NM_002227	c.A1067G	p.K356R	T	C	0.0%	0.0%	0.0%	0.9%	1.4%	1.5%	1.0%	12.6%
KCNF1	chr2	exon1	11052982	NM_002236	c.C430A	p.R144S	C	A	0.1%	0.0%	0.8%	0.9%	1.8%	1.4%	2.0%	16.2%
KCNG4	chr16	exon2	84270745	NM_172347	c.G347A	p.S116N	C	T	0.1%	0.0%	0.3%	0.0%	0.6%	0.4%	1.2%	11.2%
KCNH2	chr7	exon1	150652548	NM_172057	c.C44A	p.A15D	C	T	0.0%	0.0%	0.0%	0.7%	0.0%	0.6%	0.9%	11.4%
KCNJ14	chr19	exon1	48965276	NM_170720	c.G295A	p.A99T	G	A	0.0%	0.0%	1.0%	0.4%	0.7%	1.0%	1.4%	11.9%
KCNK2	chr1	exon2	215259925	NM_001017425	c.T261G	p.H87Q	T	G	0.0%	0.0%	0.0%	0.4%	0.5%	1.5%	1.9%	10.3%
KIAA0195	chr17	exon18	73489859	NM_014738	c.G2269A	p.A757T	G	A	0.0%	0.0%	0.0%	0.5%	0.9%	1.0%	1.5%	11.2%
KIAA0913	chr10	exon11	75553392	NM_015037	c.G2360A	p.S787N	G	A	0.0%	0.0%	0.3%	0.0%	0.7%	0.6%	1.1%	12.1%
KIAA1109	chr4	exon41	123184014	NM_015312	c.C6858G	p.D2286E	C	G	0.0%	0.0%	1.9%	0.3%	1.4%	1.4%	1.2%	15.0%
KIAA2026	chr9	exon1	6007349	NM_001017969	c.G439T	p.A147S	C	A	0.0%	0.2%	0.5%	0.6%	1.6%	1.9%	1.1%	10.2%
KIF13A	chr6	exon38	17771437	NM_022113	c.C4489T	p.P1497S	G	A	0.0%	0.0%	0.0%	0.0%	0.7%	0.7%	1.9%	11.6%
KIF21B	chr1	exon20	200959408	NM_017596	c.G2888A	p.R963Q	C	T	0.0%	0.0%	0.3%	0.5%	0.3%	1.4%	0.7%	14.0%
KIF3C	chr2	exon1	26203398	NM_002254	c.A1389C	p.E463D	T	G	0.1%	0.1%	1.2%	0.2%	0.4%	1.7%	1.3%	10.7%
KLC2	chr11	exon16	66034377	NM_001134775	c.C1819T	p.L607F	C	T	0.1%	0.0%	0.2%	0.0%	1.9%	1.2%	1.8%	13.2%
LGR5	chr12	exon11	71960667	NM_003667	c.A1045G	p.N349D	A	G	0.0%	0.0%	0.0%	0.6%	1.0%	0.5%	1.6%	10.6%
LHFPL5	chr6	exon1	35773758	NM_182548	c.G311C	p.G104A	G	C	0.1%	0.1%	0.1%	0.0%	0.0%	0.5%	0.3%	10.4%
LPPR1	chr9	exon3	104032304	NM_017753	c.C206G	p.T69S	C	G	0.0%	0.2%	0.2%	0.0%	0.3%	1.7%	1.4%	10.4%
LRBA	chr4	exon2	151935727	NM_006726	c.G68A	p.R23K	C	T	0.0%	0.0%	1.0%	0.7%	0.8%	1.4%	1.4%	11.6%
LZTS2	chr10	exon3	102763577	NM_032429	c.G722A	p.S241N	G	A	0.0%	0.2%	1.3%	0.5%	0.0%	1.5%	1.8%	16.5%
MACF1	chr1	exon86	39920703	NM_012090	c.A14832C	p.E4944D	T	C	0.0%	0.0%	0.0%	0.6%	1.3%	1.5%	1.0%	12.3%
MACF1	chr1	exon1	39796956	NM_033044	c.C16A	p.L6I	C	A	0.0%	0.0%	0.0%	0.9%	1.4%	1.3%	1.2%	14.0%
MAP1A	chr15	exon4	43817363	NM_002373	c.A3692G	p.N1231S	A	G	0.1%	0.0%	0.3%	0.2%	1.2%	0.7%	1.8%	13.3%
MAP3K10	chr19	exon4	40711082	NM_002446	c.G1067A	p.R356Q	G	A	0.0%	0.0%	0.6%	0.0%	0.0%	1.6%	1.0%	11.4%
MARK2	chr11	exon14	63670586	NM_001163296	c.G1470C	p.E490D	G	C	0.0%	0.0%	0.0%	0.8%	0.5%	0.3%	0.0%	10.1%
MED13	chr17	exon5	60111229	NM_005121	c.T733G	p.C245G	A	C	0.0%	0.0%	0.7%	0.0%	0.0%	1.9%	0.3%	9.7%
MED13	chr17	exon18	60045430	NM_005121	c.A4157G	p.K1386R	T	C	0.0%	0.0%	0.3%	0.0%	0.7%	1.3%	1.8%	11.8%
MED13	chr17	exon28	60028311	NM_005121	c.C6166A	p.P2056T	G	T	0.0%	0.0%	1.5%	0.0%	0.4%	0.9%	2.0%	14.9%
MEPCE	chr7	exon1	100028656	NM_019606	c.C1015T	p.P339S	C	T	0.0%	0.0%	0.5%	0.7%	1.3%	1.3%	1.9%	12.9%
MLL	chr11	exon3	118343405	NM_001197104	c.C1531A	p.P511T	C	A	0.0%	0.0%	0.3%	0.8%	1.2%	1.5%	1.0%	17.1%
MOSPD3	chr7	exon2	100210497	NM_001040098	c.T83C	p.L28S	T	C	0.2%	0.0%	0.4%	0.3%	0.7%	0.5%	1.7%	14.9%
MOSPD3	chr7	exon2	100210493	NM_001040098	c.C79T	p.P27S	C	T	0.0%	0.0%	0.4%	0.4%	0.7%	0.5%	1.7%	15.2%
MTA3	chr2	exon14	42936243	NM_020744	c.T1532C	p.M511T	T	C	0.0%	0.0%	0.0%	0.2%	0.4%	1.0%	1.9%	11.7%
MTA3	chr2	exon14	42936165	NM_020744	c.A1454G	p.N485S	A	G	0.0%	0.0%	0.0%	0.5%	0.3%	1.0%	1.5%	11.1%
MYL9	chr20	exon3	35176474	NM_006097	c.G224A	p.S75N	G	A	0.0%	0.0%	0.0%	0.4%	0.3%	0.5%	1.2%	16.4%
NCOA1	chr2	exon18	24974922	NM_003743	c.A3778G	p.I1260V	A	G	0.1%	0.0%	0.5%	0.1%	0.7%	1.5%	0.6%	12.3%
NFE2L1	chr17	exon6	46135812	NM_003204	c.A1128C	p.L376F	A	C	1.0%	0.4%	0.6%	0.4%	0.5%	1.0%	0.6%	10.9%
NFE2L1	chr17	exon6	46135811	NM_003204	c.T1127C	p.L376S	T	C	0.0%	0.0%	0.0%	0.0%	0.2%	0.7%	0.6%	10.4%
NPNT	chr4	exon9	106863613	NM_001184693	c.A1003G	p.I335V	A	G	0.0%	0.0%	0.8%	0.0%	0.8%	0.5%	0.7%	9.7%
NR2C2	chr3	exon4	15055162	NM_003298	c.C196T	p.P66S	C	T	0.0%	0.3%	0.8%	1.2%	0.8%	1.3%	1.2%	12.8%
NRXN3	chr14	exon9	79432620	NM_004796	c.G1529C	p.S510T	G	C	0.3%	0.0%	0.0%	0.1%	0.7%	2.0%	1.8%	13.0%
NUP153	chr6	exon20	17625037	NM_005124	c.C3929A	p.P1310H	G	T	0.0%	0.0%	0.5%	1.3%	0.0%	2.0%	1.9%	12.9%
NUP153	chr6	exon19	17626267	NM_005124	c.A3673G	p.T1225A	T	C	0.0%	0.0%	0.5%	0.2%	0.3%	1.2%	0.9%	12.4%
ODF3	chr11	exon3	197663	NM_053280	c.A212G	p.N71S	A	G	0.0%	0.0%	0.4%	0.4%	1.5%	0.5%	0.0%	14.0%
OR10A4	chr11	exon1	6898030	NM_207186	c.T152C	p.I51T	T	C	0.0%	0.0%	0.6%	0.2%	1.5%	0.9%	1.6%	15.6%
PAPPA	chr9	exon4	118974010	NM_002581	c.G1717A	p.V573I	G	A	0.0%	0.0%	0.0%	0.6%	0.4%	2.0%	0.6%	12.2%
PAX3	chr2	exon8	223066717	NM_181457	c.A1366G	p.T456A	T	C	0.0%	0.2%	0.0%	1.1%	1.0%	0.8%	0.6%	11.0%
PCDHGB5	chr5	exon1	140779521	NM_018925	c.G1827T	p.E609D	G	T	0.3%	0.0%	0.0%	0.9%	1.0%	1.0%	1.2%	14.5%
PCDHGC5	chr5	exon1	140870674	NM_032407	c.A1867G	p.T623A	A	G	0.0%	0.0%	0.0%	0.1%	0.2%	0.1%	1.7%	10.2%
PCK2	chr14	exon5	24568269	NM_004563	c.A676G	p.S226G	A	G	0.0%	0.0%	0.0%	0.5%	0.0%	1.8%	1.0%	14.8%
PCNXL3	chr11	exon31	65402848	NM_032223	c.C5113A	p.L1705M	C	A	0.1%	0.0%	0.2%	0.0%	1.5%	1.9%	1.1%	12.6%
PDIA4	chr7	exon10	148700963	NM_004911	c.G1861A	p.D621N	C	T	0.0%	0.1%	0.5%	0.2%	1.2%	0.5%	1.9%	13.2%

PDIA4	chr7	exon10	148700928	NM_004911	c.A1896T	p.E632D	T	A	0.0%	0.0%	0.3%	0.1%	0.6%	0.5%	1.5%	11.3%
PDIA4	chr7	exon10	148700981	NM_004911	c.G1843A	p.V615I	C	T	0.0%	0.0%	0.4%	0.1%	1.0%	0.4%	1.6%	12.9%
PHACTR1	chr6	exon7	13206118	NM_030948	c.A736C	p.M246L	A	C	0.0%	0.0%	0.2%	0.3%	0.5%	0.8%	1.6%	10.5%
PHF12	chr17	exon4	27251133	NM_020889	c.G509A	p.S170N	C	T	0.0%	0.0%	0.3%	0.5%	1.3%	1.7%	2.0%	16.5%
PIP5K1C	chr19	exon7	3653425	NM_001195733	c.C784A	p.R262S	G	T	0.0%	0.0%	0.4%	0.4%	0.0%	1.4%	1.2%	9.9%
PITX2	chr4	exon6	111539752	NM_153426	c.A483C	p.E161D	A	G	0.2%	0.0%	0.9%	0.2%	1.8%	1.8%	1.4%	12.1%
PITX2	chr4	exon6	111539803	NM_153426	c.T432A	p.N144K	C	T	0.0%	0.0%	1.0%	0.0%	1.0%	1.3%	1.5%	11.7%
PLEC	chr8	exon31	144998388	NM_201381	c.C5613G	p.D1871E	G	C	0.0%	0.0%	0.5%	0.3%	1.2%	1.3%	1.4%	14.3%
POF1B	chrX	exon2	84634365	NM_024921	c.G95A	p.C32Y	C	T	0.0%	0.0%	0.9%	0.4%	1.4%	1.9%	0.0%	11.4%
PPP1R9B	chr17	exon1	48226754	NM_032595	c.C1121A	p.P374H	G	T	0.1%	0.0%	0.3%	0.0%	1.4%	1.1%	1.9%	12.3%
PRPF40B	chr12	exon22	50037020	NM_001031698	c.A2157T	p.E719D	A	T	0.0%	0.0%	0.9%	0.5%	0.4%	0.9%	1.6%	13.3%
PRR14L	chr22	exon4	32108312	NM_173566	c.A5513G	p.K1838R	T	C	0.0%	0.2%	0.0%	0.6%	1.2%	2.0%	1.8%	12.6%
PTPRS	chr19	exon14	5231475	NM_002850	c.A2001C	p.E667D	T	G	0.0%	0.0%	0.7%	0.7%	0.9%	1.5%	1.7%	13.4%
PTPRS	chr19	exon14	5231458	NM_002850	c.G2018A	p.G673D	C	T	0.0%	0.0%	0.7%	0.3%	1.0%	1.2%	0.4%	11.4%
PYGM	chr11	exon5	64525293	NM_005609	c.T618A	p.H206Q	A	T	0.0%	0.0%	0.0%	0.5%	1.2%	1.0%	1.6%	13.9%
PYGM	chr11	exon5	64525294	NM_005609	c.A617G	p.H206R	T	C	0.2%	0.0%	0.0%	0.5%	1.2%	1.0%	1.6%	14.0%
R3HDM2	chr12	exon19	57651841	NM_014925	c.G2339A	p.S780N	C	T	0.0%	0.0%	0.3%	0.0%	0.8%	1.1%	1.4%	11.6%
RABGAP1L	chr1	exon7	174221655	NM_014857	c.T913A	p.L305I	T	A	0.0%	0.0%	0.0%	0.3%	1.8%	0.5%	0.9%	12.0%
RANBP17	chr5	exon25	170692728	NM_022897	c.C2820G	p.I940M	C	G	0.0%	0.0%	0.0%	0.4%	0.0%	1.7%	0.6%	10.4%
RBM33	chr7	exon5	155473553	NM_053043	c.C518G	p.T173S	C	G	0.0%	0.0%	0.3%	0.2%	0.0%	1.1%	1.0%	11.7%
RBM47	chr4	exon3	40440131	NM_019027	c.C780G	p.D260E	G	C	0.0%	0.0%	0.3%	0.2%	1.1%	1.1%	1.4%	13.8%
RNF222	chr17	exon3	8296705	NM_001146684	c.G75C	p.E25D	C	G	0.0%	0.0%	0.2%	0.3%	1.5%	1.5%	1.5%	10.9%
RNF26	chr11	exon1	119206304	NM_032015	c.G472A	p.G158S	G	A	0.0%	0.0%	0.8%	0.2%	1.0%	0.9%	1.3%	10.7%
RNFT2	chr12	exon7	117217030	NM_032814	c.G759A	p.M253I	G	A	0.0%	0.0%	0.2%	0.4%	0.2%	0.8%	1.2%	10.5%
RNFT2	chr12	exon7	117217029	NM_032814	c.T758C	p.M253T	T	C	0.0%	0.0%	0.0%	0.6%	0.2%	0.8%	1.2%	11.0%
RSPH6A	chr19	exon2	46314009	NM_030785	c.C740T	p.T247M	G	A	0.0%	0.0%	0.1%	0.0%	0.4%	0.8%	2.0%	10.6%
RSPH6A	chr19	exon2	46314034	NM_030785	c.G715A	p.V239I	C	T	0.0%	0.0%	0.2%	0.3%	0.9%	1.0%	1.9%	10.8%
RTL1	chr14	exon1	101349420	NM_001134888	c.A1706G	p.K569R	T	C	0.0%	0.0%	0.7%	0.2%	0.5%	0.4%	1.4%	10.6%
RWDD2A	chr6	exon3	83905640	NM_033411	c.T528A	p.D176E	T	A	0.0%	0.0%	0.3%	0.2%	0.6%	1.9%	1.5%	10.7%
RYR1	chr19	exon18	38948855	NM_000540	c.C2090G	p.A697G	C	G	0.0%	0.0%	0.6%	0.2%	0.3%	1.2%	0.0%	11.4%
RYR1	chr19	exon18	38948828	NM_000540	c.C2063G	p.T688S	C	G	0.0%	0.0%	0.6%	0.0%	0.8%	1.0%	0.3%	12.7%
RYR1	chr19	exon18	38948840	NM_000540	c.C2075G	p.T692S	C	G	0.0%	0.0%	0.6%	0.0%	0.3%	1.1%	0.0%	12.6%
SCNN1A	chr12	exon2	6483718	NM_001159575	c.C301A	p.Q101K	G	T	0.0%	0.0%	0.3%	0.0%	0.2%	0.6%	1.9%	12.1%
SCNN1B	chr16	exon2	23360011	NM_000336	c.G91A	p.D31N	G	A	0.0%	0.0%	0.4%	0.5%	1.6%	1.8%	1.0%	13.4%
SETD5	chr3	exon16	9490257	NM_001080517	c.C2289G	p.I763M	C	G	0.0%	0.0%	0.3%	0.0%	0.2%	1.9%	1.5%	11.8%
SGK2	chr20	exon10	42204969	NM_016276	c.A979G	p.S327G	A	G	0.0%	0.0%	0.0%	0.0%	0.6%	0.6%	0.7%	10.3%
SGSM3	chr22	exon13	40803481	NM_015705	c.C1433T	p.S478L	C	T	0.0%	0.0%	0.7%	1.4%	1.4%	2.0%	1.8%	13.8%
SHANK2	chr11	exon22	70333755	NM_012309	c.G2452A	p.G818R	C	T	0.0%	0.0%	0.0%	0.0%	0.5%	0.5%	0.0%	12.7%
SHANK2	chr11	exon22	70333749	NM_012309	c.C2458T	p.L820F	G	A	0.0%	0.0%	0.0%	0.0%	0.5%	0.5%	0.0%	13.0%
SHANK2	chr11	exon22	70333766	NM_012309	c.C2441T	p.P814L	G	A	0.0%	0.0%	0.0%	0.0%	0.5%	0.5%	0.0%	13.3%
SHANK2	chr11	exon22	70333772	NM_012309	c.A2435C	p.Q812P	T	G	0.0%	0.0%	0.0%	0.0%	0.5%	0.4%	0.0%	12.9%
SHANK2	chr11	exon22	70333791	NM_012309	c.T2416C	p.S806P	A	G	0.0%	0.0%	0.0%	0.2%	0.5%	0.4%	0.0%	12.6%
SLC6A20	chr3	exon5	45812790	NM_022405	c.T743C	p.F248S	A	G	0.0%	0.0%	0.0%	0.2%	1.1%	1.5%	0.7%	10.4%
SLC6A9	chr1	exon5	44474154	NM_201649	c.A680C	p.H227P	T	G	0.0%	0.0%	0.6%	0.9%	0.9%	1.3%	1.0%	11.2%
SMOC1	chr14	exon11	70490043	NM_001034852	c.G1170T	p.M390I	C	T	0.0%	0.0%	0.0%	0.2%	1.7%	1.7%	1.1%	10.5%
SND1	chr7	exon22	127729628	NM_014390	c.G2506A	p.G836S	G	A	0.0%	0.0%	0.4%	0.3%	1.0%	1.3%	1.1%	11.7%
SNRNP200	chr2	exon15	96959158	NM_014014	c.C1932A	p.D644E	C	T	0.0%	0.2%	0.7%	0.2%	0.6%	1.9%	0.9%	14.5%
SNRNP200	chr2	exon15	96959125	NM_014014	c.G1965C	p.M655I	T	G	0.5%	0.2%	0.5%	0.5%	0.6%	1.5%	0.5%	11.0%
SNX17	chr2	exon15	27599537	NM_014748	c.A1364C	p.D455A	A	C	0.0%	0.0%	0.0%	0.1%	0.2%	0.4%	0.2%	10.9%
SNX8	chr7	exon2	2317839	NM_013321	c.C196T	p.H66Y	G	A	0.2%	0.0%	0.0%	0.3%	0.7%	1.5%	1.6%	12.7%
SRGAP2	chr1	exon19	206632033	NM_001170637	c.A2309G	p.E770G	A	G	0.1%	0.1%	0.2%	0.0%	1.2%	1.2%	0.8%	10.3%
SRGAP2	chr1	exon19	206632041	NM_001170637	c.C2317T	p.P773S	C	T	0.0%	0.0%	0.2%	0.0%	1.9%	1.6%	0.8%	12.0%

SRGAP2	chr1	exon19	206632083	NM_001170637	c.C2359T	p.P787S	C	T	0.1%	0.0%	0.0%	0.0%	1.7%	1.1%	1.3%	11.0%
SRGAP2	chr1	exon19	206632062	NM_001170637	c.A2338G	p.R780G	A	G	0.0%	0.0%	0.0%	0.0%	1.8%	1.3%	1.1%	11.0%
ST7L	chr1	exon9	113124647	NM_138728	c.C1036G	p.P346A	G	C	0.0%	0.0%	0.3%	0.7%	0.7%	1.4%	1.1%	12.8%
SYTL2	chr11	exon9	85431943	NM_032943	c.A1519T	p.M507L	T	A	0.0%	0.5%	0.6%	0.0%	0.9%	0.9%	1.3%	12.0%
TAB2	chr6	exon5	149700061	NM_015093	c.A1010G	p.N337S	A	G	0.0%	0.0%	0.4%	0.1%	1.1%	1.5%	2.0%	14.0%
TCEAL8	chrX	exon3	102508616	NM_153333	c.A292T	p.M98L	T	A	0.0%	0.0%	0.7%	0.0%	1.1%	1.4%	0.8%	10.8%
TCF20	chr22	exon1	42607204	NM_005650	c.T4108G	p.S1370A	A	C	0.0%	0.0%	0.3%	0.0%	0.9%	0.4%	1.2%	10.2%
TET3	chr2	exon1	74274176	NM_144993	c.C727T	p.P243S	C	T	0.1%	0.0%	0.5%	0.2%	2.0%	1.6%	1.7%	11.4%
TMEM180	chr10	exon8	104233371	NM_024789	c.T970C	p.S324P	T	C	0.1%	0.0%	0.7%	0.1%	1.1%	0.9%	1.2%	10.9%
TMEM64	chr8	exon1	91657447	NM_001146273	c.G687C	p.E229D	C	G	0.0%	0.0%	0.6%	1.6%	1.4%	1.7%	0.6%	13.0%
TMEM64	chr8	exon1	91657454	NM_001146273	c.G680A	p.S227N	C	T	0.0%	0.0%	1.1%	1.6%	1.4%	1.7%	1.3%	13.6%
TNRC6B	chr22	exon5	40662599	NM_015088	c.G2365A	p.A789T	G	A	0.0%	0.0%	0.5%	1.6%	1.6%	2.0%	1.9%	15.4%
TPP2	chr13	exon13	103288598	NM_003291	c.G1534A	p.V512I	G	A	0.0%	0.0%	0.0%	0.3%	0.0%	0.5%	0.5%	11.1%
TSSK1B	chr5	exon1	112770071	NM_032028	c.A466G	p.S156G	T	C	0.0%	0.0%	0.7%	0.3%	1.9%	1.8%	1.0%	11.6%
TTN	chr2	exon127	179458058	NM_003319	c.C31682T	p.A10561V	G	A	0.0%	0.0%	0.3%	0.0%	0.7%	1.5%	1.3%	12.0%
TTN	chr2	exon164	179415860	NM_003319	c.A64203C	p.E21401D	T	G	0.4%	0.0%	0.0%	0.3%	0.8%	1.4%	1.7%	11.9%
TTN	chr2	exon164	179415864	NM_003319	c.A64199G	p.N21400S	T	C	0.0%	0.0%	0.0%	0.3%	0.9%	1.9%	1.4%	11.6%
TTN	chr2	exon153	179441424	NM_003319	c.A42352G	p.S14118G	T	C	0.1%	0.0%	0.2%	0.5%	1.6%	1.8%	1.4%	11.6%
TTN	chr2	exon74	179587114	NM_133378	c.C18668T	p.T6223I	G	A	0.0%	0.0%	1.2%	0.3%	0.5%	1.7%	1.8%	12.4%
UBN2	chr7	exon15	138969124	NM_173569	c.T3473C	p.V1158A	T	C	0.1%	0.0%	1.0%	0.5%	0.2%	1.5%	1.6%	11.5%
UNC13B	chr9	exon14	35376157	NM_006377	c.A1501C	p.I501L	A	C	0.0%	0.0%	1.7%	1.7%	1.7%	1.6%	1.7%	11.5%
UNC45A	chr15	exon7	91479610	NM_001039675	c.C301A	p.Q101K	C	A	0.0%	0.0%	0.0%	0.3%	0.9%	1.6%	1.4%	14.3%
UNC5A	chr5	exon14	176306442	NM_133369	c.G2316C	p.R772S	G	C	0.0%	0.0%	0.6%	0.0%	0.7%	0.9%	1.0%	10.6%
UROC1	chr3	exon12	126219599	NM_001165974	c.A1264T	p.T422S	T	A	0.0%	0.0%	0.0%	0.0%	1.7%	0.9%	1.7%	10.8%
USP24	chr1	exon5	55637255	NM_015306	c.G799A	p.V267I	C	T	0.0%	0.0%	0.2%	0.2%	0.7%	1.7%	1.9%	11.3%
VWA5B2	chr3	exon11	183955086	NM_138345	c.A1606G	p.T536A	A	G	0.0%	0.0%	0.5%	0.2%	0.3%	1.7%	1.0%	12.8%
WNT16	chr7	exon3	120971860	NM_016087	c.G445C	p.A149P	G	C	0.0%	0.0%	0.0%	0.5%	0.9%	1.9%	0.5%	12.9%
XRN2	chr20	exon30	21369966	NM_012255	c.A2843G	p.N948S	A	G	0.0%	0.0%	0.0%	0.5%	0.4%	1.2%	0.9%	9.8%
YOD1	chr1	exon2	207222492	NM_018566	c.G920A	p.R307K	C	T	0.0%	0.0%	0.5%	0.5%	1.1%	1.8%	1.8%	13.3%
ZFHX2	chr14	exon3	24001988	NM_033400	c.G2347A	p.A783T	C	T	0.0%	0.0%	0.0%	2.0%	1.6%	1.8%	1.6%	15.8%
ZNF609	chr15	exon6	64972488	NM_015042	c.T3874G	p.S1292A	T	G	0.0%	0.0%	0.0%	0.1%	0.7%	0.9%	1.0%	10.6%
ZNF609	chr15	exon6	64972480	NM_015042	c.C3866G	p.T1289S	C	G	0.0%	0.0%	0.0%	0.1%	0.6%	0.9%	0.9%	9.9%
ZNF688	chr16	exon2	30582361	NM_145271	c.A280G	p.K94E	T	C	0.0%	0.0%	0.2%	0.4%	0.8%	1.5%	1.9%	11.4%

Table S12. SNVs in clonally derived tumors from CT38

Gene	CHR	Location	Position	Type	NCBI Ref	Coding	Protein	RS	Ref. Allele	Var. Allele	Variant Allele Frequency (%)	
											Type I derived tumor	Type V derived tumor
BRCA1	chr17	exon10	41,244,000	nonsynonymous SNV	NM_007300	c.A3548G	p.K1183R	rs16942	T	C	68.4%	70.0%
BRCA1	chr17	exon10	41,244,936	nonsynonymous SNV	NM_007300	c.C2612T	p.P871L	rs799917	G	A	30.0%	17.3%
CDH1	chr16	exon13	68,857,441	synonymous SNV	NM_004360	c.T2076C	p.A692A	rs1801552	T	C	99.4%	99.0%
CDKN2A	chr9	UTR3	21,968,199					rs11515	C	G	40.0%	24.4%
EGFR	chr7	exon20	55,249,063	synonymous SNV	NM_005228	c.G2361A	p.Q787Q	rs1050171	G	A	48.3%	47.1%
EGFR	chr7	exon25	55,268,916	synonymous SNV	NM_005228	c.C2982T	p.D994D	rs2293347	C	T	39.7%	36.5%
FGFR3	chr4	exon12	1,807,894	synonymous SNV	NM_022965	c.G1617A	p.T539T	rs7688609	G	A	99.5%	99.5%
FGFR3	chr4	exon9	1,806,131	nonsynonymous SNV	NM_001163213	c.T1156C	p.F386L	rs17881656	T	C	47.1%	45.7%
FLT3	chr13	intronic	28,610,183					rs2491231	A	G	99.9%	99.9%
FLT3	chr13	intronic	28,589,267					rs4073630	C	T	46.5%	38.5%
MLH1	chr3	exon8	37,053,568	nonsynonymous SNV	NM_000249	c.A655G	p.I219V	rs1799977	A	G	36.8%	31.6%
MLH1	chr3	intronic	37,083,740					rs9876116	A	G	48.1%	39.2%
NF1	chr17	intronic	29,654,876					rs2285894	T	A	51.6%	47.5%
PDGFRA	chr4	exon23	55,161,391	synonymous SNV	NM_006206	c.T3222C	p.D1074D	rs7685117	T	C	99.8%	99.9%
RET	chr10	exon13	43,613,843	synonymous SNV	NM_020630	c.G2307T	p.L769L	rs1800861	G	T	100.0%	98.9%
TP53	chr17	exon4	7,579,472	nonsynonymous SNV	NM_001126114	c.C215G	p.P72R	rs1042522	G	C	99.6%	99.8%
TP53	chr17	intronic	7,579,801					rs1642785	G	C	99.2%	99.1%

Table S13. SNVs in clonally derived tumors from CT59

Gene	CHR	Location	Position	Type	NCBI Ref	Coding	Protein	RS	Ref. Allele	Var. Allele	Variant Allele Frequency (%)	
											Type I derived tumor	Type II derived tumor
APC	chr5	exon12	112,162,855	nonsynonymous SNV	NM_000038	c.G1459A	p.G487R		G	A	19.2%	21.3%
APC	chr5	exon12	112,162,854	synonymous SNV	NM_000038	c.T1458C	p.Y486Y	rs2229992	T	C	99.8%	99.6%
APC	chr5	exon16	112,176,325	synonymous SNV	NM_000038	c.G5034A	p.G1678G	rs42427	G	A	99.2%	99.1%
BRAF	chr7	exon15	140,453,136	nonsynonymous SNV	NM_004333	c.T1799A	p.V600E	rs113488022	A	T	65.3%	68.6%
CDH1	chr16	intronic	68,771,372					rs3743674	C	T	100.0%	97.4%
CDH1	chr16	exon13	68,857,441	synonymous SNV	NM_004360	c.T2076C	p.A692A	rs1801552	T	C	99.4%	99.7%
CDKN2A	chr9	UTR3	21,968,199					rs11515	C	G	100.0%	100.0%
EGFR	chr7	exon20	55,249,063	synonymous SNV	NM_005228	c.G2361A	p.Q787Q	rs1050171	G	A	99.4%	99.3%
FBXW7	chr4	exon3	153,268,144	stopgain SNV	NM_001013415	c.C310T	p.R104X		G	A	50.2%	54.3%
FBXW7	chr4	exon9	153,247,224	nonsynonymous SNV	NM_001013415	c.G1224T	p.W408C		C	A	46.2%	55.3%
FGFR2	chr10	exon6	123,298,158	synonymous SNV	NM_001144917	c.A696G	p.V232V	rs1047100	T	C	52.7%	44.6%
FGFR3	chr4	exon12	1,807,894	synonymous SNV	NM_022965	c.G1617A	p.T539T	rs7688609	G	A	99.6%	99.9%
FLT3	chr13	intronic	28,610,183					rs2491231	A	G	99.5%	99.9%
HRAS	chr11	exon2	534,270	nonsynonymous SNV	NM_176795	c.C53T	p.A18V		G	A	48.5%	50.6%
JAK2	chr9	exon6	5,050,706	synonymous SNV	NM_004972	c.C489T	p.H163H	rs10429491	C	T	99.4%	99.7%
KIT	chr4	exon20	55,603,362	synonymous SNV	NM_001093772	c.C2706T	p.C902C		C	T	53.5%	60.0%
NF1	chr17	intronic	29,654,876					rs2285894	T	A	99.4%	99.7%
PDGFRA	chr4	exon23	55,161,391	synonymous SNV	NM_006206	c.T3222C	p.D1074D	rs7685117	T	C	99.9%	99.8%
PDGFRA	chr4	exon18	55,152,040	synonymous SNV	NM_006206	c.C2472T	p.V824V	rs2228230	C	T	47.7%	47.4%
PDGFRA	chr4	exon10	55,139,771	nonsynonymous SNV	NM_006206	c.T1432C	p.S478P	rs35597368	T	C	50.9%	45.4%
PDGFRA	chr4	exon12	55,141,054	nonsynonymous SNV	NM_006206	c.C1700T	p.P567L		C	T	50.7%	51.6%
PIK3CA	chr3	intronic	178,922,274					rs2699896	C	A	100.0%	99.0%
RB1	chr13	intronic	48,919,358					rs198617	T	G	99.4%	100.0%
RET	chr10	exon13	43,613,843	synonymous SNV	NM_020975	c.G2307T	p.L769L	rs1800861	G	T	100.0%	100.0%
TP53	chr17	intronic	7,579,801					rs1642785	G	C	98.5%	99.0%
TP53	chr17	exon4	7,579,472	nonsynonymous SNV	NM_001126114	c.C215G	p.P72R	rs1042522	G	C	99.6%	99.6%
TP53	chr17	exon8	7,577,090	nonsynonymous SNV	NM_001126114	c.G848A	p.R283H		C	T	48.0%	52.8%
TP53	chr17	exon5	7,578,430	nonsynonymous SNV	NM_001126114	c.A500C	p.Q167P		T	G	25.8%	27.0%
TP53	chr17	exon6	7,578,263	stopgain SNV	NM_001126114	c.C586T	p.R196X		G	A	49.8%	47.6%

References

1. M. Greaves, C. C. Maley, Clonal evolution in cancer. *Nature* **481**, 306 (2012). doi:10.1038/nature10762 Medline

2. S. Nik-Zainal *et al.*; Breast Cancer Working Group of the International Cancer Genome Consortium, The life history of 21 breast cancers. *Cell* **149**, 994 (2012). doi:10.1016/j.cell.2012.04.023 Medline

3. M. Gerlinger *et al.*, Intratumor heterogeneity and branched evolution revealed by multiregion sequencing. *N. Engl. J. Med.* **366**, 883 (2012). doi:10.1056/NEJMoa1113205 Medline

4. K. Anderson *et al.*, Genetic variegation of clonal architecture and propagating cells in leukaemia. *Nature* **469**, 356 (2011). doi:10.1038/nature09650 Medline

5. F. Notta *et al.*, Evolution of human BCR-ABL1 lymphoblastic leukaemia-initiating cells. *Nature* **469**, 362 (2011). doi:10.1038/nature09733 Medline

6. E. Clappier *et al.*, Clonal selection in xenografted human T cell acute lymphoblastic leukemia recapitulates gain of malignancy at relapse. *J. Exp. Med.* **208**, 653 (2011). doi:10.1084/jem.20110105 Medline

7. C. G. Mullighan *et al.*, Genomic analysis of the clonal origins of relapsed acute lymphoblastic leukemia. *Science* **322**, 1377 (2008). doi:10.1126/science.1164266 Medline

8. X. Wu *et al.*, Clonal selection drives genetic divergence of metastatic medulloblastoma. *Nature* **482**, 529 (2012). doi:10.1038/nature10825 Medline

9. W. Liu *et al.*, Copy number analysis indicates monoclonal origin of lethal metastatic prostate cancer. *Nat. Med.* **15**, 559 (2009). doi:10.1038/nm.1944 Medline

10. M. E. Gorre *et al.*, Clinical resistance to STI-571 cancer therapy caused by BCR-ABL gene mutation or amplification. *Science* **293**, 876 (2001). doi:10.1126/science.1062538 Medline

11. C. Roche-Lestienne, J. L. Laï, S. Darré, T. Facon, C. Preudhomme, A mutation conferring resistance to imatinib at the time of diagnosis of chronic myelogenous leukemia. *N. Engl. J. Med.* **348**, 2265 (2003). doi:10.1056/NEJMc035089 Medline

12. M. J. Bissell, M. A. Labarge, Context, tissue plasticity, and cancer: Are tumor stem cells also regulated by the microenvironment? *Cancer Cell* **7**, 17 (2005). doi:10.1016/S1535-6108(04)00375-7 Medline

13. V. Sanz-Moreno *et al*., Rac activation and inactivation control plasticity of tumor cell movement. *Cell* **135**, 510 (2008). doi:10.1016/j.cell.2008.09.043 Medline

14. S. L. Spencer, S. Gaudet, J. G. Albeck, J. M. Burke, P. K. Sorger, Non-genetic origins of cell-to-cell variability in TRAIL-induced apoptosis. *Nature* **459**, 428 (2009). doi:10.1038/nature08012 Medline

15. A. Roesch *et al*., A temporarily distinct subpopulation of slow-cycling melanoma cells is required for continuous tumor growth. *Cell* **141**, 583 (2010). doi:10.1016/j.cell.2010.04.020 Medline

16. S. V. Sharma *et al*., A chromatin-mediated reversible drug-tolerant state in cancer cell subpopulations. *Cell* **141**, 69 (2010). doi:10.1016/j.cell.2010.02.027 Medline

17. P. B. Gupta *et al*., Stochastic state transitions give rise to phenotypic equilibrium in populations of cancer cells. *Cell* **146**, 633 (2011). doi:10.1016/j.cell.2011.07.026 Medline

18. K. Ishizawa *et al*., Tumor-initiating cells are rare in many human tumors. *Cell Stem Cell* **7**, 279 (2010). doi:10.1016/j.stem.2010.08.009 Medline

19. P. N. Kelly, A. Dakic, J. M. Adams, S. L. Nutt, A. Strasser, Tumor growth need not be driven by rare cancer stem cells. *Science* **317**, 337 (2007). doi:10.1126/science.1142596 Medline

20. S. Jones *et al*., Comparative lesion sequencing provides insights into tumor evolution. *Proc. Natl. Acad. Sci. U.S.A.* **105**, 4283 (2008). doi:10.1073/pnas.0712345105 Medline

21. A. Marusyk, V. Almendro, K. Polyak, Intra-tumour heterogeneity: A looking glass for cancer? *Nat. Rev. Cancer* **12**, 323 (2012). doi:10.1038/nrc3261 Medline

22. M. Kærn, T. C. Elston, W. J. Blake, J. J. Collins, Stochasticity in gene expression: From theories to phenotypes. *Nat. Rev. Genet.* **6**, 451 (2005). doi:10.1038/nrg1615 Medline

23. M. Loreau *et al*., Biodiversity and ecosystem functioning: Current knowledge and future challenges. *Science* **294**, 804 (2001). doi:10.1126/science.1064088 Medline

24. D. F. Flynn, N. Mirotchnick, M. Jain, M. I. Palmer, S. Naeem, Functional and phylogenetic diversity as predictors of biodiversity—ecosystem-function relationships. *Ecology* **92**, 1573 (2011). doi:10.1890/10-1245.1 Medline

25. H. B. Fraser, A. E. Hirsh, G. Giaever, J. Kumm, M. B. Eisen, Noise minimization in eukaryotic gene expression. *PLoS Biol.* **2**, e137 (2004). doi:10.1371/journal.pbio.0020137 Medline

26. H. L. True, S. L. Lindquist, A yeast prion provides a mechanism for genetic variation and phenotypic diversity. *Nature* **407**, 477 (2000). doi:10.1038/35035005 Medline

27. J. M. Raser, E. K. O'Shea, Control of stochasticity in eukaryotic gene expression. *Science* **304**, 1811 (2004). doi:10.1126/science.1098641 Medline

28. K. Lewis, Persister cells, dormancy and infectious disease. *Nat. Rev. Microbiol.* **5**, 48 (2007). doi:10.1038/nrmicro1557 Medline

29. A. M. Abulafi, N. S. Williams, Local recurrence of colorectal cancer: The problem, mechanisms, management and adjuvant therapy. *Br. J. Surg.* **81**, 7 (1994). doi:10.1002/bjs.1800810106 Medline

30. J. M. Raser, E. K. O'Shea, Noise in gene expression: Origins, consequences, and control. *Science* **309**, 2010 (2005). doi:10.1126/science.1105891 Medline

31. G. Guenechea *et al*., Transduction of human $CD34^+$ $CD38^-$ bone marrow and cord blood-derived SCID-repopulating cells with third-generation lentiviral vectors. *Mol. Ther.* **1**, 566 (2000). doi:10.1006/mthe.2000.0077 Medline

32. A. Kreso, C. A. O'Brien, *Curr. Protoc. Stem Cell Biol.* Chap. 3, Unit 3 1 (2008).

33. S. Pounds *et al*., Reference alignment of SNP microarray signals for copy number analysis of tumors. *Bioinformatics* **25**, 315 (2009). doi:10.1093/bioinformatics/btn624 Medline

34. A. B. Olshen, E. S. Venkatraman, R. Lucito, M. Wigler, Circular binary segmentation for the analysis of array-based DNA copy number data. *Biostatistics* **5**, 557 (2004). doi:10.1093/biostatistics/kxh008 Medline

35. C. Li, W. Hung Wong, *Genome Biol.* **2**, RESEARCH0032 (2001).

36. O. Harismendy *et al*., Detection of low prevalence somatic mutations in solid tumors with ultra-deep targeted sequencing. *Genome Biol.* **12**, R124 (2011). doi:10.1186/gb-2011-12-12-r124 Medline

37. R. Tewhey *et al*., Microdroplet-based PCR enrichment for large-scale targeted sequencing. *Nat. Biotechnol.* **27**, 1025 (2009). doi:10.1038/nbt.1583 Medline

38. M. A. DePristo *et al*., A framework for variation discovery and genotyping using next-generation DNA sequencing data. *Nat. Genet.* **43**, 491 (2011). doi:10.1038/ng.806 Medline

39. K. Wang, M. Li, H. Hakonarson, ANNOVAR: Functional annotation of genetic variants from high-throughput sequencing data. *Nucleic Acids Res.* **38**, e164 (2010). doi:10.1093/nar/gkq603 Medline

40. K. D. Siegmund, P. Marjoram, S. Tavaré, D. Shibata, High DNA methylation pattern intratumoral diversity implies weak selection in many human colorectal cancers. *PLoS ONE* **6**, e21657 (2011). doi:10.1371/journal.pone.0021657 Medline

41. A. G. Uren *et al*., A high-throughput splinkerette-PCR method for the isolation and sequencing of retroviral insertion sites. *Nat. Protoc.* **4**, 789 (2009). doi:10.1038/nprot.2009.64 Medline

42. D. M. Muzny *et al*.; Cancer Genome Atlas Network, Comprehensive molecular characterization of human colon and rectal cancer. *Nature* **487**, 330 (2012). doi:10.1038/nature11252 Medline

43. D. Shibata, Inferring human stem cell behaviour from epigenetic drift. *J. Pathol.* **217**, 199 (2009). doi:10.1002/path.2461 Medline

44. J. E. Dick, M. C. Magli, D. Huszar, R. A. Phillips, A. Bernstein, Introduction of a selectable gene into primitive stem cells capable of long-term reconstitution of the hemopoietic system of W/Wv mice. *Cell* **42**, 71 (1985). doi:10.1016/S0092-8674(85)80102-1 Medline

45. G. Keller, C. Paige, E. Gilboa, E. F. Wagner, Expression of a foreign gene in myeloid and lymphoid cells derived from multipotent haematopoietic precursors. *Nature* **318**, 149 (1985). doi:10.1038/318149a0 Medline

46. I. R. Lemischka, D. H. Raulet, R. C. Mulligan, Developmental potential and dynamic behavior of hematopoietic stem cells. *Cell* **45**, 917 (1986). doi:10.1016/0092-8674(86)90566-0 Medline

47. J. E. Dick, Stem cell concepts renew cancer research. *Blood* **112**, 4793 (2008). doi:10.1182/blood-2008-08-077941 Medline

48. J. L. McKenzie, O. I. Gan, M. Doedens, J. C. Wang, J. E. Dick, Individual stem cells with highly variable proliferation and self-renewal properties comprise the human hematopoietic stem cell compartment. *Nat. Immunol.* **7**, 1225 (2006). doi:10.1038/ni1393 Medline

49. C. A. O'Brien, A. Pollett, S. Gallinger, J. E. Dick, A human colon cancer cell capable of initiating tumour growth in immunodeficient mice. *Nature* **445**, 106 (2007). doi:10.1038/nature05372 Medline

50. L. Ricci-Vitiani *et al*., Identification and expansion of human colon-cancer-initiating cells. *Nature* **445**, 111 (2007). doi:10.1038/nature05384 Medline

51. P. Dalerba *et al*., Phenotypic characterization of human colorectal cancer stem cells. *Proc. Natl. Acad. Sci. U.S.A.* **104**, 10158 (2007). doi:10.1073/pnas.0703478104 Medline

52. M. Todaro *et al*., Colon cancer stem cells dictate tumor growth and resist cell death by production of interleukin-4. *Cell Stem Cell* **1**, 389 (2007). doi:10.1016/j.stem.2007.08.001 Medline

53. N. Haraguchi *et al*., $CD133^{+}CD44^{+}$ population efficiently enriches colon cancer initiating cells. *Ann. Surg. Oncol.* **15**, 2927 (2008). doi:10.1245/s10434-008-0074-0

54. P. Chu *et al*., Characterization of a subpopulation of colon cancer cells with stem cell-like properties. *Int. J. Cancer* **124**, 1312 (2009). doi:10.1002/ijc.24061 Medline

55. E. H. Huang *et al*., Aldehyde dehydrogenase 1 is a marker for normal and malignant human colonic stem cells (SC) and tracks SC overpopulation during colon tumorigenesis. *Cancer Res.* **69**, 3382 (2009). doi:10.1158/0008-5472.CAN-08-4418 Medline

56. C. A. O'Brien *et al*., ID1 and ID3 regulate the self-renewal capacity of human colon cancer-initiating cells through p21. *Cancer Cell* **21**, 777 (2012). doi:10.1016/j.ccr.2012.04.036 Medline